

LAMINAR HEAT TRANSFER TO TIME-INDEPENDENT NON-NEWTONIAN FLUIDS IN TUBES

By

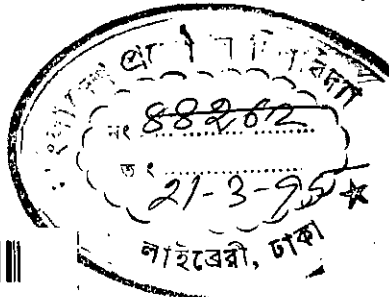
ANANDA MOHAN MONDAL

A Thesis Submitted to the Department of Chemical Engineering
in Partial Fulfilment of the Requirements for the Degree of

Master of Science
in
Chemical Engineering

FEBRUARY 1995

88261



#88261#

BANGLADESH UNIVERSITY OF ENGINEERING AND TECHNOLOGY
DHAKA-1000, BANGLADESH

660.2844
1995
MON

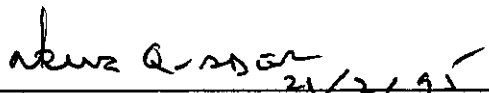
LAMINAR HEAT TRANSFER TO TIME-INDEPENDENT
NON-NEWTONIAN FLUIDS IN TUBES

A THESIS

BY


ANANDA MOHAN MONDAL

Approved as to style and content by:



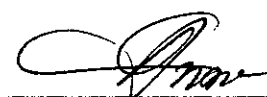
Dr. A. K. M. A. Quader
Professor
Department of Chemical Engineering
BUET, Dhaka-1000

:Chairman



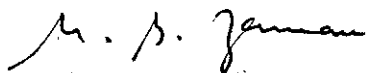
Dr. M. Sabder Ali
Professor and Head
Department of Chemical Engineering
BUET, Dhaka-1000

:Member
(Ex-officio)



Dr. J. A. Naser
Assistant Professor
Department of Mechanical Engineering
BUET, Dhaka-1000

:Member



M. Badiuzzaman
Sr. General Manager
Bangladesh Chemical Industries Corpn.
BCIC Bhaban,
30-31, Dilkusha
Dhaka

:Member
(External)

ABSTRACT

Heat transfer characteristics for the heating of the dilute solutions of different types of Cellofas in straight tubes are studied numerically in laminar condition with constant wall temperature considering viscous dissipation. The scope of this study is limited to numerical prediction of velocity profile, temperature profile and the rate of heat transfer at steady fully developed condition.

"TEACH-T", a general computer program has been used for this purpose. After sufficient testing against bench-mark experimental and analytical data, the computer program was used for the prediction of flow and heat transfer data.

The present study is confined to a tube of fixed diameter 17.4 mm. Power law model describes the flow behaviour of the fluids and the fluid consistency, K is temperature dependent. To study the effect of heating on velocity profile, temperature profile and the rate of heat transfer, three different temperature ratio T_w/T_1 , namely, 1.068, 1.13 and 1.233 were considered.

Present study indicates that velocity profile becomes flatter with the increase of pseudoplasticity and temperature ratio. The effect of pseudoplasticity on temperature profile is small but the effect of temperature ratio is significant. Effect of pseudoplasticity and viscous dissipation on heat transfer rates are interrelated. This combined effect is small because the fluids considered do not have large values for consistency, K .

ACKNOWLEDGEMENTS

The author expresses his sincere gratitude to his supervisor, Dr. A. K. M. A. Quader, Professor of Chemical Engineering, BUET, Dhaka for his guidance and encouragement all through this work.

The author is much indebted to Dr. J. A. Naser, Assistant Professor of Mechanical Engineering, BUET, for his constructive suggestions and help for having this work completed.

The author is also grateful to Dr. M. Sabder Ali, Professor and Head, Department of Chemical Engineering, BUET, for providing assistance at different stages of the work.

CONTENTS

Title	Page
Abstract	i
Acknowledgement	ii
Contents	iii
List of Symbols	vi
List of Figures	x
CHAPTER-I INTRODUCTION	1
1.1 Background	1
1.2 Motivation Behind the Selection of the study	2
1.3 Importance of Numerical investigation	2
1.4 The Present Contribution	3
1.5 Thesis Outline	4
CHAPTER-II LITERATURE REVIEW	5
2.1 Introduction	5
2.2 Laminar Heat transfer to Newtonian Fluids in Closed Conduits	6
2.2.1 The Leveque Solution	6
2.2.2 The Classical Graetz Solution	8
2.2.3 Extension of the Graetz Problem; Velocity Profile Fully Developed	11
2.2.4 Laminar Heat Transfer With Developing Flow	13
2.2.5 Empirical Correlations of Laminar Flow Heat Transfer Data	15
2.3 Laminar Heat Transfer to Non-Newtonian Fluids in Closed Conduits	16
2.3.1 The Graetz Nusselt Problem for a Power Law Non-Newtonian Fluid	17
2.3.2 Extension of the Leveque Approximation to Non-Newtonian Systems	18
2.3.3 Experimental work on Heat Transfer to Non-Newtonian Fluids	21

2.3.4 Heat Transfer to Non-Newtonian Fluids with Temperature dependent Flowbehavior Characteristics	22
2.3.5 Heat Transfer to Non-Newtonian Fluids Considering Viscous Generation	29
2.3.6 Heat Transfer to Non-Newtonian Fluids Considering Natural Convection	32
2.3.7 Empirical Correlations of Laminar Flow Heat Transfer Data of Non-Newtonian Fluids	35
2.3.8 Heat Transfer to Laminar Non-Newtonian Flow in Curved Tubes	38
CHAPTER-III STATEMENT OF THE OBJECTIVES	40
CHAPTER-IV FORMULATION OF THE PROBLEM	42
CHAPTER-V COMPUTER PROGRAM	46
5.1 Description	46
5.2 Contents of the Program	46
5.3 Verification of the Program	48
CHAPTER-VI NUMERICAL SOLUTION	50
6.1 Introduction	50
6.2 The Method of Discretization	51
6.3 Differencing Scheme	52
6.4 Solution Procedure	54
6.4.1 Grid and Variable Arrangement	54
6.4.2 Calculation of Pressure	54
6.5 Boundary Conditions	55
6.6 Solution Algorithm	55
CHAPTER-VII RESULTS AND DISCUSSIONS	57
7.1 Introduction	57
7.2 Domain of Solution and Computational Grid	57
7.3 Grid Independence Test	58

7.4	Presentation of Results	58
7.4.1	Physical Property Used	58
7.4.2	Variables/Parameters Used in the Presentation	59
7.4.3	Description of the Graphs	62
7.5	Discussion of Results	64
7.5.1	Velocity Profiles	64
7.5.2	Temperature Profiles	65
7.5.3	Heat Transfer Rates	66
CHAPTER-VIII CONCLUSIONS		69
CHAPTER-IX SUGGESTIONS FOR FUTURE WORK		71
REFERENCES		72
FIGURES		77
APPENDIX-A Finite Difference Form of Equation		132

LIST OF SYMBOLS

Symbol	Meaning
Latin Letters:	
a	constant in eq.(2.78)
A	constant in eq.(2.43), N.s ⁿ /m ²
A _w	heat transfer area/surface area of tube
b	constant in eq.(2.78)
B	Boltzman constant per mole in eq.(2.43)
Br	Brinkmann number, $\frac{u_{av}^{n+1} K_i}{k T_i R^{n-1}}$
c	constant
c _n	coefficient of Graetz solution
C _p	heat capacity of fluid
D	diameter of tube
Gr	Grashof number, $\frac{g \epsilon D^3 \Delta t \rho^2}{\mu^2}$
Gz	Graetz number, WC _p /kx
h	heat transfer coefficient
k	thermal conductivity of fluid
k'	fluid consistency index, $\frac{\tau_w}{(8u_{av}/D)^n}$ or $\frac{D \Delta P / 4L}{(8u_{av}/D)^n}$
K	fluid consistency index in power law
L	length
n	power law index
n'	flow behavior index, $\frac{d(\ln D \Delta P / 4L)}{d(\ln 8u_{av}/D)}$
Nu	Nusselt number, hD/k
P	pressure
Pe	Peclet number, RePr

Pe'	Peclet number (of radius). $Re'Pr'$
Pr	Prandtl number, $C_p\mu/k$
Pr'	Prandtl number(of radius), $(KC_p/k)(R/u_{av})^{1-n}$
q	rate of heat flow
r	radial distance
R	radius of tube
R'	dimensionless radial distance, r/R
Re'	generalized Reynolds number $\frac{D^n u_{av}^{2-n} \rho}{k/8^{n-1}}$ Reynolds number for power law fluid $\frac{D^n u_{av}^{2-n} \rho}{\frac{K}{8} \left(\frac{6n+2}{n}\right)^n}$
t	temperature
T	temperature; Absolute temperature, eq.(2.43); $t-t_1$, eq.(2.52).
T ₁	fluid temperature as it enters the heating or cooling section
u	x-direction velocity/axial velocity
U	dimensionless axial velocity, u/u_{av}
v	y-direction velocity/radial velocity
w	z-direction velocity
W	mass flow rate
x	axial distance
X	$(x/R)(1/Pe')$, eq.(2.51); $kx/\rho u_{av} R^2 C_p = \pi/Gz$, eq.(2.62); [dimensionless]

Greek Letter

α	thermal diffusivity
α'	velocity gradient at the wall
β	parameter representing the temperature dependence effect, $\beta_1 T_1$
β_i	constant characterising temperature dependent properties, eq.(2.57)
β_n	exponents of the Graetz solution
γ	$-1/\mu \, d\mu/dT$ or $-1/K \, dK/dT$ in eqn.(2.83); shear rate, du/dr or du/dz
Δ	$(3n+1)/4n$
ΔH	activation energy for flow in eq.(2.43)
ΔT	$q_w D/2k$
δ	ratio of velocity gradient at wall of a pipe for non-Newtonian fluid to velocity gradient for Newtonian fluid at same flow rate or small increment
ϵ	coefficient of volume expansion, $1/^\circ C$
ζ	defined as $(k/\rho C_p u_{max} R^2) x$
η	non-Newtonian viscosity, Pa.s
θ	dimensionless temperature defined as $T/(q_w R/k)$, eq.(2.51); $(T-T_1)/T_1$, eq.(2.58); $(T-T_1)/(T_w-T_1)$, eq.(2.46)

μ	viscosity, Kg/m.s
μ_a	apparent viscosity, $K\left(\frac{\partial u}{\partial r}\right)^{n-1}$
ρ	fluid density, Kg/m ³
τ	shear stress, N/m ²
ϕ	T_w/T_i
ψ	$q_w R/kT_i$

Subscripts

a.m.	arithmetic mean
av	average
b	bulk
c	curvature
cp,n	power law fluid with constant properties
e	entrance
eff	effective
i	inlet
m	mean
max	maximum
o	outlet
vp,n	power law fluid with variable properties
w	wall
x	local
y	yield
∞	infinity or asymptotic

LIST OF FIGURES

Figure No.	Name	Page
Fig. 2.1	Condition for the Leveque Solution	77
Fig. 2.2	Boundary Conditions for the Classical Graetz Solution	77
Fig. 2.3	Local Nusselt Number for Laminar Flow in Tubes. Velocity Profile Fully Developed	78
Fig. 2.4	Local Nusselt Number for Laminar Flow in the entrance of a Tube ($Pr=0.7$)	78
Fig. 2.5	Mean Nusselt Number for Laminar Flow in the Entrance of a Tube ($Pr=0.7$)	79
Fig. 2.6	Mean Nusselt Number for Fully Developed Laminar Flow in Tubes	79
Fig. 4.1	Flow Configuration	80
Fig. 5.1	Program Flow Chart	81
Fig. 5.2	Isothermal Flow Development of Newtonian Fluid	82
Fig. 5.3	Isothermal Flow Development of Carbopol. $n=0.6$, $EPSY=.9$	83
Fig. 5.4	Local Nusselt Number for Laminar Flow in Tubes. Velocity Profile Fully Developed	84
Fig. 5.5	Velocity Profile for Newtonian Oil-heating. $Gz=323$, $T_w/T_i=1.29$ and $D=14.8$ mm	85
Fig. 5.6	Velocity Profile for Carbopol heating. $n=0.6$, $Gz=359$, $T_w/T_i=1.233$ and $D=17.4$ mm	86
Fig. 5.7	Temperature Profile for Newtonian oil-heating $Gz=323$, $T_w/T_i=1.29$ and $D=14.8$ mm	87
Fig. 5.8	Temperature Profile for Carbopol Heating. $n=0.6$, $Gz=359$, $T_w/T_i=1.233$ and $D=17.4$ mm	88
Fig. 6.1	Two Dimensional Computational Cell	89
Fig. 6.2	Control Volume for Continuity Equation	89

Fig. 6.3	Control Volume for U	90
Fig. 6.4	Control Volume for V	90
Fig. 6.5	Computational Grid, Local and Control Volumes(cells) of Scalar Variables and Axial and Radial Velocities	91
Fig. 6.6	Schematic Presentation of CDS	92
Fig. 6.7	Schematic Presentation of UDS	92
Fig. 7.1a	Velocity Profiles for Different Types Cellofas. $Gz=232$, $T_w/T_i=1.068$, $D=17.4$ mm	93
Fig. 7.1b	Velocity Profiles for Different Types Cellofas. $Gz=232$, $T_w/T_i=1.130$, $D=17.4$ mm	94
Fig. 7.1c	Velocity Profiles for Different Types Cellofas. $Gz=232$, $T_w/T_i=1.233$, $D=17.4$ mm	95
Fig. 7.2	Velocitiy Profiles for 1% Cellofas B-10 at Different T_w/T_i . $Gz=232$, $D=17.4$ mm	96
Fig. 7.3	Velocitiy Profiles for 0.5% Cellofas B-300 at Different T_w/T_i . $Gz=232$, $D=17.4$ mm	97
Fig. 7.4	Velocitiy Profiles for .15% Cellofas B-3500 at Different T_w/T_i . $Gz=232$, $D=17.4$ mm	98
Fig. 7.5	Velocitiy Profiles for .27% Cellofas B-3500 at Different T_w/T_i . $Gz=232$, $D=17.4$ mm	99
Fig. 7.6	Velocitiy Profiles for .40% Cellofas B-3500 at Different T_w/T_i . $Gz=232$, $D=17.4$ mm	100
Fig. 7.7	Velocitiy Profiles for 1% Cellofas B-10 at Different Gz . $T_w/T_i=1.130$, $D=17.4$ mm	101
Fig. 7.8	Velocitiy Profiles for 0.5% Cellofas B-300 at Different Gz . $T_w/T_i=1.130$, $D=17.4$ mm	102
Fig. 7.9	Velocitiy Profiles for .15% Cellofas B-3500 at Different Gz . $T_w/T_i=1.130$, $D=17.4$ mm	103
Fig. 7.10	Velocitiy Profiles for .27% Cellofas B-3500 at Different Gz . $T_w/T_i=1.130$, $D=17.4$ mm	104
Fig. 7.11	Velocitiy Profiles for .40% Cellofas B-3500 at Different Gz . $T_w/T_i=1.130$, $D=17.4$ mm	105
Fig. 7.12a	Temperature Profiles for Different Types Cellofas. $Gz=232$, $T_w/T_i=1.068$, $D=17.4$ mm	106

Fig. 7.12b	Temperature Profiles for Different Types Cellofas. $Gz=232$, $T_w/T_i=1.130$, $D=17.4$ mm	107
Fig. 7.12c	Temperature Profiles for Different Types Cellofas. $Gz=232$, $T_w/T_i=1.233$, $D=17.4$ mm	108
Fig. 7.13	Temperature Profiles for 1% Cellofas B-10 at Different T_w/T_i . $Gz=232$, $D=17.4$ mm	109
Fig. 7.14	Temperature Profiles for .5% Cellofas B-300 at Different T_w/T_i . $Gz=232$, $D=17.4$ mm	110
Fig. 7.15	Temperature Profiles for .15% Cellofas B-3500 at Different T_w/T_i . $Gz=232$, $D=17.4$ mm	111
Fig. 7.16	Temperature Profiles for .27% Cellofas B-3500 at Different T_w/T_i . $Gz=232$, $D=17.4$ mm	112
Fig. 7.17	Temperature Profiles for .40% Cellofas B-3500 at Different T_w/T_i . $Gz=232$, $D=17.4$ mm	113
Fig. 7.18	Temperature Profiles for 1% Cellofas B-10 at Different Gz . $T_w/T_i=1.130$, $D=17.4$ mm	114
Fig. 7.19	Temperature Profiles for .5% Cellofas B-300 at Different Gz . $T_w/T_i=1.130$, $D=17.4$ mm	115
Fig. 7.20	Temperature Profiles for .15% Cellofas B-3500 at Different Gz . $T_w/T_i=1.130$, $D=17.4$ mm	116
Fig. 7.21	Temperature Profiles for .27% Cellofas B-3500 at Different Gz . $T_w/T_i=1.130$, $D=17.4$ mm	117
Fig. 7.22	Temperature Profiles for .40% Cellofas B-3500 at Different Gz . $T_w/T_i=1.130$, $D=17.4$ mm	118
Fig. 7.23	Local Nusselt Number for Laminar Flow in Tubes. Velocity Profile Fully Developed. $T_w/T_i=1.130$, $D=17.4$ mm.	119
Fig .7.24	Local Nusselt Number for 1% Cellofas B-10 at Different T_w/T_i . Velocity Profile Fully Developed, $D=17.4$ mm.	120
Fig .7.25	Local Nusselt Number for .5% Cellofas B-300 at Different T_w/T_i . Velocity Profile Fully Developed, $D=17.4$ mm.	121
Fig .7.26	Local Nusselt Number for .15% Cellofas B-3500 at Different T_w/T_i . Velocity Profile Fully Developed, $D=17.4$ mm.	122

Fig .7.27	Local Nusselt Number for .27% Cellofas B-3500 at Different T_w/T_1 . Velocity Profile Fully Developed, $D=17.4$ mm.	123
Fig .7.28	Local Nusselt Number for .40% Cellofas B-3500 at Different T_w/T_1 . Velocity Profile Fully Developed, $D=17.4$ mm.	124
Fig. 7.29	Nu_w vs Gz for the Heating of 1% Cellofas B-10 with Constant Temperature at the Wall.	125
Fig. 7.30	Nu_w vs Gz for the Heating of .5% Cellofas B-300 with Constant Temperature at the Wall.	126
Fig. 7.31	Nu_w vs Gz for the Heating of .15% Cellofas B-3500 with Constant Temperature at the Wall.	127
Fig. 7.32	Nu_w vs Gz for the Heating of .27% Cellofas B-3500 with Constant Temperature at the Wall.	128
Fig. 7.33	Nu_w vs Gz for the Heating of .40% Cellofas B-3500 with Constant Temperature at the Wall.	129
Fig. 7.34	Nu_w vs Gz for the Heating of Cellofas B-3500 with Different Composition at $T_w/T_1=1.130$.	130
Fig. A.1	Computational Grid	131

CHAPTER-I

INTRODUCTION



1.1 Background

The processing of non-Newtonian fluids is of great industrial importance. These fluids are characterized by a nonlinear rheogram or shear stress-shear rate relationship. Emulsions, slurries, and polymeric melts, solutions, and dispersions are mostly of non-Newtonian nature. Of the many types of non-Newtonian fluids considered in the literature, pseudoplastic fluids are most commonly encountered.

The rheograms for most of these pseudoplastic fluids are quite accurately represented by the equation suggested by Eyring et al (1955).

$$B'\tau = \gamma \frac{S}{A'} + \sinh^{-1} \frac{S}{A'} \quad (1.1)$$

where A' , B' and γ are constants, and S is shear rate.

The occurrence of the shear rate in both the linear and inverse hyperbolic sine terms of eq.(1.1) makes this relationship somewhat cumbersome for many engineering purposes. Consequently the empirical Ostwald-de-Waele or power law equation eq.(4.1) has often been used as an approximate representation of pseudoplastic rheology (10, 13, 19, 31, 50).

In some cases eq. (4.1) has been found to fit rheological data as well as or better than eq. (1.1). In the present study, eq.(4.1) is used to describe the fluid rheology.

1.2 Motivation Behind the Selection of the Study

The industrial importance of non-Newtonian behavior is generally known and the types of non-Newtonian behavior encountered have been discussed by many authors; nevertheless, not a single satisfactory method is available for the prediction of heat transfer rates to highly non-Newtonian fluids such as viscous slurries, gels, and polymeric melts and solutions(38). A study of the literature indicates that methods for predicting heat transfer to pseudoplastic fluids in laminar flow did not adequately incorporate the effect of the viscosity-temperature dependency. Those who considered the temperature-dependent rheology is specific to the fluids are involved. One of the purposes of this investigation was to determine a realistic viscosity-temperature dependency of Cellofas solutions and, based on this, to develop accurate methods for the prediction of heat transfer coefficients for the heating of these pseudoplastic fluids in laminar flow in tubes of circular cross section with constant wall temperature.

1.3 Importance of Numerical Investigation

The emergence of computers together with the development of

more versatile and efficient numerical solution method has led to a substantial increase in the assembly of mathematical modelling of flow process. Now a days, in the engineering design of heat transfer related problems, designers are looking for computational investigations to seek the optimum design, as experiments with either model or full scale prototype are generally laborious, expensive, and time consuming.

The theoretical prediction enables to operate an existing equipment more safely and efficiently. Prediction of the relevant process help in forecasting and even controlling potential dangers. These predictions offer economic advantages too.

1.4 The Present Contribution

The present study deals with the numerical investigation of heat transfer with specific time-independent non-Newtonian fluids. The fluids are dilute solutions of Cellofas of different grades and concentrations.

The specific contribution of this study are :

- a. variation of velocity profile with pseudoplasticity, n ;
temperature ratio, T_w/T_1 ; and Graetz number, Gz .

- b. variation of temperature profile with pseudoplasticity, n ; temperature ratio, T_w/T_b ; and Graetz number, Gz .
- c. variation of heat transfer rate with temperature ratio, T_w/T_b and viscous dissipation.

1.5 Thesis Outline

The remaining part of the thesis is divided into eight chapters. In Chapter II, relevant literature is briefly reviewed in this area. The objectives of the present work are listed in Chapter III.

Formulation of the problem is presented in Chapter IV. Computer program used in this work is described in Chapter V and the method of solution is in Chapter VI.

The results and discussions are presented in Chapter VII. Finally in Chapters VIII and IX, the findings of the present work and suggestions for future work are presented respectively.

CHAPTER-II

LITERATURE REVIEW

2.1 Introduction

The study of laminar heat transfer with non-Newtonian fluids is of considerable industrial importance. Several studies have been carried out on heat transfer to non-Newtonian fluids in tubes in laminar condition(10,11,12,19,20,35,36,38,50). These fluids are characterized by a nonlinear shear stress-shear rate relationship.

There are different kinds of non-Newtonian fluids, but the most important type to-date from the industrial viewpoint is pseudo-plastic behaviour. Most of these pseudoplastic fluids are satisfactorily represented by the empirical Ostwald-de-Waele or power law equation.

$$\tau = -K \left(\frac{du}{dr} \right)^n \quad (2.1)$$

In section 2.2 literature on laminar heat transfer to Newtonian fluids and subsequent developments are discussed. Heat transfer to non-Newtonian fluids are presented in section 2.3.

2.2 Laminar Heat Transfer to Newtonian Fluids in Closed Conduits.

When heat transfer occurs during laminar flow of a fluid, the transfer through the fluid is by conduction alone. No mixing of the fluid, like that occurring during turbulent flow, takes place. In practice it is difficult to obtain truly laminar flow during heat transfer except in very small passages. Natural convection currents are usually present, and under these conditions conduction alone is not the only mode of heat transfer to be considered.

2.2.1 The Leveque Solution.

One of the simplest solutions for the laminar flow heat transfer coefficient in circular tubes is that of Leveque(1928). The analysis applies directly to laminar flow heat transfer on a flat plate, but the results may be easily applied to circular tubes. The Leveque solution yields a solution in the region near the wall considering a fluid flowing over a surface under the following conditions(Figure 2.1):

- (1) The fluid properties are constant.
- (2) The surface temperature is uniform at T_w .
- (3) The undisturbed fluid temperature is T_∞ .
- (4) Heat transfer is due to conduction alone.
- (5) The velocity of the fluid is

$$u = cy \quad , \quad v = 0 \quad , \quad w = 0$$

where y = direction outward normal to surface

c = constant

The fluid temperature T is a function of x and y . For small values of y , $\partial^2 T / \partial x^2 \ll \partial^2 T / \partial y^2$. Also $\partial^2 T / \partial z^2$ may be considered negligible. Using these simplifying assumptions, the differential equation for laminar flow heat transfer without viscous dissipation becomes,

$$cy \frac{\partial T}{\partial x} = \alpha \frac{\partial^2 T}{\partial y^2} \quad (2.2)$$

where, $\alpha = k / C_p \rho$ and boundary conditions are:

B. C. 1: At $x = 0$ and $y > 0$; $T = T_w$

B. C. 2: At $x > 0$ and $y = 0$; $T = T_w$

Introducing a new variable X , where $X = y(c/9\alpha x)^{1/3}$ eq.(2.2)

becomes,

$$\frac{d^2 T}{dX^2} + 3X^2 \frac{dT}{dX} = 0 \quad (2.3)$$

and boundary conditions are:

B. C. 1: At $X = 0$, $T = T_w$

B. C. 2: At $X = \infty$, $T = T_w$

The solution of eq.(2.3) is

$$\frac{T - T_w}{T_w - T_w} = \frac{1}{0.893} \int_0^X e^{-X^3} dX \quad (2.4)$$

Temperature profile, eq.(2.4), is used to derive the expression for the local Nusselt number(Nu_x) on the surface a distance x from the leading edge and the Nusselt number(Nu_x) for laminar flow in the entrance region of a circular tube as

$$Nu_x = \frac{hx}{k} = \frac{x}{0.893} \left(\frac{c}{9\alpha x} \right)^{1/3} \quad (2.5)$$

and

$$Nu_x = 1.077 (Pe)^{1/3} \left(\frac{D}{x} \right)^{1/3} \quad (2.6)$$

In general, eq.(2.6) is applicable in the range $100 < Pe(D/x) < 5,000$ and in this region it agrees with experimental data.

2.2.2 The Classical Graetz Solution.

One of the earliest analysis of laminar heat transfer with Newtonian fluids in tubes was made by Graetz in 1885. It has been thoroughly described by Drew(1931) and Jakob(1949). The analysis has been extended to include a variety of boundary conditions.

The assumptions of the classical Graetz problem for laminar-flow heat transfer in circular tubes(Figure 2.2) are:

1. Steady state has been attained,
2. Heat conduction in the x -direction is negligible in comparison with heat transport in the x -direction by the overall fluid flow,
3. The fluid properties are constant,
4. Heat produced by viscous dissipation is negligible,

5. There are no external (body) forces acting on the fluid,
6. Laminar parabolic velocity profile is assumed to be established before heating or cooling of the fluid,
7. At $x = 0$ the temperature of the tube wall changes from T_1 to T_2 and is uniform at this value for $x > 0$.

The continuity and momentum equations for this situation are:

Continuity :

$$\frac{du}{dx} = 0 \quad (2.7)$$

Momentum :

$$0 = -\frac{dp}{dx} - \frac{1}{r} \frac{d}{dr} (r\tau) \quad (2.8)$$

The velocity profile obtained is

$$u = 2u_{av} \left[1 - \left(\frac{r}{R} \right)^2 \right] \quad (2.9)$$

Assuming radial symmetry and neglecting heat conduction in x -direction (the term containing $\partial^2 T / \partial x^2$), energy balance equation becomes,

$$u \frac{\partial T}{\partial x} = \frac{k}{C_p \rho} \left[\frac{1}{r} \frac{\partial}{\partial r} \left(r \frac{\partial T}{\partial r} \right) \right] \quad (2.10)$$

Combining eqs. (2.9) and (2.10),

$$2u_{av} \left[1 - \left(\frac{r}{R} \right)^2 \right] \frac{\partial T}{\partial x} = \frac{k}{C_p \rho} \left[\frac{1}{r} \frac{\partial}{\partial r} \left(r \frac{\partial T}{\partial r} \right) \right] \quad (2.11)$$

Boundary conditions:

B.C.1: At $x = 0$ and at any r ; $T = T_2$.

B.C.2: At $x > 0$ and $r = R$; $T = T_1$.

Solution of eq.(2.11) gives T as a function of x and r . This partial differential equation is solved by assuming that $T-T_w$ is the product of two functions, one which is a function of x and the other is the function of r . The solution takes the form of an infinite series as follows:

$$\frac{T-T_w}{T_v-T_w} = \sum_{n=0}^{\infty} c_n \phi_n(r/R) \exp \frac{-\beta_n^2(x/R)}{Pe} \quad (2.12)$$

where c_n are coefficients, $\phi_n(r/R)$ are functions of (r/R) determined by the boundary conditions, and β_n^2 are exponents determined by the boundary conditions.

The local Nusselt number for laminar flow in circular tubes predicted by the Graetz solution is

$$Nu_x = \frac{\sum_{n=0}^{\infty} \frac{c_n \phi_n'(1)}{2} \exp \frac{-\beta_n^2(x/R)}{Pe}}{2 \sum_{n=0}^{\infty} \frac{c_n \phi_n'(1)}{2\beta_n^2} \exp \frac{-\beta_n^2(x/R)}{Pe}} \quad (2.13)$$

Hausen(1943) proposed the following equation for the mean Nusselt number over a length of pipe x as representing the Graetz solution for constant wall temperature and parabolic velocity distribution.

$$Nu_m = 3.66 + \frac{0.0668[(x/D)/Pe]^{-1}}{1+0.04[(x/D)/Pe]^{-2/3}} \quad (2.14)$$

where $Nu_m = h_m D/k$ for circular tubes.

Application of eq.(2.13) requires the use of a large number of terms when $(x/D)/Pe$ is small. For this case Sellars, Tribus, and Klein(1956) proposed the relation

$$Nu_x = 1.357 \left(\frac{x/R}{Pe} \right)^{-1/3}; \quad \text{for} \quad \frac{x/R}{Pe} \leq 0.01 \quad (2.15)$$

which is essentially the same as that obtained by Leveque solution shown in eq.(2.6).

From eq.(2.13) the value of the local Nusselt number, Nu_x , as $(x/R)/Pe$ becomes large is

$$Nu_\infty = 3.656; \quad \text{for} \quad \frac{x/R}{Pe} > 0.25 \quad (2.16)$$

where Nu_∞ is the asymptotic value of the Nusselt number when $(x/R)/Pe$ becomes greater than 0.25. Equation(2.13) is shown in Figure 2.3 in the range $0.0001 < (x/D)/Pe < 1.0$.

2.2.3 Extension of the Graetz Problem; Velocity Profile Fully Developed.

Sellars, Tribus, and Klein(1956) provided a useful extension of the classical Graetz solution by considering boundary conditions other than constant wall temperature.

Case 1. Constant Wall Heat Flux. The differential eq.(2.11) is applicable. The boundary conditions are:

B.C.1: At $x = 0$ and at any r ; $T = T_w$.

B.C.2: At all x ; $\frac{q_w}{A_w} = \text{const}$ and $\frac{\partial T_b}{\partial x} = \text{const}$

The Nusselt number is

$$Nu_x = \frac{1}{\frac{11}{48} + \frac{1}{2} \sum_{m=0}^{\infty} \frac{\exp(-\beta_m^2(x/R)/Pe)}{\beta_m^4 \phi_m'(-\beta_m^2)}} \quad (2.17)$$

For small values of $(x/R)/Pe$

$$Nu_x = 1.639 \left(\frac{x/R}{Pe} \right)^{-1/3} ; \quad \text{for } \frac{x/R}{Pe} < 0.01 \quad (2.18)$$

For large values of $(x/R)/Pe$

$$Nu_x = 4.364 ; \quad \text{for } \frac{x/R}{Pe} \geq 0.25 \quad (2.19)$$

Equation (2.17) is plotted in Figure 2.3.

Case 2. Linear Wall Temperature. The differential eq.(2.11) is applicable. The boundary conditions are:

B.C.1: At $x = 0$ and at any r ; $T = T_w$.

B.C.2: At $x > 0$ and $r = R$;

$$T = T_w \text{ and } T_w - T_w = cx, \text{ where } c = \text{const}$$

The Nusselt number becomes

$$Nu_x = \frac{\frac{1}{2} + 4 \sum_{n=0}^{\infty} \frac{c_n \phi_n'(1)}{2\beta_n^2} \exp \frac{-\beta_n^2(x/R)}{Pe}}{\frac{88}{768} + 8 \sum_{n=0}^{\infty} \frac{c_n \phi_n'(1)}{2\beta_n^4} \exp \frac{-\beta_n^2(x/R)}{Pe}} \quad (2.20)$$

For small values of $(x/R)/Pe$

$$Nu_x = 2.035 \left(\frac{x/R}{Pe} \right)^{-1/3} ; \quad \text{for } \frac{x/R}{Pe} < 0.01 \quad (2.21)$$

For large values of $(x/R)/Pe$

$$Nu_w = 4.364 \quad ; \quad \text{for} \quad \frac{x/R}{Pe} \geq 0.5 \quad (2.22)$$

The limiting Nusselt number for case 1 is the same as for case 2; however, for the former the limiting Nusselt number is reached when $(x/R)/Pe = 0.25$, while in the latter it is reached when $(x/R)/Pe = 0.5$. This means that the thermal entrance length (at constant Peclet number) for constant wall heat flux (case 1) is one-half the thermal entrance length for linear wall temperature (case 2). The thermal entrance length is that distance from the beginning of heat transfer at which the Nusselt number becomes independent of length.

2.2.4 Laminar Heat Transfer With Developing Flow.

Since heat transfer often occurs at the actual entrance of a tube, the velocity profile is not parabolic but is developing. The Graetz solutions based on the parabolic velocity distribution are not valid in these circumstances. This problem was considered by Kays(1955), who obtained a numerical solution of eq.(2.10) in which the laminar velocity profile was assumed to develop according to the relation derived by Langhaar(1942). Kays considered three boundary conditions:

- (1) Constant wall temperature ($Pr = 0.7$)
- (2) Constant wall heat flux ($Pr = 0.7$)
- (3) Constant temperature difference ($Pr = 0.7$)

The results of the numerical solution are shown in Figures 2.4 and 2.5. In Figure 2.4 values of the local Nusselt number are plotted as a function of $(x/D)/Pe$ for the three boundary conditions. Experimental data of Kroll(1951) are included, indicating good agreement with the numerical solution. Equation (2.13), the classical Graetz solution is shown in Figure 2.4 for comparison. Figure 2.5 is a plot of the mean Nusselt number over a length of tube x versus $(x/D)/Pe$ for two of the boundary conditions considered by Kays. Experimental data reported by Kays(1951) are shown in Figure 2.5. Good agreement with the numerical solution is found.

Kays also reported relationships for the mean and local Nusselt numbers for the boundary conditions. These relationships are summarized below.

1. Constant wall temperature ($Pr = 0.7$):

$$Nu_m = 3.66 + \frac{0.104[(x/D)/Pe]^{-1}}{1 + 0.016[(x/D)/Pe]^{-0.8}} \quad (2.23)$$

2. Constant temperature difference ($Pr = 0.7$):

$$Nu_m = 4.36 + \frac{0.10[(x/D)/Pe]^{-1}}{1 + 0.016[(x/D)/Pe]^{-0.8}} \quad (2.24)$$

3. Constant wall heat flux ($Pr = 0.7$):

$$Nu_x = 4.36 + \frac{0.036[(x/D)/Pe]^{-1}}{1 + 0.0011[(x/D)/Pe]^{-1}} \quad (2.25)$$

Equations (2.23) to (2.25) may be used to predict Nusselt numbers

for laminar flow in the entrance section of circular tubes. They are strictly applicable to the flow of air or the common gases since they were derived for a fluid with a Prandtl number of 0.7.

2.2.5 Empirical Correlations of Laminar flow Heat transfer

Data.

Experimental data are not plentiful; nor have all the available data been obtained under conditions for which analytical solutions are available, i.e., constant wall temperature, constant heat input, etc. Another difficulty encountered in comparing analytical and experimental results is due to variable fluid properties. Most theoretical work assumes constant fluid properties, but in practice the assumption is valid only in the limit where temperature differences approach zero. In dealing with experimental data the further question arises of whether natural convection plays a significant role in the heat transfer. Some experimental results are shown in Figures 2.4 and 2.5, and a good agreement with theoretical work is obtained.

Boehm(1943) studied the laminar flow heat transfer for the cooling of oil in a tube. The heat transfer was studied after the velocity profile was established, and Nusselt numbers based on the arithmetic mean temperature difference were determined over a section having a length-to-diameter ratio x/D of 124. Since the data were obtained at essentially constant wall temperature, they may be compared with classical Graetz solution. Figure 2.6 is a plot of $Nu_{a,m}$ versus $(x/D)/Pe$, where $Nu_{a,m} = h_{a,m}D/k$, in which $h_{a,m}$

is defined as

$$\frac{q_w}{A_w} = h_{a.m.} (T_w - T_b)_{a.m.} \quad (2.26)$$

Boehm's data fall much below the curve for eq. (2.14) and agree well with a curve for cooling obtained by Kraussold(1931). Kraussold's curve for heating lies above that for cooling. Nusselt's laminar-flow data for air are plotted on Figure 2.6. They were obtained at fairly high values of $(x/D)/Pe$ and fall close to eq. (2.14). The following equation, proposed by Sieder and Tate(1936), is also plotted on Figure 2.6:

$$Nu_{a.m.} = 1.86 \left(\frac{x/D}{Pe} \right)^{-1/3} \left(\frac{\mu_b}{\mu_w} \right)^{0.14} \quad (2.27)$$

(Properties evaluated at bulk temperature)

where μ_b is the viscosity of the fluid at its arithmetic mean bulk temperature. Equation (2.27) gives Nusselt numbers somewhat higher than the analytical Graetz solution.

The relatively poor agreement of experimental data with theoretical results is probably due to natural-convection effects, which are difficult to eliminate.

2.3 Laminar Heat Transfer to Non-Newtonian Fluids in Closed Conduits.

This section presents theoretical and numerical analyses, and empirical correlations on heat transfer with non-Newtonian fluids. Analytical and theoretical results are compared with some of the experimental data.

2.3.1 The Graetz-Nusselt Problem for a Power law Non-Newtonian Fluid.

Lyche and Bird(1956) showed how the Graetz-Nusselt problem can be extended to non-Newtonian flow. They introduced a non-Newtonian model, "Power Law", for the fluid instead of the Newtonian one.

Using the assumptions, the equations of motion and energy in cylindrical tubes become

$$0 = -\frac{dP}{dx} - \frac{1}{r} \frac{d}{dr} (r\tau) \quad (2.28)$$

and

$$u \frac{\partial T}{\partial x} = \frac{k}{C_p \rho} \left[\frac{1}{r} \frac{\partial}{\partial r} \left(r \frac{\partial T}{\partial r} \right) \right] \quad (2.29)$$

where,

$$\tau = -K \left| \frac{du}{dr} \right|^{n-1} \frac{du}{dr} \quad (2.30)$$

in which K and n are constants of the power law, obtainable from experimental flowcurve.

Solution of eq. (2.28) gives the velocity profile as

$$u = \frac{R^{\frac{1}{n}-1}}{K \left(\frac{1}{n} + 1 \right)} \left(-\frac{1}{2} \frac{dP}{dx} \right)^{1/n} \left(1 - \frac{r}{R} \right)^{\frac{1}{n}+1} = u_{\max} (1-R^*)^{\frac{1}{n}+1} \quad (2.31)$$

where, $R^* = r/R$, and the solution of eq. (2.29) gives the temperature profile as

$$\theta(R^*, \zeta) = \frac{T - T_w}{T_\infty - T_w} = \sum_{i=1}^{i=\infty} (-1)^{i+1} B_i \psi_i(\zeta) \phi_i(R^*) \quad (2.32)$$

where B_i are constants, $\phi_i(R^*)$ are the eigenfunctions, and $\psi_i(\zeta) = \exp(-c_i \zeta)$. c_i are the eigenvalues.

Average outlet temperature and the local Nusselt number for laminar flow in circular tubes predicted by this solution are:

$$\theta_{av} = \frac{T_{av} - T_w}{T_\infty - T_w} = \frac{\int_0^{2\pi} \int_0^1 \theta(R^*, \zeta) u(R^*) R^* dR^* d\phi}{\int_0^{2\pi} \int_0^1 u(R^*) R^* dR^* d\phi} \quad (2.33)$$

and

$$Nu_x = \frac{1 - \theta_{av}(\zeta)}{\zeta u_{max} / u_{av}} \quad (2.34)$$

Lyche and Bird made the calculations for $n=1, 1/2, 1/3,$ and 0 to find the velocity and temperature distributions as a function of dimensionless radial coordinate. Their calculations were the first step in the study of heat conduction in non-Newtonian flow systems. There were no experimental data to make comparisons with the theoretical data.

2.3.2 Extension of the Leveque Approximation to Non-Newtonian Systems.

The Leveque approximation for the average Nusselt number for laminar flow in a pipe has been given as

$$Nu_{av} = \frac{h_{av}D}{k} = 1.62 \left(\frac{\alpha' C_p \rho D^3}{8kL} \right)^{1/3} \quad (2.35)$$

where α' is the velocity gradient at the wall. For Newtonian fluid α' is $8u_{av}/D$ and in this case it becomes

$$Nu_{av} = \frac{h_{av}D}{k} = 1.75 \left(\frac{WC_p}{kL} \right)^{1/3} \quad (2.36)$$

Pigford(1955) has rewritten this in the form

$$Nu_{av} = \frac{h_{av}D}{k} = 1.75 \delta^{1/3} \left(\frac{WC_p}{kL} \right)^{1/3} \quad (2.37)$$

where δ is the ratio of the velocity gradient at the wall for the non-Newtonian fluid, α' , to that for a Newtonian fluid, $8u_{av}/D$, i.e. δ is defined as

$$\delta = \frac{\alpha'}{8u_{av}/D} \quad (2.38)$$

Pigford has also shown that δ for Bingham plastics is given by

$$\delta = \frac{(1 - \tau_y/\tau_w)}{1 - \frac{4}{3}(\tau_y/\tau_w) + \frac{1}{3}(\tau_y/\tau_w)^4} \quad (2.39)$$

and in general, for all time-independent fluids by

$$\delta = \frac{(3n'+1)}{4n'} \quad (2.40)$$

Using this value of δ , eq.(2.37) applies for high flow rates (with Graetz numbers greater than 100) and values of n' above 0.1. These conditions will normally be encountered in practice; so this restriction is not serious. For the rare case of fluids showing extreme pseudoplasticity at low Graetz numbers, Metzner,

Vaughn and Houghton(1957) have presented an empirical correction in place of δ which is in the form of an interpolation between the two limiting theoretical solutions for $n' = 0$ and $n' = 1$.

It is worth noting here that the correction for dilatant fluids is never very great, for in the limiting case of 'infinite dilatancy' $n' = \infty$, and Eqn.(2.40) gives $\delta = 3/4$. Hence from eq.(2.37) one gets for infinite dilatancy

$$Nu_{av} = \frac{h_{av}D}{k} = 1.59 \left(\frac{WC_P}{kL} \right)^{1/3} \quad (2.41)$$

which is slightly different from eq.(2.35) for Newtonian fluids. The correction for pseudoplasticity could be greater as shown by Figure 2.6 which shows the curves for a Newtonian fluid, eq.(2.36), together with those for infinite dilatancy, eq.(2.41), and 'infinite pseudoplasticity' $n' = 0$, which is identical with the case for piston flow.

Metzner et al.(1957) have also suggested an empirical correction factor to take into account deviations from theory caused by the distortion of the velocity profile by changes in viscosity due to the radial temperature gradient. This is a generalization of the Sieder-Tate viscosity ratio, $(\mu/\mu_w)^{0.14}$, which is widely used in heat transfer correlations for Newtonian fluids. The denominator in the generalized Reynolds number is $k'8^{n'-1}$ and this takes the place of the viscosity in the conventional Reynolds number. Therefore, in place of the Sieder-Tate correction Metzner et al. have suggested $(m/m_w)^{0.14}$ where $m = k'8^{n'-1}$. m is evaluated

at the mean bulk temperature and m_w at the wall temperature. The final correlation for the average heat transfer coefficient then becomes

$$Nu_{av} = \frac{h_{av}D}{k} = 1.75\delta^{1/3} \left(\frac{WC_p}{kL} \right)^{1/3} \left(\frac{m}{m_w} \right)^{1/3} \quad (2.42)$$

This equation was tested experimentally(38), and found to be satisfactory, over the following range of variables:

$$n' \quad : \quad 0.18 \text{ to } 0.70$$

$$WC_p/kL \quad : \quad 100 \text{ to } 2050$$

$$Re' \quad : \quad 0.65 \text{ to } 2100$$

The inclusion of the correction factor $(m/m_w)^{0.14}$ in eq. (2.42) considerably improved the correlation of the experimental results.

2.3.3 Experimental Work on Heat Transfer to Non-Newtonian Fluids.

A number of analytical solutions of the equations of energy and motion applicable to heat transfer to molten polymers have been published. These include the work of Topper(1956), who considered systems with a heat generation term constant across a tube both for a parabolic velocity profile and potential flow; that of Lyche and Bird(1956), who studied the Graetz-Nusselt problem for an incompressible power law fluid without heat generation; and various papers by Toor which dealt with the effect of expansion on temperatures with little heat generation (1956), heat generation and conduction in a viscous compressible fluid (1957),

and heat transfer in forced convection with internal heat generation (1958). None of forgoing studies presented any experimental data other than calculated quantities.

Griskey and Wiehe (1966) developed a precise, reproducible method for measuring temperature profiles in flowing molten polymers with heat transfer. They carried out experiments on heat transfer to molten polyethylene and polypropylene. Experimental data determined by this method showed that viscous dissipation occurred, but not at the level predicted theoretically. Nusselt numbers calculated from the data checked theoretical Graetz-Nusselt solutions.

2.3.4. Heat Transfer to Non-Newtonian Fluids with Temperature-Dependent Flowbehavior Characteristics.

Early experiments indicated that neither Graetz's nor Leveque's solutions were capable of correlating experimental data owing to failure to incorporate the effect of temperature on fluid properties. Christiansen and Craig (1962) proposed a temperature dependent equation

$$\tau = A \left[\frac{du}{dr} \exp\left(\frac{\Delta H}{BT}\right) \right]^n \quad (2.43)$$

to represent the rheological properties of pseudoplastic fluids. In the analysis natural convection and thermal energy generation are negligible. Problem was solved numerically for heating of both Newtonian and non-Newtonian fluids in laminar flow in tubes of circular cross section with constant wall temperature.

The energy equation for steady laminar flow after neglecting longitudinal heat conduction and frictional heat generation terms, is

$$u \frac{\partial t}{\partial x} = \frac{k}{\rho C_p} \left(\frac{\partial^2 t}{\partial r^2} + \frac{1}{r} \frac{\partial t}{\partial r} \right) \quad (2.44)$$

The fluid enters the heating section with a fully developed velocity profile given by

$$U = \frac{u}{u_{av}} = \frac{1}{2} \frac{\int_{R^*}^1 (R^*)^{1/n} e^{\Delta H/BT} dR^*}{\int_0^1 R^* \int_{R^*}^1 (R^*)^{1/n} e^{-\Delta H/BT} dR^* dR^*} \quad (2.45)$$

The energy equation can be written in a dimensionless form as

$$\frac{\partial \theta}{\partial \left(\frac{1}{Gz} \right)} = \frac{\pi}{U} \left(\frac{\partial^2 \theta}{\partial R^{*2}} + \frac{1}{R^*} \frac{\partial \theta}{\partial R^*} \right) \quad (2.46)$$

Although analytical solutions to this equation are unknown, numerical solutions were obtained through standard finite difference techniques. The general procedure was to divide the reduced radius into j equal parts of δR^* each and then to start at a reduced length $1/Gz$ equal to zero and to compute the temperature distribution for steps of length $\delta(1/Gz)$. Second-order approximations were used to evaluate all partial derivatives in eq.(2.46). The result of these second-order approximations was a series of j simultaneous algebraic equations in $\theta(R^*, Gz)$ to be solved for each step of $\delta(1/Gz)$. This set of simultaneous equations was found to be especially adaptable to solution by the Crout reduction method. When the reduced

temperature distribution had been found at each reduced length, the Nusselt number was determined from the solution of the equation

$$Nu_x = \frac{1}{\pi} Gz \frac{\int_0^1 2R^* U \theta dR^*}{1 - \frac{1}{2} \int_0^1 2R^* U \theta dR^*} \quad (2.47)$$

The numerical solutions obtained are in good agreement with experimental heat transfer data for heating of a 3% aqueous suspension of CMC and a 0.75% aqueous suspension of CPM in laminar flow in tubes with L/D ratios varying from 6 to 230, fluid temperature increases up to 30°C, and temperature potentials up to 70°C. The solutions are believed to be essentially exact for plug flow for $Nu < 1,000$ and for Newtonian and pseudoplastic flow at $Nu < 100$.

Christiansen, Jensen, and Tao (1966) extended the previous work of Christiansen et al (1962) for the heating of non-Newtonian fluids to the case of cooling at constant wall temperature. They compared the numerical results with experimental data for the cooling of 1.5 and 0.35% CPM solutions in water at constant tube wall temperatures. The mean deviation of experimental data from the numerical solutions was $\pm 8\%$.

Mizushima et al (1967) performed experimental and analytical studies in laminar horizontal flow heat transfer in non-Newtonian pseudoplastic fluids, under conditions of constant heat flux at the wall. They have taken into account variation in viscosity

with respect to temperature by including a correction term in the consistency index. Their final correlation is of the form

$$Nu = 1.41 \left(\frac{3n+1}{4n} \right)^{1/3} Gz \left(\frac{K}{K_w} \right)^{0.1/n^{0.7}} \quad (2.48)$$

where K is the power law fluid consistency index, and K_w is the value of K at wall temperature.

Mitsuishi and Miyatake (1966) applied the Ellis model to develop analytical solutions and these solutions were subsequently verified by them experimentally (1968), using a viscosity correction of the form similar to that used by Mizushima et al. For the constant wall temperature case, analytical and experimental data have been published by Christiansen et al (10, 11), Metzner et al (39).

Mahalingam, Tilton, and Coulson (1975) developed analytical solutions for heat transfer to non-Newtonian power law pseudoplastic fluids in laminar flow in circular conduits. The wall boundary conditions are constant heat flux and step change in heat flux. Experimental data showed that the consistency index as a function of temperature can be correlated as

$$K = ae^{bt} \quad (2.49)$$

The energy equation remains the same as eq.(2.44). The fluid enters the heating section with a fully developed velocity profile given by

$$U = \frac{u}{u_{av}} = \frac{1}{2} \frac{\int_0^1 R^{1/n} e^{bt/n} dR}{\int_0^1 R \cdot \int_0^1 R^{1/n} e^{bt/n} dR \cdot dR} \quad (2.50)$$

The energy equation can be written in a non-dimensional form as

$$U \frac{\partial \theta}{\partial X} = \frac{\partial^2 \theta}{\partial R^2} + \frac{1}{R} \frac{\partial \theta}{\partial R} \quad (2.51)$$

or as

$$U \frac{\partial T}{\partial X} = \frac{\partial^2 T}{\partial R^2} + \frac{1}{R} \frac{\partial T}{\partial R} \quad (2.52)$$

In order to evaluate the Nusselt numbers, the mean bulk temperature can be obtained from

$$T_{av} = \int_0^1 2R \cdot UT dR \quad (2.53)$$

and the local Nusselt number from

$$Nu_x = \frac{2(q_w R/k)}{T_w - T_{av}} \quad (2.54)$$

The partial differential equation is solved using finite difference solution technique. The 'marching solution' method has been used for the numerical solution. In order to calculate the wall temperature and center-line temperature, the temperature profile is approximated to a power series. A 3-term series given by

$$T_w = \frac{1}{3} \left[4T_{(1-\Delta R')} - T_{(1+2\Delta R')} + \frac{2\Delta R' q_w R}{k} \right] \quad (2.55)$$

has been found to be adequate. For cases wherein step increase in wall heat flux has to be studied, the step-change heat fluxes are induced via this equation.

In numerical solutions Mahalingam et al consider the cases of low heat fluxes wherein natural convection effects are negligible. Effect of viscosity variation has been taken into account in the numerical computation. Numerical results are good in agreement with experimentally measured values.

Forrest and Wilkinson (1973) investigated the heat transfer to temperature dependent non-Newtonian fluid numerically. They used a temperature dependent rheology given by the equation:

$$\tau = \tau_y + K(\dot{\gamma})^n \quad (2.56)$$

Consistency K is given by

$$K = \frac{K_i}{1 + \beta_i (T - T_i)^n} \quad (2.57)$$

where K_i is the value of K at the fluid inlet temperature T_i and β_i is a constant which characterizes the temperature dependent properties of the fluid. This model includes both power law and Bingham plastic behavior. The two boundary conditions of constant wall temperature and constant wall heat flux are considered for both heating and cooling.

The energy equation eq.(2.44) is applicable. The fluid enters the heating section with a fully developed velocity profile given by

$$U = \frac{u}{u_{av}} = \frac{1}{2} \frac{\int_{R'}^1 (1 + \beta\theta) (R' - R'y)^{1/n} dR'}{\int_0^1 R' \int_{R'}^1 (1 + \beta\theta) (R' - R'y)^{1/n} dR' dR'} \quad (2.58)$$

The energy equation can be written in a dimensionless form as eq.(2.51). Nusselt numbers are

Constant wall temperature:

$$Nu_{av} = \frac{h_{av} D}{k} = \frac{Gz}{\pi} \frac{\theta_0}{(\theta_w - \frac{1}{2}\theta_0)} \quad (2.59)$$

Constant wall heat flux:

$$Nu_q = \frac{Dh_q}{k} = \frac{2}{(\theta_w - \theta_0)} \psi \quad (2.60)$$

where

$$\theta_0 = \int_0^1 2R' U \theta dR' \quad (2.61)$$

The equations are solved numerically to yield solutions as functions of a number of dimensionless parameters, viz:

Constant wall temperature:

$$U_{R',x} \theta_{R',x} = f[Gz, n, (\tau_y/\tau_w)_i, \beta, \Phi] \quad (2.62)$$

Constant wall heat flux:

$$U_{R',x} \theta_{R',x} = f[Gz, n, (\tau_y/\tau_w)_i, \beta, \Psi] \quad (2.63)$$

The numerical technique used to solve the partial differential equation consisted of a Crank-Nicholson, Thomas algorithm implicit finite-difference scheme using 100 radial increments and

an initial axial step length of 10^{-6} . Numerical results obtained by Forrest and Wilkinson are good in agreement with the previous work of Jensen (11) and Hirai (28).

Faghri and Welty (1977) performed a complete solution for laminar, fully developed flow in a circular pipe with uniform entrance temperature subjected to a wall heat flux which is uniform axially but circumferentially variable. Non-Newtonian fluid behavior characterized by a power law constitutive relationship was used in the analysis. The expressions for fluid temperature, wall temperature, and local Nusselt number are given in terms of the wall heat flux distribution. Any circumferential distribution is allowed so long as it may be expressed in Fourier series form.

2.3.5 Heat Transfer to Non-Newtonian Fluids Considering Viscous Heat Generation.

Popovska and Wilkinson (1977) studied numerically the problem of laminar heat transfer to Newtonian and non-Newtonian fluids in tubes considering viscous dissipation. They used the power law model for fluid rheology. Consistency index K is represented by a polynomial of the form

$$\log K = A + BT + CT^2 + \dots \quad (2.64)$$

In order to simplify the problem it is assumed that

1. The flow is laminar and steady and the radial component of velocity can be neglected.

2. Conduction of heat in the axial direction is negligible, which is justified when $RePr \gg 100$.
3. The heat capacity, C_p , and the thermal conductivity, k , are constant.
4. The density, ρ , is independent of temperature and natural convection effects can be ignored.

The initial and boundary conditions for the problem are:

- a) The velocity profile at the tube inlet is fully developed and the temperature is uniform.
- b) The tube wall temperature is constant.

On this basis the simplified equations of motion, energy and continuity are as follows:

Equation of motion:

$$-\frac{\partial P}{\partial x} = \frac{1}{r} \frac{\partial}{\partial r} (r\tau) \quad (2.65)$$

Equation of energy:

$$\rho C_p u \frac{\partial T}{\partial x} = \frac{k}{r} \frac{\partial}{\partial r} \left(r \frac{\partial T}{\partial r} \right) - \tau \frac{\partial u}{\partial r} \quad (2.66)$$

Equation of continuity:

$$W = 2\pi\rho \int_0^R r u dr \quad (2.67)$$

The average Nusselt number is defined on the basis of an average heat transfer coefficient as

$$Nu_{av} = \frac{h_{av} D}{k} = \frac{Gz}{\pi} \frac{(T_0 - T_i)}{T_w - (T_0 + T_i)/2} \quad (2.68)$$

The theoretical predictions have been confirmed by comparing them with experimental temperature and velocity profiles obtained for a Newtonian oil and non-Newtonian polymer solutions. Both heating and cooling experiments have been carried out for a range of Reynolds numbers from 2-700. The Graetz number variation was from 80-1600. The experimental Nusselt numbers were also compared with the theoretical predictions and with those calculated from the generally accepted design correlations of the Leveque form. The agreement between the theoretical predictions and the experimental results was good. Empirical design correlations gave poor predictions for cooling cases.

Dinh and Armstrong (1982) performed an approximate analytical solutions for estimating the local temperature rise from viscous heating in slit and tube flow of non-Newtonian fluids with small Nahme-Griffith numbers, i.e., fluids whose viscosities are independent of temperature. An arbitrary values of h as well as the limiting cases of infinite h (isothermal wall) and h equal to zero (insulated wall) are considered in the solution.

Assumptoins made in the solution are:

1. The physical properties of the fluid, in particular the viscosity, are independent of temperature.
2. The velocity profile is fully developed prior to $x=0$.
3. Axial conduction is small compared to axial convection.

For the assumptions given above, the equations of motion and energy for this problem in rectangular coordinates are:

$$0 = -\frac{dp}{dx} + \frac{d}{dz} \eta \frac{du}{dz} \quad (2.69)$$

$$\rho C_p u \frac{\partial T}{\partial x} = k \frac{\partial^2 T}{\partial z^2} + \eta (\gamma) (\gamma)^2 \quad (2.70)$$

These equations are solved analytically using the WKB-J method. For the slit flow problem and the tube flow problem, the lowest eigenvalues, which will be the least accurate, obtained by the WKB-J method are in good agreement (10% error in the worst case) with numerical results. The higher eigenvalues are practically indistinguishable from the numerical values.

2.3.6 Heat Transfer to Non-Newtonian Fluids Considering Natural Convection.

In forced convection heat transfer problems, there are situations where the natural convection effects are significant. For the case of Newtonian fluids, the presence of natural convection may increase the rate of heat transfer by a factor of 3-4. This effect has been examined by Colburn(1933), Martinelli and Boelter(1962), McComas and Eckert(1966), Shannon and Depew (1969), and Pigford(1955). The natural convection correction term is the group $(GrPr(D/L))$, which is added to the forced convection group. Jackson, Spurlock and Purdey (1961) were the first to discard the factor (D/L) from the natural convection group, based on experimental data for flow in horizontal tubes. In addition to natural convection, there is also viscosity variation with temperature. This causes velocity profile distortion and has been

considered by Sieder-Tate by including the bulk-wall viscosity ratio. Oliver (1962) investigated the effects of natural convection and radial viscosity variation in an experimental study of laminar heat transfer to water, glycerol, and ethyl alcohol in a horizontal tube, with constant temperature at the wall. He concluded that the natural convection effects are independent of D/L . His relationship is expressed as

$$\left(\frac{h_{av}D}{k}\right) \left(\frac{\mu_w}{\mu_b}\right)^{0.75} = 1.75 [Gz_b + 0.0083 (Gr_b Pr_b)^{0.75}]^{1/3} \quad (2.71)$$

In the case of non-Newtonian fluids, Metzner and Gluck (1960) have used the Eubank and Proctor (1951) relationship to correlate data on ammonium alginate ($n=0.5$), apple sauce ($n=0.65$) and banana puree ($n=0.46$). For conditions of constant wall temperature, their final correlation is

$$\frac{h_{av}D}{k\delta^{1/3}} \left(\frac{\mu_{eff_v}}{\mu_{eff_b}}\right)^{0.14} = 1.75 [Gz_b + 12.6 (Gr_w Pr_w D/L)^{0.4}]^{1/3} \quad (2.72)$$

Oliver and Jensen (1964) correlated their data on pseudoplastic fluids in the following form

$$Nu_b = 1.75 \left(\frac{\mu_{eff_b}}{\mu_{eff_v}}\right)^{0.14} [Gz_b + 0.0083 (Gr_w Pr_w)^{0.75}]^{1/3} \quad (2.73)$$

and suggested that the Metzner-Gluck correlation over-corrected for natural convection at large temperature differences.

Mahalingam et al. (1975) correlated their data on Newtonian fluids using these equations

$$Nu_b \left(\frac{\mu_w}{\mu_b} \right)^{0.14} = 1.418 [Gz_b + 12.6 (Gr_w Pr_w D/L)^{0.40}]^{1/3} \quad (2.74)$$

$$Nu_b \left(\frac{\mu_w}{\mu_b} \right)^{0.14} = 1.418 [Gz_b + 0.0083 (Gr_w Pr_w)^{0.75}]^{1/3} \quad (2.75)$$

Equation (2.75) which does not include the D/L term is, however, more successful in correlating the data, if the constant term is modified to 1.50. The success of eq.(2.75) also indicates the insignificance of D/L ratio and is similar to the observations of Oliver and Jensen, eq.(2.73). The criterion for the onset of natural convection effects is the ratio Gr/Re. This ratio expresses the buoyancy forces in relation to inertia forces. Based on the results of Mahalingam et al(1975), the criteria may be expressed as:

$$Gr/Re > 2.0$$

$$Gr/Re^2 > 30 \times 10^{-4}$$

They also correlated the data on non-Newtonian pseudoplastic fluids considering natural convection using the following relations

$$Nu_b \left(\frac{K_w}{K_b} \right)^{0.14} \frac{1}{\Delta_w^{1/3}} = 1.46 [Gz_b + 12.6 (Gr_w Pr_w D/L)^{0.4}]^{1/3} \quad (2.76)$$

$$Nu_b \left(\frac{K_w}{K_b} \right)^{0.14} \frac{1}{\Delta_w^{1/3}} = 1.46 [Gz_b + 0.0083 (Gr_w Pr_w)^{0.75}]^{1/3} \quad (2.77)$$

Equation (2.77) is seen to fit the data better than eq.(2.76). As in the Newtonian case, the criteria for the significance of

natural convection are

$$Gr/Re > 1.0$$

$$Gr/Re^2 > 7.0 \times 10^{-4}$$

2.3.7 Empirical Correlations of Laminar flow Heat transfer Data of Non-Newtonian Fluids.

Joshi and Bergles (1981) studied the problem of heat transfer to laminar flow pseudoplastic fluids in circular tubes with constant heat flux. A correlation of these results includes temperature-dependent K effects for entrance and fully developed regions. In formulating the equation the following assumptions were made:

1. The flow is steady and axisymmetric.
2. Axial conduction is negligible.
3. Free convection effects are negligible.
4. The usual boundary layer approximations are valid: since pseudoplastic fluids exhibit flat velocity and temperature profiles near the tube centerline and sharp profile gradients near the wall.
5. K is temperature-dependent according to the constitutive equation of most industrial fluids as

$$K = ae^{-bT} \quad (2.78)$$

With these assumptions, the general governing equations in cylindrical coordinates reduce to

Continuity:

$$\frac{\partial}{\partial x}(\rho u r) + \frac{\partial}{\partial r}(\rho v r) = 0 \quad (2.79)$$

Momentum (x-direction):

$$\rho u \frac{\partial u}{\partial x} + \rho v \frac{\partial u}{\partial r} = -\frac{dp}{dx} - \frac{1}{r} \frac{\partial}{\partial r} (r\tau) \quad (2.80)$$

Energy:

$$\rho u C_p \frac{\partial T}{\partial x} + \rho v C_p \frac{\partial T}{\partial r} = \frac{k}{r} \frac{\partial}{\partial r} \left(r \frac{\partial T}{\partial r} \right) + \mu_a \left(\frac{\partial u}{\partial r} \right)^2 \quad (2.81)$$

Far away from the tube inlet, fully developed velocity and temperature profiles exist. In this region, $v = 0$, $\partial u / \partial x = 0$, and $\partial T / \partial x = dT / dx$. With these simplifications, eqs.(2.79) to (2.81) reduce to the fully developed governing equations.

The numerical method utilizes a form of DuFort-Frankel differencing which results in a scheme for which the axial step size is not severely constrained due to stability consideration of the axial pressure gradient for each axial step. This is accomplished by numerically integrating the finite-difference form of the axial momentum equation over the tube cross-section and employing the overall conservation of mass constraint to eliminate the integral of the axial velocity from the equation. The pressure gradient can then be evaluated explicitly.

The correlation strategy was to correlate various property effects in the entrance region and in the fully developed region. An interpolation formula was then devised to correlate both regions with a single equation. The following general relation is proposed for the thermal entrance region:

$$\left(\frac{Nu_{vp,n}}{Nu_{cp,n}} \right)_e = \left(\frac{K}{K_w} \right)^m \quad (2.82)$$

where $m = 0.58 - 0.44n$.

For the fully developed region, the data are correlated as

$$\frac{Nu_{vp,n}}{Nu_{cp,n}} = 1 + (0.12392 - 0.0542n)\sqrt{\Delta\Gamma} - (0.010133 - 0.0068n)(\sqrt{\Delta\Gamma})^2 \quad (2.83)$$

This equation is valid up to $\sqrt{\Delta\Gamma} = 6$, which covers the range of normally encountered heat fluxes.

The above two asymptotic correlations were combined by the interpolation technique suggested by Churchill and Usagi (1972) as

$$Nu_{vp,n} = Nu_{cp,n-1} \frac{(Nu_{cp,n}/Nu_{cp,n=1})}{\frac{1}{(Nu_{vp,n}/Nu_{cp,n})_\infty} \left(\left[\frac{(Nu_{vp,n}/Nu_{cp,n})_\infty}{(Nu_{vp,n}/Nu_{cp,n})_e} \right]^{30} + 1 \right)^{1/30}} \quad (2.84)$$

This equation represents an accurate, explicit correlation of the numerical predictions, which is very convenient for design purposes.

No experimental data are available in the fully developed region and in the transition region from the thermal entrance region to the fully developed region. Data are needed in these regions to examine the accuracy of this correlation.

2.3.8 Heat Transfer to Laminar Non-Newtonian Flow in Curved Tubes.

Curved tubes are often used in different types of process equipment. The study of flow and heat transfer in such tubes is required for the proper design of the corresponding equipment. Although the Newtonian flow in curved tube has been extensively analyzed, there appears to be little theoretical work on the non-Newtonian flow in curved tubes.

Hsu and Patankar (1982) for the first time performed a numerical solutions of the differential equations that govern the laminar fully developed velocity and temperature fields of a power law fluid flowing in a curved tube. Results for the velocity and temperature fields, the friction factor, and the Nusselt number are presented for different values of the Dean number ($Re(R/R_c)^{1/2}$), the Prandtl number, and the power law index. For large radius of curvature, the non-Newtonian flow is governed by the power law index and by the modified Dean number. The heat transfer is additionally governed by the Prandtl number. The axial velocity profiles are distorted by the centrifugal force, although they tend to be flatter for lower values of the power law index. The secondary flow in the tube cross section exhibits an interesting boundary layer behavior, especially at high Dean numbers. The friction factor increases with the Dean number and also with the power law index.

The overall heat transfer coefficient also increases with the Dean number. Indeed, the increase in the heat transfer coefficient is more pronounced than that in the friction factor. Thus a curved tube appears to be an attractive device for heat transfer enhancement for all the values of the power law index considered.

The local heat transfer coefficient varies significantly over the circumference of the tube for low Prandtl numbers. The heat transfer coefficient becomes more uniform as the Prandtl number increases.

CHAPTER-III

STATEMENT OF THE OBJECTIVES

The objective of this work is to carry out a numerical analysis of heat transfer to time-independent non-Newtonian fluids considering viscous dissipation and temperature dependence of the related physical and thermal properties.

The specific objectives are:

1. To predict the temperature and velocity profiles for non-Newtonian fluids during heat transfer in laminar flow in tubes with constant wall temperature.
2. To predict the heat transfer rates for non-Newtonian fluids with the same condition as mentioned above.

The fluids considered are:

- * 1.00% Cellofas B-10
- * 0.50% Cellofas B-300
- * 0.15% Cellofas B-3500
- * 0.27% Cellofas B-3500
- * 0.40% Cellofas B-3500

"Cellofas" is the trade name of Sodium Carboxymehtyl Cellulose produced by ICI(UK) and "B-10" etc. indicate different grades based on molecular weight.

Rheological data of these fluids obey the power law model. Consistency index, K , depends on temperature and a polynomial expression has been used to describe this effect. The temperature dependent density, heat capacity and thermal conductivity data of water are used in the analysis because the solutions are dilute.

CHAPTER-IV

FORMULATION OF THE PROBLEM

This work is concerned with heat transfer to time-independent non-Newtonian fluids in steady laminar flow in straight tubes. The rheological equation used in this work is the well known power law, viz;

$$\tau_{rx} = K \left(-\frac{du}{dr} \right)^n \quad (4.1)$$

where τ_{rx} is the shear stress, n is a temperature-independent exponent which is less than unity in the present work and consistency index, K , is temperature-dependent according to the equation given below:

$$\log_{10} K(T) = A + BT + CT^2 + \dots \quad (4.2)$$

This relationship is superior to the analytical forms previously used (10,11) or the hyperbolic relationships(20).

The problem of heat transfer in laminar flow in straight tubes is considered for the boundary condition of constant wall temperature for heating (Fig. 4.1). The other conditions are:

1. The velocity profile at the inlet of heat transfer section is fully developed.
2. The temperature at the inlet of heat transfer section is uniform at T_1 .

3. The flow is laminar and steady.
4. The axial velocity u_x , hereafter designated as u , is only function of r while u_r and u_θ are zero.
5. The fluid density, ρ , thermal conductivity, k , and heat capacity, C_p , are temperature dependent. These are water properties as the solutions are dilute.
6. The radial velocity profile within the heated section will change as a result of changes in the rheological properties with temperature.

For the assumptions stated above, the equations of continuity, momentum and energy for this problem in cylindrical coordinates are:

Continuity :

$$\frac{\partial}{\partial x} (\rho u) = 0 \quad (4.3)$$

Momentum :

$$-\frac{\partial P}{\partial x} = \frac{1}{r} \frac{\partial}{\partial r} (r \tau_{rx}) \quad (4.4)$$

Energy :

$$\rho C_p u \frac{\partial T}{\partial x} = k \left[\frac{1}{r} \frac{\partial}{\partial r} \left(r \frac{\partial T}{\partial r} \right) + \frac{\partial^2 T}{\partial x^2} \right] - \tau_{rx} \frac{\partial u}{\partial r} \quad (4.5)$$

The expression for shear stress, τ_{rx} , is given in eq.(4.1).

Boundary conditions for eq.(4.2) and (4.3) are:

B.C.1: At $r = 0$ $\tau_{rx} = 0$

B.C.2: At $r = R$ $u_r = 0$ (no slip at the wall)

Boundary conditions for eq.(4.5) are:

B.C.1: At $x = 0$ and at any r ; $T = T_i$

B.C.2 and 3: At $x \geq 0$ and $r = R$; $T = T_w$

Equations (4.3) to (4.5) are used in the present study. The numerical methodology used for solving these equations are given in chapter VI.

Definition of Nusselt numbers

It is useful to represent the results of heat transfer calculations by plotting Nusselt numbers against the Graetz numbers.

Mean Nusselt Number: For constant wall temperature, a mean Nusselt number may be defined as:

$$Nu_m = h_m D / k \quad (4.6)$$

The mean heat transfer coefficient, h_m , for a tube of length x is defined in terms of the terminal temperatures as

$$h_m = \frac{WC_p (T_0 - T_i)}{\pi D x (T_w - \frac{1}{2} (T_i + T_0))} \quad (4.7)$$

where T_0 is the bulk outlet (i.e. cup mixing) temperature, and W is the fluid mass flow rate. Further we have

$$WC_p(T_0 - T_i) = 2\pi C_p \rho \int_0^R ru(T - T_i) dr \quad (4.8)$$

hence,

$$Nu_m = \frac{2\rho C_p \int_0^R ru(T - T_i) dr}{kx(T_w - \frac{1}{2}(T_i + T_0))} \quad (4.9)$$

Local Nusselt Number: Local Nusselt number for flow through a tube with constant wall temperature can be defined as:

$$Nu_x = \frac{h_x D}{k} \quad (4.10)$$

The local convection heat transfer coefficient, h_x , is defined as

$$h_x = -\frac{k}{T_w - T_b} \left(\frac{\partial T}{\partial r} \right)_w \quad (4.11)$$

hence,

$$Nu_x = -\frac{D}{T_w - T_b} \left(\frac{\partial T}{\partial r} \right)_w \quad (4.12)$$

where T_b is the bulk temperature at x .

CHAPTER-V

COMPUTER PROGRAM

5.1 Description

The program used in this work is TEACH-T, a general computer program for solving conservation equations for heat, mass, momentum, etc. by finite difference method. The program is written by A.D. Gosman and F.J.K. Ideriah (1976).

TEACH-T is a general program for steady, 2-dimensional flows. The flow may be laminar or turbulent, and of variable properties. It can be made to handle compressible flows. It should be noted that the program can conveniently be used for unsteady, 1-dimensional cases, and it can easily be extended to encompass 3-D flows. The program is for flows which can be represented in Cartesian or cylindrical coordinates, and the grid may be non-uniform.

5.2 Contents of the Program.

There are six general subroutines relevant for any particular variable to be solved : CONTRO, INIT, PROPS, PROMOD, LISOLV and PRINT. In addition, there is a major set of CALC ϕ subroutines, where ϕ is the particular variable solved. The inter-connection between the various subroutines is shown in Figure 5.1.

The functions of different subroutines are described bellow:

CONTRO: Overall control is exerted by the main subroutine CONTRO.

The functions of this subroutine are

1. Specification of grid, control parameters, constants of problem, etc.
2. Calculation of grid parameters, initialization of arrays (via INIT), prescription of fixed boundary values, preliminary output, etc.
3. Initialization and control of iteration. It also gives intermediate outputs.
4. Final operations, like calculation of shear stress coefficient, normalization of profiles, etc., as well as the final output, are carried out.

CALC ϕ : These subroutines make the main calculations of the finite difference equations for each variable ϕ . Functions are

1. Calculation of the coefficients over the entire field.
2. Modification of the sources and boundary coefficients to suit the particular problem through PROMOD.
3. Assemble all the coefficients and also caculates the residual sources.
4. Finally equations are solved by LBL(line-by-line) procedure through LISOLV.

INIT : It performs initialization tasks. Functions are

1. Calculation of grid co-ordinates, inter-node distances, cell dimensions and so on.
2. Initialization of the dependent variables. Specifically, the starting variable fields (except density and viscosity)

are set to zero.

PROPS : Fluid properties (viscosity, density, etc.) based on user-supplied formula are calculated by this subroutine.

PROMOD : Modifications of sources and boundary conditions are made in PROMOD.

LISOLV : This subroutine performs LBL (line-by-line) iteration.

PRINT : Provides output of dependent variable arrays.

INIT, LISOLV, PRINT, and the set of CALC ϕ subroutines are independent of problem type. Modifications to suit individual problems are required only in CONTRO, PROMOD, and in rare instances PROPS.

5.3 Verification of the Program.

The computer program used here is tailored by modifying TEACH-T which can solve flow and heat transfer problems for Newtonian fluids. A number of tests were carried out by solving a variety of flow and heat transfer problems to assess the usefulness of this tailored program. During the test runs, the flow condition was always laminar.

The cases examined during the test runs include :

- a. developing laminar flow for a Newtonian fluid with flat velocity profile at the inlet,
- b. developing laminar flow for a power law fluid with flat velocity profile at the inlet,
- c. classical Graetz problem,

- d. heat transfer with temperature dependent viscosity for Newtonian fluid, and
- e. heat transfer with temperature dependent K for a power law fluid.

Computed results were graphically presented along with available analytical solutions and experimental data. Figures 5.2 and 5.3 show the velocity profiles for Newtonian and non-Newtonian fluids in the developing region respectively. Figure 5.4 shows the Graetz problem in the form of a plot of Nu_x (local Nusselt number) against $Pe/(x/D)$. Figures 5.5 and 5.6 show the plot of velocity profiles for both Newtonian and non-Newtonian fluids for the case of heating respectively. Similarly figures 5.7 and 5.8 show the plot of temperature profiles.

Computed results are found to agree with the analytical solution and available data. The deviations observed in case of available data are likely due to error in regression analysis to fit viscosity and consistency index, K data and size of the grids used for computation.

CHAPTER-VI

NUMERICAL SOLUTION

6.1 Introduction

This chapter represents the numerical solution procedure of the governing differential equations presented in chapter IV, i.e. eq.(4.3) to (4.5). The general form of the governing differential equations is:

$$\frac{1}{r} \left[\frac{\partial}{\partial x} (\rho r u \phi) - \frac{\partial}{\partial x} (r \Gamma \frac{\partial \phi}{\partial x}) - \frac{\partial}{\partial r} (r \Gamma \frac{\partial \phi}{\partial r}) \right] = S_{\phi} \quad (6.1)$$

where, ϕ = variable of interest

= unity for continuity

= u for momentum

= T for energy

$$\Gamma = \mu_{eff} (=K \left| -\frac{du}{dr} \right|^{n-1}) \text{ for momentum}$$

= k/C_p for energy

S_{ϕ} = source or generation term

= zero for continuity (mass can't be generated)

= $-\frac{\partial P}{\partial x}$ for momentum

= $-\tau \frac{\partial u}{\partial r} / C_p$ for energy

6.2 The Method of Discretization.

The governing differential equations can be discretized in many ways. An overview of the discretization method for the numerical solution of the fluid flow problems is given by Patankar(1980). In the present study the finite volume approach, as described by Gosman et al (1969) and others, is adopted. In this approach, the governing differential equations are discretized by integrating them over a finite number of control volumes or computational cells, into which the solution domain are divided. A typical computational cell is shown in Figure 6.1. Typical discretized transport equation (e.g. eq. 6.1) will take the following quasilinear form.

$$(a_p - b)\phi_p = \sum a_{nb}\phi_{nb} + c \quad (6.2)$$

where, the a_{nb} are coefficients multiplying the values of ϕ at the neighbouring nodes surrounding the central node P. The number of neighbour depends on the interpolation practice or differencing scheme used. The a_{nb} contains combined convection and diffusion contribution at the control volume faces, i.e.

$$a_{nb} = a_{nb}^C + a_{nb}^D \quad (6.3)$$

a_p is the coefficient of ϕ_p given by

$$a_p = \sum a_{nb} \quad (6.4)$$

and, b and c are obtained by linearizing the source term as follows.

The source term, right hand term of eq.(6.1), is evaluated by integrating the volumetric source s_ϕ over the volume of the computational cell and expressed as

$$-\int_V s_\phi dv = b\phi_p + c \quad (6.5)$$

where, c stands for the constant part of the source term where b is the coefficient of ϕ_p and often a function of ϕ_p .

Since the direct solution methods (i.e. matrix inversion) require very large computer storage and time and since the governing transport equations are non-linear, (the discretized governing transport equations are seemingly linear but a_p being the function of ϕ_p makes them virtually nonlinear) the discretized equations are solved using the SIMPLE (Semi-Implicit Method for Pressure-Linked Equations) algorithm of Patankar and Spalding(1972) by repeated sweeps of a line-by-line application of the Tri-Diagonal Matrix Algorithm (TDMA) (Patankar[1980]).

6.3 Differencing Scheme.

Central differencing scheme (CDS) is used to describe the diffusion terms in the present study. If a piece-wise linear profile of ϕ is assumed between P and E (Figure 6.6), the cell face value ϕ_e is given by

$$\phi_e = \phi_E f_p + \phi_P (1 - f_p) \quad (6.6)$$

where f_p is a linear interpolation factor defined as

$$f_p = \frac{\Delta x_p}{\Delta x_p + \Delta x_E} \quad (6.7)$$

Here Δx_p and Δx_E are the cell dimensions along x coordinate for P and E cells (Figures 6.1 and 6.6).

In this scheme a_e and a_n are always negative and if the convection process dominates this can cause the whole coefficient a_{nb} to assume negative value. As a result the Scarborough criteria fails and produce unbounded solutions (Spalding[1972], Rahtby and Torrance [1974]). At high Peclet number the CDS also violates the transportive property by employing downstream nodes in expressions given above. For These reasons application of CDS is limited to low Reynolds number problems.

Upwind differencing scheme(UDS) is used to discretize convection terms in the present study. In the UDS convection term is calculated assuming that the value of ϕ at an interface (see Figure 6.7) is equal to the value of ϕ at the grid point of the upwind side of the faces. Thus

$$\begin{aligned} \phi_e &= \phi_p \quad \text{if } f_e > 0 \\ &= \phi_E \quad \text{if } f_e < 0 \end{aligned}$$

In this scheme all the coefficients contributing to a_p are always non-negative. As a result Scarborough criteria is satisfied. UDS also satisfies the property of transportiveness, and thus the

boundness of the solution is guaranteed.

In terms of Taylor Series Truncation Error(TSTE) analysis, the UDS is first order approximate.

6.4 Solution Procedure

6.4.1 Grid and Variable Arrangement

In the present study, the numerical solution is accomplished on a variably spaced staggered mesh [see for example Caretto et al (1972) and Patankar (1980)], in which the scalar quantities (including pressure, density, viscosity, thermal conductivity) are defined at the centre and the normal velocities at cell faces, as shown in Figure 6.5. It has the advantage that the variables u , v , p are stored such that the pressure gradients which drive the velocities u and v are easy to evaluate and moreover the velocities are located where they are needed for the calculation of convective flux.

6.4.2 Calculation of Pressure

The pressure gradient forming part of the source term in the momentum equation is to be obtained before the velocity field is calculated and it is the pressure field through which the continuity equation is satisfied.

The SIMPLE method of Patankar and Spalding(1972) is used in the present study to obtain pressure.

6.5 Boundary Conditions

The forms of boundary conditions encountered in the present study and their implementations are described below.

- (i) Inlet Boundaries : Fully developed velocity profile and uniform temperature are specified.
- (ii) Outlet Boundaries : The gradients of all variables in the axial direction are zero, i.e., $\frac{d\phi}{dx}=0$.
- (iii) Wall Boundary : at the solid wall velocities are set to zero, and constant temperature is specified.
- (iv) Symmetry-axis Boundary : The gradients of all variables are zero, i.e., $\frac{d\phi}{dr}=0$, at the axis of symmetry.

6.6 Solution Algorithm

The important operation in the order of their execution are

- (i) Initialise all field values by an initial guess.
- (ii) Solve momentum equations and obtain u. The u velocity at this stage is not accurate because it is obtained with guessed pressure field.
- (iii) Solve the continuity equation to obtain the pressure p. This pressure field satisfies both the momentum and continuity equation.
- (iv) Calculate correct u from the values obtained in step(ii) and newly calculated pressure p.

- (v) Solve the discretized equation for other variables if they influence the flow field through fluid properties, source terms etc.
- (vi) Treat the corrected pressure p as a new guessed pressure and return to step (ii) and repeat the whole procedure until a converged solution is obtained.

In the present study, the convergence criterion is that the sum of the normalised absolute residuals at all computational nodes, defined

$$R_\phi^i = \sum_N |(a_p^i - b^{(i-1)})\phi_p^{(i-1)} - \sum a_{nb}^i \phi_{nb}^{(i-1)} - c^{(i-1)}| / N_f \quad (6.8)$$

should fall below a specified level $R_\phi^i < 10^{-3}$. Here N is the total number of nodes, r the iteration counter and N_f the normalization factor.

CHAPTER-VII

RESULTS AND DISCUSSIONS

7.1 Introduction

In this chapter, the results of the numerical prediction of laminar heat transfer with time-independent non-Newtonian fluids in straight tubes considering viscous dissipation are presented. Cellofas (trade name of Sodium Carboxymethyl Cellulose) of different grades and concentrations are used as working fluid in the present work. Rheological data of these fluids obey the power law model. Consistency index, K , is a strong function of temperature. A polynomial expression has been used to describe this effect. As the solutions are dilute, density, heat capacity and thermal conductivity of water are used in the analysis.

7.2 Domain of Solution and Computational Grid

The solution domain shown in Figure A.1 is bounded by the inlet plane, exit plane, solid wall and the axis of symmetry. The entire computational domain is divided into 20 vertical grid lines and 20 horizontal grid lines. The grid distribution in the calculation domain is uniform in the x -direction and non-uniform in the y -direction. The mesh is contracted near the tube wall region all over the whole calculation domain such that the ratio between the two successive steps in space is constant and equal to .90 .

7.3 Grid Independence Test

To obtain a solution independent of the number and spacing of the grid nodes, grid dependence test was performed. The test was done at Reynolds number 126 for two grid sizes: 16X16 and 20X20. Each time close spacing was maintained near the tube wall, where rapid changes of the flow variables occur. For this test, predicted u-velocity and T-profiles are compared at various axial distances for two different grid sizes. The predictions for both the grid sizes remain the same and hence the solution is independent for any grid sizes.

7.4 Presentation of Results

7.4.1 Physical Property Used

In the present work five different non-Newtonian fluids are used. These are cellofas of different grades and concentration such as:

- 1.00% cellofas B-10
- 0.50% cellofas B-300
- 0.15% cellofas B-3500
- 0.27% cellofas B-3500
- 0.40% cellofas B-3500

As the solutions are very dilute, physical properties such as density, thermal conductivity and heat capacity of water are used in the calculation. Temperature dependent equations are used for these properties. The equations are:

Density:

$$\rho = 1000.186 + 8.77 \times 10^{-3} T - 5.98 \times 10^{-5} T^2 + 2.15 \times 10^{-5} T^3 - 4.50 \times 10^{-8} T^4$$

Thermal Conductivity:

$$k = .5529 + 2.48 \times 10^{-3} T - 1.47 \times 10^{-5} T^2 + 2.58 \times 10^{-8} T^3 + 6.77 \times 10^{-12} T^4$$

Heat Capacity:

$$C_p = 4217.07 - 2.609 T + 4.99 \times 10^{-2} T^2 - 3.46 \times 10^{-4} T^3 + 1.03 \times 10^{-6} T^4$$

The rheological data were taken from the work of Quader and Wilkinson (59), see Table 7.1. The flow behavior index, n , is independent of temperature, whereas the consistency index, K , is a strong function of temperature. K can be expressed as a polynomial of the form

$$\log_{10} K = a + bT + cT^2 \quad (4.2)$$

where K is in M.K.S unit and T is in $^{\circ}\text{C}$. The values of constants a , b and c are found by regression analysis and are given in Table 7.2.

7.4.2 Variables/Parameters Used in the Presentation

The computed results are presented graphically in Figures 7.1-7.34 and the main features are discussed in the subsequent section. Variables/parameters used in the presentation are described below.

TABLE 7.1

The values of consistency index, K and flow behavior index, n.

Temp. °C	n	K (C.G.S. units)
1.00% Cellofas B-10		
8.5	1.000	0.099
16.0	1.000	0.076
27.5	1.000	0.0525
0.50% Cellofas B-300		
21.0	0.835	0.558
40.8	0.835	0.335
58.5	0.835	0.218
0.15% Cellofas B-3500		
21.0	0.850	0.241
40.8	0.850	0.158
58.9	0.850	0.101
0.27% Cellofas B-3500		
19.0	0.705	1.085
43.8	0.705	0.635
58.5	0.705	0.410
0.40% Cellofas B-3500		
17.8	0.64	3.04
41.8	0.64	1.80
58.3	0.64	1.27

TABLE 7.2

Values of constants of eq.(4.2)

a	$b \times 10^3$	$c \times 10^6$
1.00% Cellofas B-10		
-1.8646	-17.04	70.52
0.50% Cellofas B-300		
-1.0113	-11.70	8.25
0.15% Cellofas B-3500		
-1.4569	-6.85	-38.96
0.27% Cellofas B-3500		
-0.86096	-3.75	-89.69
0.40% Cellofas B-3500		
-.34275	-9.93	7.49

88261

R' : Dimensionless radius, r/R

U : Dimensionless velocity, u/u_{av}

Theta: Dimensionless temperature, $(T-T_i)/T_i$

T_w/T_i : Ratio of wall temperature and inlet fluid temperature, $T_w/T_i > 1$ for heating

Gz : Graetz number, WC_p/kx

Gz' : Another form of Graetz number, $(4/\pi)Gz = Pe/(x/D)$

Nu_x : Local Nusselt number, $h_x D/k = -\frac{D}{T_w - T_b} \left(\frac{\partial T}{\partial r} \right)_w$

Nu_m : Mean Nusselt number, $Nu_m = \frac{2\rho C_p \int_0^R ru(T-T_i)dr}{kx(T_w - \frac{1}{2}(T_i + T_0))}$

Br : Brinkmann number, $\frac{u_{av}^{n+1} K_i}{kT_i R^{n-1}}$

7.4.3 Description of the Graphs

Velocity profiles:

Figures 7.1-7.11 represent the velocity profiles, i.e. dimensionless velocity as a function of dimensionless radius. In Figures 7.1a-c parameter is concentration or pseudoplasticity, n . These are plots at a particular dimensionless axial distance, i.e. Graetz number, Gz , for different temperature ratios T_w/T_i .

Figures 7.2-7.6 represent the velocity profiles for individual cellofas at a particular axial distance. T_w/T_i is the parameter of these plots. Figures 7.7-7.11 represent the velocity profiles for different types of cellofas at a particular temperature ratio. Dimensionless axial distance, Gz , is the parameter of these plots.

Temperature profiles:

Figures 7.12-7.22 represent the temperature profiles, i.e. dimensionless temperature, θ , as a function of dimensionless radial distance, R^* . Figures 7.12a-c represent the temperature profiles at particular Graetz number, Gz , for different temperature ratios, T_w/T_i . Concentration of the solutions or pseudoplasticity, n , is the parameters of these plots.

88262
Figures 7.13-7.17 represent the temperature profiles for individual cellofas at a particular axial distance. Temperature ratio, T_w/T_i , is the parameter of these plots. Figures 7.18-7.22 represent the temperature profiles for individual fluids at constant temperature ratio, $T_w/T_i=1.13$. Here Graetz number, Gz , is the parameter.

Heat transfer rates:

Heat transfer data have been evaluated in the form of both local Nusselt number, Nu_x , and mean Nusselt number, Nu_m . Figures 7.23-7.28 represent the local Nusselt number as a function of Gz' or $Pe/(x/D)$. Figure 7.23 is a plot for different types of cellofas at constant temperature ratio, $T_w/T_i=1.13$. Here concentration of the solutions or pseudoplasticity, n , or Brinkmann number, BR , is the parameter. Figures 7.24-7.28 represent Nu_x as a function of $Pe/(x/D)$ for individual fluids. Temperature ratio, T_w/T_i and Brinkmann number, Br , are the parameters.

Figures 7.29-7.33 show the plots of mean Nusselt number, Nu_m , as a function of Graetz number, Gz , for individual fluids. T_w/T_i and

Br are the parameters for these plots. Figure 7.34 show the plot of Nu_w vs Gz for the heating of B-3500 with different concentration at constant temperature ratio, $T_w/T_i=1.13$. Pseudoplasticity, n , and Brinkmann number, Br, are used as the parameters.

7.5 Discussion of Results.

7.5.1 Velocity Profiles

Effect of Pseudoplasticity, n , on Velocity Profile:

Figures 7.1a-c show the velocity profiles for five cellofas solutions for different T_w/T_i at constant Gz. It is seen that at a given value of T_w/T_i , as n decreases, the velocity profile becomes flatter, i.e. velocity gradients are increased in the tube wall region and decreased near the tube centre.

Effect of T_w/T_i on Velocity Profile:

Figures 7.2-7.6 show the velocity profiles for each of five cellofas solutions at different T_w/T_i . It can be seen that for particular fluid at a given Graetz number, Gz, as T_w/T_i increases, the velocity profile becomes flatter, i.e. velocity gradients are increased near the tube wall region and decreased near the tube centre. The increase in temperature in the wall region decreases the fluid consistency. This leads to increased velocity gradients near the wall.

Effect of Gz on Velocity Profiles:

Development of velocity profiles for heating of Cellofas solutions are shown in Figures 7.7-7.11. It is seen that at a given temperature ratio, as the Graetz number decreases, the velocity profile becomes flatter, i.e. velocity gradients are increased in the tube wall region and decreased near the tube centre. For a particular temperature, as the Graetz number decreases, the temperature gradients near the wall decreases, Figure 7.18, i.e. the temperature of the streams near the tube wall is high in comparison to the streams near the tube centre. At higher temperature fluid consistency decreases, which leads to increased velocity gradients near the wall at low Graetz number.

7.5.2 Temperature Profiles

Effect of Pseudoplasticity, n , on Temperature Profile:

Figures 7.12a-c show the temperature profiles for five cellofas solutions for different T_w/T_i at constant Gz . At low temperature ratio, i.e. at $T_w/T_i=1.068$, temperature profiles remain almost same. At higher temperature ratio, it is seen that at a given dimensionless axial distance, i.e. the Graetz number, temperature gradients near the wall increase as the value of n decreases, Figures 7.12b-c.

Effect of T_w/T_i on Temperature profile :

Temperature profiles for individual fluid at different T_w/T_i are shown in Figures 7.13-7.17. It is seen and obvious that at a

given Graetz number, temperature gradients are high for higher temperature ratio near the wall. As temperature increases, consistency index of fluid decreases, which leads to increased temperature gradient.

Effect of Graetz Number, Gz , on Temperature Profile:

Figures 7.18-7.22 present the temperature profiles for individual fluid at different Graetz number, Gz . It is clear that for any of five fluids, as the Graetz number increases, the temperature gradients near the wall increase, i.e. at entrance region temperature gradients near the tube wall are higher than that of the region away from the entrance. For this reason, at the entrance region, i.e. at large Graetz number, heat transfer rate is high, Figure 7.23.

7.5.3 Heat Transfer Rates.

Heat transfer data have been evaluated in the form of both local Nusselt number, Nu_x , and mean Nusselt number, Nu_m . These are shown in Figures 7.23-7.34.

Effect of Pseudoplasticity and Viscous Dissipation on Heat Transfer:

Local Nusselt numbers for different types of cellofas as a function of Gz' are shown in Figure 7.23. It is seen from the figure that at a given temperature, as pseudoplasticity increases, i.e. n decreases, rate of heat transfer increases slightly. It is also seen that Brinkmann number, Br , i.e. shear

heating effect increases with the increase of pseudoplasticity. As the solutions are not so viscous, the value of Br is small and the viscous dissipation effect is also small. As pseudoplasticity increases, velocity gradients near the tube wall region increase slightly, Figure 7.1b, which enhances the heat transfer rate slightly by the increase in Nu_x , Figure 7.23.

Figure 7.34 shows Nu_m as a function of Gz for the heating of Cellofas B-3500 with different concentration. It is seen that at a constant temperature ratio, as n decreases, Br increases, which results in high heat transfer at large Gz , i.e. near the entrance. At a constant temperature ratio, velocity gradients near the tube wall region increase as the pseudoplasticity increases, i.e. n decreases. These increased velocity gradients result in high viscous dissipation. It is evident that consistency of fluid increases with the decrease of n , which results in high viscous dissipation.

Effect of Temperature Ratio on Heat Transfer:

Local Nusselt number for individual fluids at different temperature ratio are presented in Figures 7.24-7.28. It is clear from the figures that for any of five fluids, Nu_x or rate of heat transfer increases with the increase of temperature ratio. As the temperature increases, consistency of fluid decreases, which increases velocity gradients near the tube wall region. This results in high heat transfer at higher temperature ratio.

Mean Nusselt number as a function of Graetz number for individual fluid at different temperature ratio are presented in Figures 7.29-7.33. It is also seen that Nu_m or rate of average heat transfer increases with temperature ratio at large Graetz number but it remains same at very low Graetz number. At entrance region, i.e. at large Graetz number temperature gradients are high at higher temperature ratio and hence the higher rate of heat transfer. Velocity gradients are also high near the tube wall region at higher temperature ratio in the entrance region. This leads to high viscous dissipation and consequently high heat transfer. Far away from the entrance, i.e. at very small Graetz number, temperature profiles are fully developed and these remain same at different temperature ratio. For this reason heat transfer rates remain constant at low Graetz number for different temperature ratio.

Range of variables in the investigation are:

n : 0.64 - 1.0
Re : 0.88 - 24.0
Pr : 40 - 1300
Gz : 2 - 10000
Br : 4.0×10^{-8} - 1.74×10^{-6}
 T_w/T_f : 1.068 - 1.233

CHAPTER-VIII

CONCLUSIONS

This study of heat transfer with time-independent non-Newtonian fluids in laminar flow condition in tubes with constant wall temperature for heating leads to the following conclusions:

1. For a particular temperature ratio velocity profile becomes flatter as the pseudoplasticity increases, i.e. value of n decreases.
2. For a particular fluid, velocity profile also becomes flatter as the value of temperature ratio, T_w/T_i , increases.
3. The effect of pseudoplasticity on temperature profile is small. For a particular temperature ratio, T_w/T_i , temperature gradients near the wall increase slightly as the pseudoplasticity increases.
4. The effect of temperature ratio on temperature profile is significant. For a particular fluid, temperature gradients are high for higher temperature ratio near the wall.
5. Temperature profile is also a strong function of Graetz number, Gz . Temperature gradients near the wall increase markedly with the increase of Graetz number.

6. Effect of pseudoplasticity and viscous dissipation on heat transfer rate are interrelated. Viscous dissipation is a direct function of fluid consistency, K , and K increases with the pseudoplasticity. This combined effect is small because these fluids do not have large values for K . Heat transfer rate increases slightly with the increase of pseudoplasticity.
7. Effect of temperature ratio on heat transfer is significant at higher Graetz number. At low Graetz number effect is small.

CHAPTER-IX

SUGGESTIONS FOR FUTURE WORK

The scope of extension and development of the present study are given below:

1. The same prediction can be carried out with large number of fine grids which may produce more accurate results.
2. Similar study can be made in developing region.
3. Present work can be extended for the flow through concentric tubes, and also for the flow through helical tube.
4. The same prediction can be made for cooling with constant temperature at the tube wall.
5. Present work can be extended with constant heat flux at the tube wall both for heating and cooling.
6. Experimental measurements are required to verify the theoretical prediction.

REFERENCES

1. Acrivos, A., Shah, M. J. and Petersen, E. E., "Momentum and Heat Transfer in Laminar Boundary-Layer Flows of Non-Newtonian Fluids Past External Surfaces", *AIChE Journal*, 6, 312-317(1960).
2. Bassett, C. E. and Welty, J. R., "Non-Newtonian Heat Transfer in the Thermal Entrance Region of Uniformly Heated, Horizontal Pipes", *AIChE Journal*, 21, 699-706 (1975).
3. Bird, R. B. "Viscous Heat Effects in Extrusion of Molten Plastics", *SPE Journal*, 35-42, September(1955).
4. Brodkey, R. S. "Translating Terms for Non-Newtonian Flow", *Industrial and Engineering Chemistry*, 54, 45-48, September (1962).
5. Brown, J. M. and George, M. B., "Heat or Mass Transfer in a Fluid in Laminar Flow in a Circular or Flat Conduit", *AIChE Journal*, 6, 179-183(1960).
6. Broyer, E., Gutfinger, C., and Tadmor, Z., "Evaluating Flows of Non-Newtonian Fluids by the Method of Equivalent Newtonian Viscosity", *AIChE Journal*, 21, 198-200(1975).
7. Burka, M. K. "Solution of Stiff Ordinary Differential Equation by Decomposition and Orthogonal Collocation", *AIChE Journal*, 28, 11-20(1982).
8. Carey, G. E. and Finlayson, B. A., "Orthogonal Collocation in Finite Elements", *Chemical Engg. Sc.*, 30, 587-596 (1975).
9. Chapra, S. C. and Canale, R. P., "Numerical Methods for Engineers", McGraw-Hill International Editions, New York, 1990.
10. Christiansen, E. B. and Craig, Jr. S. E., "Heat Transfer to Pseudoplastic Fluids in Laminar Flow", *AIChE Journal*, 8, 154-160(1962).
11. Christiansen, E. B., Jensen, G. E. and Tao, F. S., "Laminar-flow Heat Transfer", *AIChE Journal*, 12, 1196-1202(1966).
12. Christiansen, E. B. and Kelsey, S. J., "Isothermal and non-isothermal, Laminar, Inelastic, Non-Newtonian Tube-entrance flow following a Contraction", *Chemical Engg. Sc.*, 28,1099-1113(1973).
13. Chu, J. C., Brown, F. and Burridge, K. G., "Heat Transfer Coefficients of Pseudo-Plastic Fluids", *Industrial and Engineering Chemistry*, 45, 1686-1696(1953).

14. Darby, R. and Rogers, B. A., "Non-Newtonian Viscous Properties of Methanol Suspensions", *AIChE Journal*, 26, 310-312(1980).
15. Dinh, S. M. and Armstrong, R. C., "Non-Isothermal Channel Flow of Non-Newtonian Fluids with Viscous Heating", *AIChE Journal*, 28, 294-301(1982).
16. Dodge, D. W. and Metzner, A. B., "Turbulent Flow of Non-Newtonian Systems", *AIChE Journal*, 5, 189-204(1959).
17. Douglas, J. Jr., and Peaceman, D. W., "Numerical Solution of Two-dimensional Heat-flow Problems", *AIChE Journal*, 1, 505-512(1955).
18. Edwards, M. F., Nellist, D. A. and Wilkinson, W. L., "Unsteady, Laminar Flows of Non-Newtonian Fluids in Pipes", *Chemical Engg. Sc.*, 27, 297-306(1972).
19. Faghri, M. and Welty, J. R., "Analysis of Heat Transfer for Laminar Power-law Pseudoplastic Fluids in a Tube with an Arbitrary Circumferential Wall Heat Flux", *AIChE Journal*, 23, 288-294(1977).
20. Forrest, G. and Wilkinson, W. L., "Laminar Heat Transfer to Temperature-Dependent Bingham Fluids in Tubes". *International Journal of Heat and Mass Transfer*, vol.16, p.2377-2391, Pergamon Press, 1973.
21. Friend, W. L. and Metzner, A. B., "Turbulent Heat Transfer Inside Tubes and the Analogy Among Heat, Mass, and Momentum Transfer", *AIChE Journal*, 4, 393-402(1958).
22. Gorla, R. S. R., "Unsteady Heat Transfer in Laminar Non-Newtonian Boundary Layer Over a Wedge", *AIChE Journal*, 28, 56-60(1982).
23. Gosman, A. D. and Ideriah, F. J. K., "TEACH-T: A General Computer Program for Two-dimensional, Turbulent, Recirculating Flows", Department of Mechanical Engineering, Imperial College London, S. W. 7, 1976.
24. Griskey, R. G. and Wiehe, I. A., "Heat Transfer to Molten Flowing Polymers", *AIChE Journal*, 12, 308-312(1966).
25. Gucuyener, H. I. and Mehmetoglu, T., "Flow of Yield-Pseudo-plastic Fluids Through a Concentric Annulus", *AIChE Journal*, 38, 1139-1143(1992).
26. Heeht, A. M., "Theoretical Non-Newtonian Pipe-flow Heat Transfer", *AIChE Journal*, 19, 197-199(1973).
27. Hildebrand, F. B. "Introduction to Numerical Analysis", McGraw-Hill, New York, 1956.

28. Hirai, E., "Theoretical Explanation of Heat Transfer in Laminar Region of Bingham Fluids", *AIChE Journal*, 5, 130-133(1959).
29. Hsu, C. F. and Patankar, S. V., "Analysis of Laminar Non-Newtonian Flow and Heat Transfer in Curved Tubes", *AIChE Journal*, 28, 610-616(1982).
30. Inman, R. M., "Experimental Study of Temperature Distribution in Laminar Tube Flow of a Fluid with Internal Heat Generation", *Int. J. of Heat and Mass Transfer*, 5, 1053-1058(1962).
31. Joshi, S. D. and Bergles, A. E., "Heat Transfer to Laminar In-tube Flow of Pseudoplastic Fluids", *AIChE Journal*, 27, 872-875(1981).
32. Knudsen, J. G. and Katz, D. L., "Fluid Dynamics and Heat Transfer", McGraw-Hill Book Company, Inc., New York, 1958.
33. Kubair, V. G. and Pei, D. C. T., "Combined Laminar Free and Forced Convection Heat Transfer to Non-Newtonian Fluids", *Int. Journal of Heat and Mass Transfer*, 11, 855-869(1968).
34. Laura, P. A. A. and Cortinez, V. H., "Optimisation of Eigenvalues When Using the Galerkin Method", *AIChE Journal*, 32, 1025-1026(1986).
35. Lyche, B. C. and Bird, R. B., "The Graetz-Nusselt Problem for a Power-law Non-Newtonian Fluid", *Chemical Engg. Sc.*, 6, 35-41(1954).
36. Mahalingam, R., Tilton, L. O. and Coulson, J. M., "Heat Transfer in Laminar Flow of Non-Newtonian Fluids", *Chemical Engg. Sc.*, 30, 921-929(1975).
37. Metzner, A. B. and Reed, J. C., "Flow of Non-Newtonian Fluids --- Correlation for the Laminar, Transition, and Turbulent Flow Regions", *AIChE Journal*, 1, 434-440(1955).
38. Metzner, A. B. and Gluck, D. F., "Heat Transfer to Non-Newtonian Fluids Under Laminar-Flow Conditions", *Chemical Engineering Science*, 12, 185-190(1960).
39. Metzner, A. B., Vaughn, R. D. and Haughton, G. L., "Heat Transfer to Non-Newtonian Fluids", *AIChE Journal*, 3, 92-100(1957).
40. Milton, A., "On the Solution of the Differential Equation Occurring in the Problem of Heat Convection in the Laminar Flow Through a Tube", *Journal of Mathematics and Physics*, 32, 184-187(1953).

41. Mizushima, T. and Kuriwaki, Y., "Turbulent Heat Transfer in Non-Newtonian Fluids", 197-212(1966).
42. Nouri, J. M., Umur, H. and Whitelaw, J. H., "Flow of Newtonian and non-Newtonian Fluids in Concentric and Eccentric Annuli", Journal of Fluid Mech., 253, 617-641 (1993).
43. Orr, C. Jr. and Dallavalle, J. M., "Heat-Transfer Properties of Liquid-Solid Suspensions", Symposium --- Heat Transfer, 50, 29-45.
44. Orville, G. S., Owen, T. H. and Gelibter, M., "Turbulent Non-Newtonian Transport in a Circular Tube", AIChE Journal, 22, 1142-1145(1976).
45. Papoutsakis, E., "Nusselt Numbers Near Entrance of Heat-Exchange Section in Flow Systems", AIChE Journal, 27, 687-689(1981).
46. Papoutsakis, E., Ramkrishna, D. and Lim, H. C., "The Extended Graetz Problem with Prescribed Wall Flux", AIChE Journal, 26, 779-787(1980).
47. Patankar, S. V. "Numerical Heat Transfer and Fluid Flow", Hemisphere, Washington D. C., 1980.
48. Patankar, S. V. and Spalding, D. B., "Heat and Mass Transfer in Boundary Layers", 2nd edn, Intertext Books, London, 1970.
49. Petersen, A. W. and Christiansen, E. B., "Heat Transfer to Non-Newtonian Fluids in Transitional and Turbulent Flow", AIChE Journal, 12, 221-232(1966).
50. Popovska, F. and Wilkinson, W. L., "Laminar Heat Transfer to Newtonian and Non-Newtonian Fluids in Tubes", Chemical Engg. Sc., 32, 1155-1164(1977).
51. Raghavan, N. S. and Ruthven, D. M., "Numerical Simulation of Fixed-Bed Adsorption Column by the Method of Orthogonal Collocation", AIChE Journal, 29, 922-925 (1983).
52. Rosenberg, D. E. and Hellums, J. D., "Flow Development and Heat Transfer in Variable-viscosity Fluids", I & EC Fundamentals, Vol 4, No 4, 417-422(1965).
53. Shaver, R. G. and Merrill, E. W., "Turbulent Flow of Pseudoplastic Polymer Solutions in Straight Cylindrical Tubes", AIChE Journal, 5, 181-188(1959).
54. Shenoy, A. V., "A Correlating Equation for Combined Laminar Forced and Free Convection Heat Transfer to Power-law Fluids", AIChE Journal, 26, 505-507(1980).

55. Shenoy, A. V., "Combined Laminar Forced and Free Convection Heat Transfer to Viscoelastic Fluids", *AIChE Journal*, 26, 683-686(1980).
56. Skelland, A. H. P., "Non-Newtonian Flow and Heat Transfer", John Wiley and Sons, Inc., New York, 1967.
57. Toor, H. L., "The Energy Equation for Viscous Flow--- Effect of Expansion on Temperature Profiles", *Industrial and Engineering Chemistry(Engineering, Design, and Process Development)*, 48, 922-926(1956).
58. Wilkinson, W.L., "Non-Newtonian Fluids-- Fluid Mechanics, Mixing and Heat Transfer", Pergamon Press, New York, 1960.
59. Quader, A. K. M. A. and Wilkinson, W. L., "Correlation of Turbulent Flow Rate-Pressure Drop Data for Non-Newtonian Solutions and Slurries", *Int. J. Multiphase Flow*, 6, 553-561(1980).
60. Ybarra, R. M. and Eckert, R. E., "Transport Eigenvalue Problems --- Effect of Order of Approximation and Step Size on Solution Accuracy"., *AIChE Journal*, 31, 1755-1757 (1985).
61. Yuan, S. W., "Foundations of Fluid Mechanics", Prentice-Hall of India Private Limited, New Delhi, 1969.

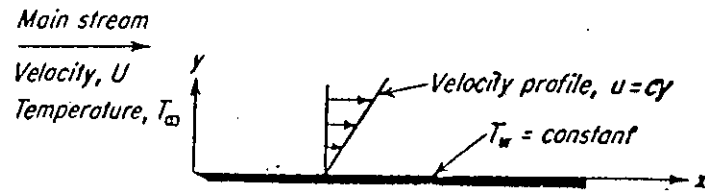


Fig. 2.1 Conditions for the Leveque solution.

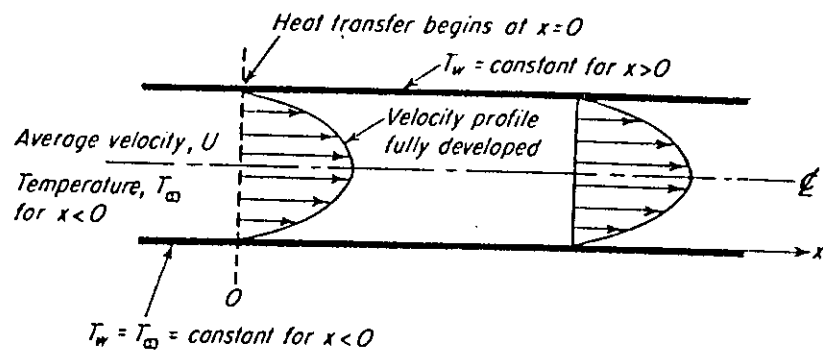


Fig. 2.2 Boundary conditions for the classical Graetz solution.

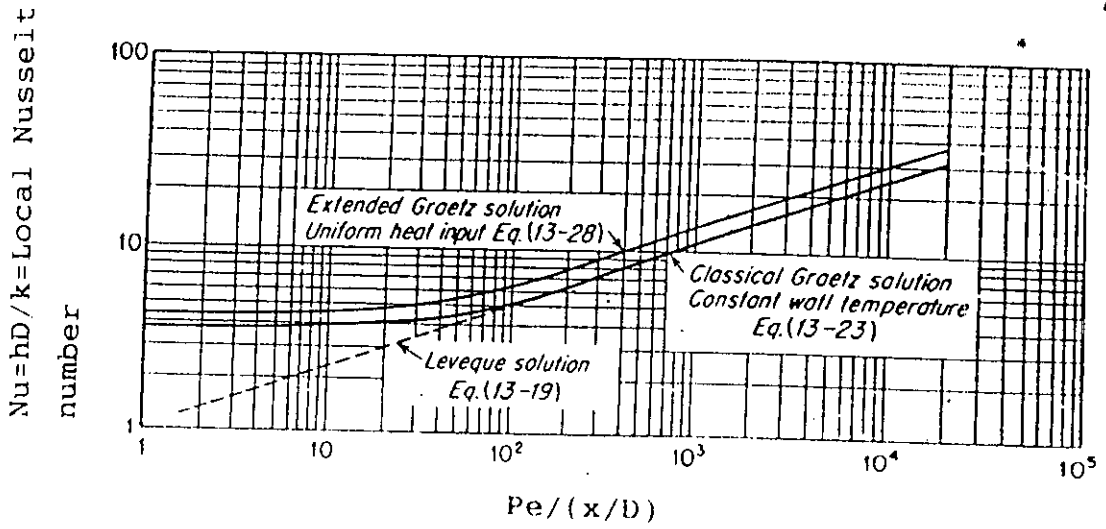


Fig. 2.3 Local Nusselt number for laminar flow in tubes. Velocity profile fully developed.

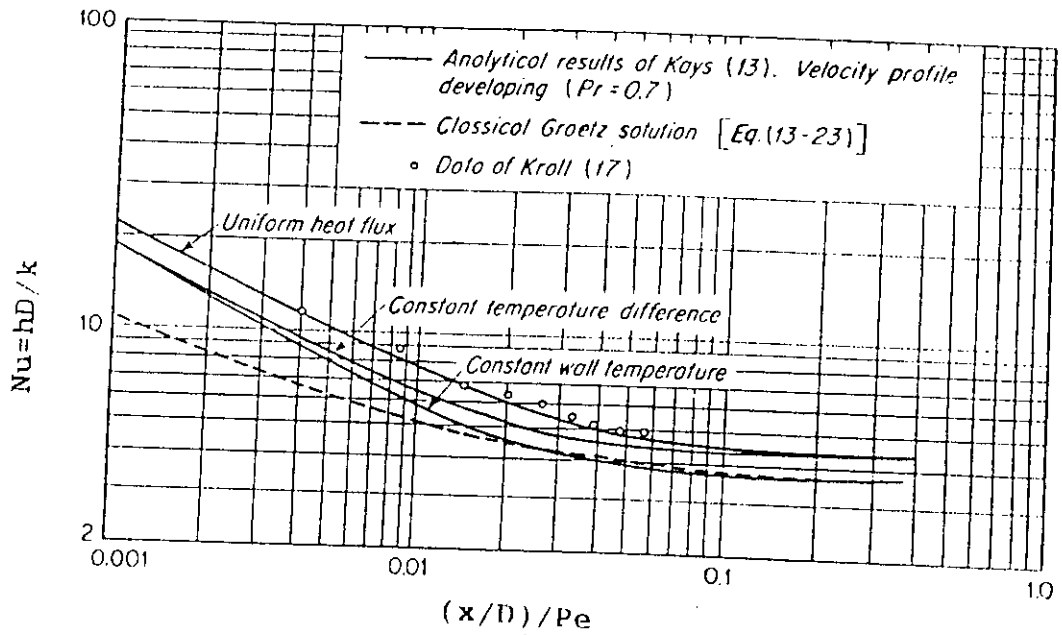


Fig. 2.4 Local Nusselt number for laminar flow in the entrance of a tube ($Pr=0.7$).

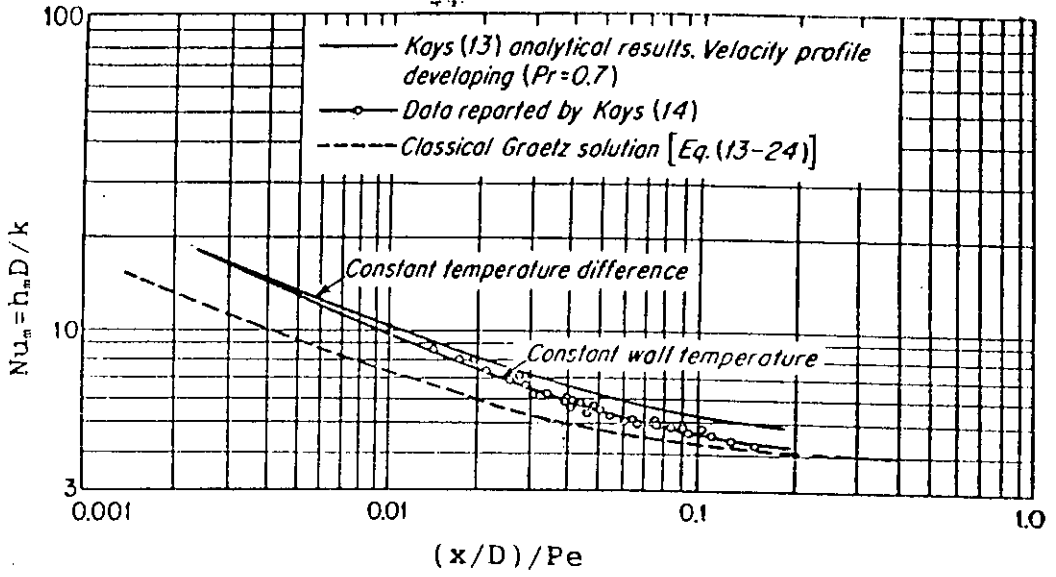


Fig. 2.5 Mean Nusselt number for laminar flow in the entrance of a tube ($Pr=0.7$).

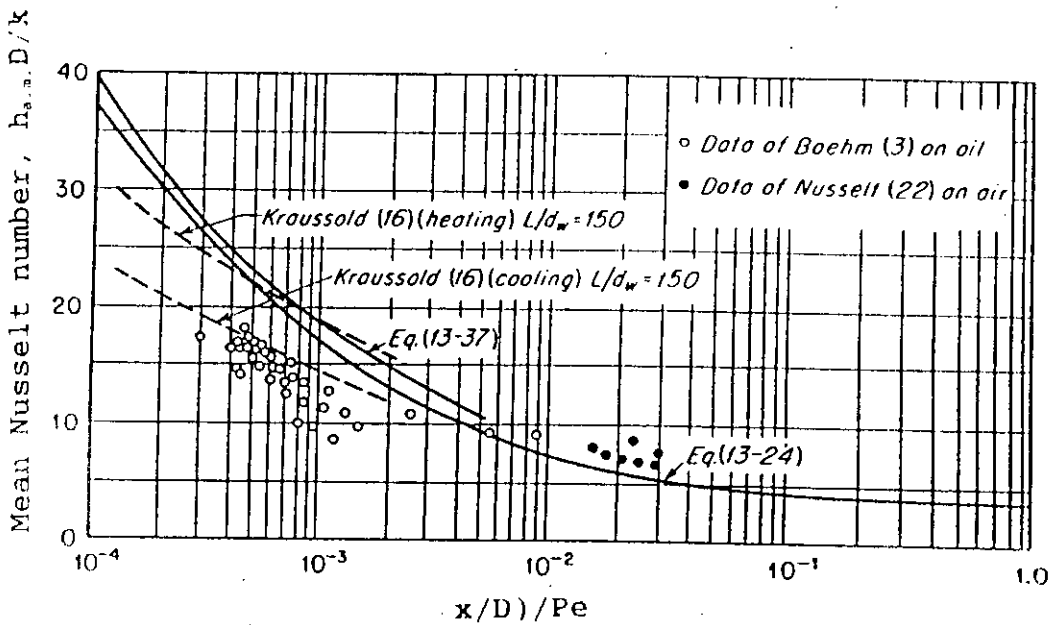


Fig. 2.6 Mean Nusselt number for fully developed laminar flow in tubes.

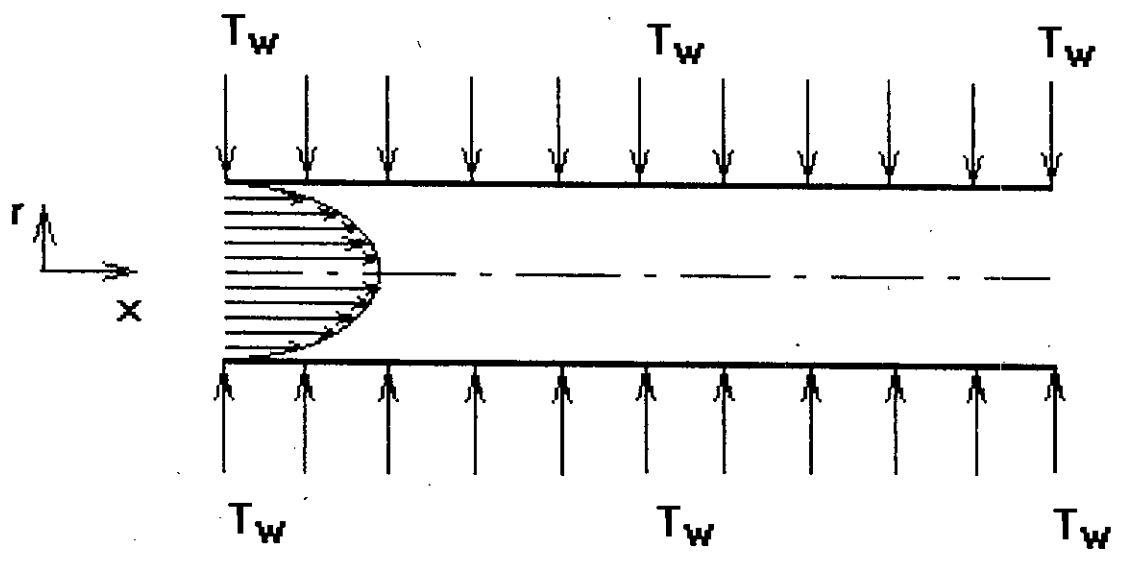


Fig. 4.1 Flow Configuration

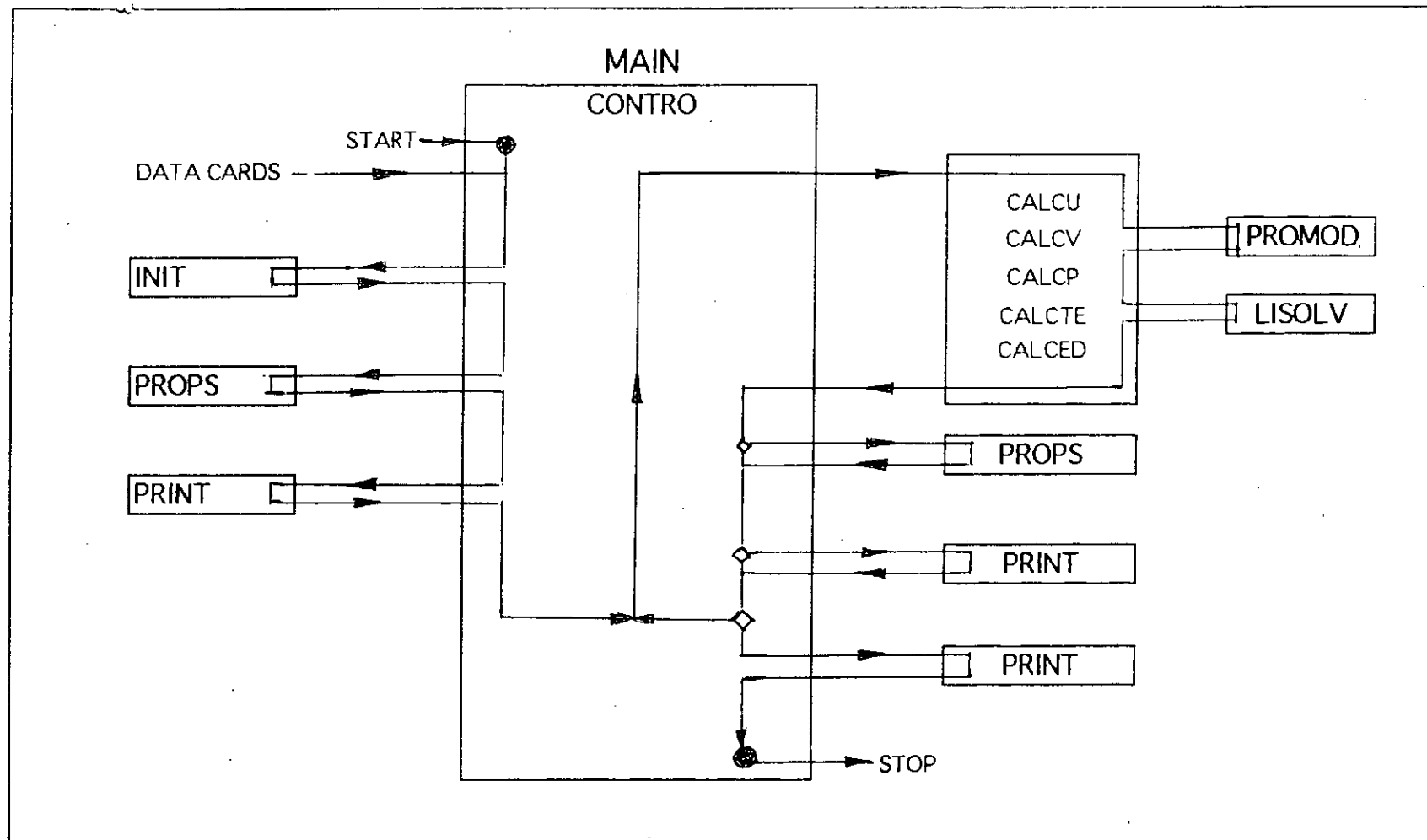


Fig. 5.1 Program Flow Chart

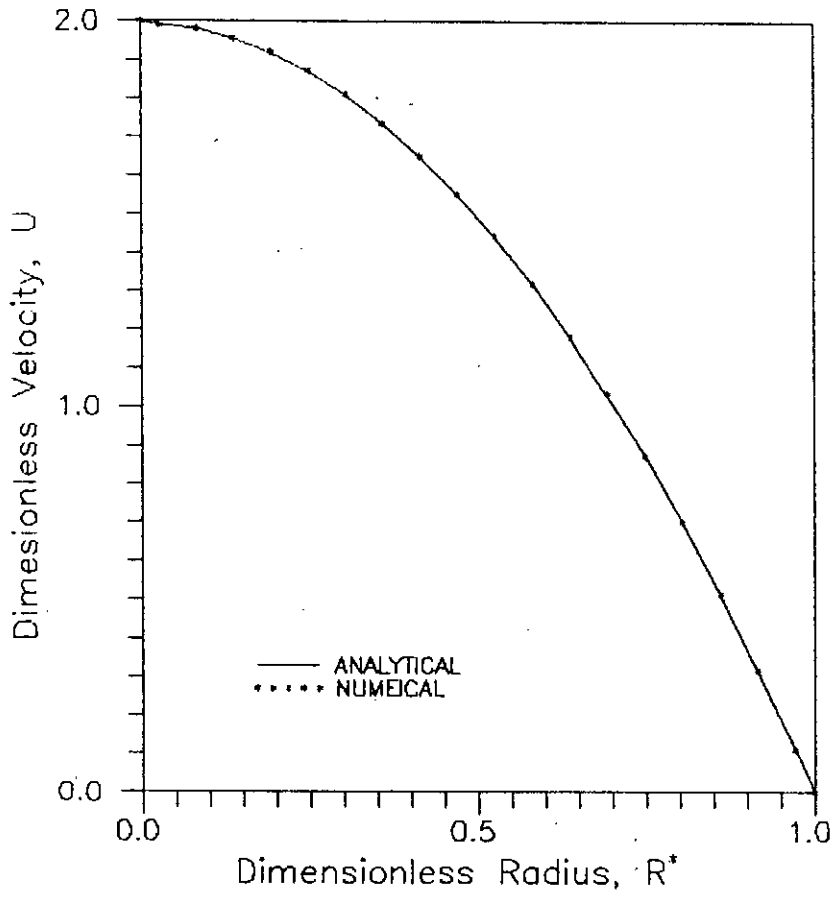


FIG.5.2 Isothermal Flow Development of Newtonian Fluid.

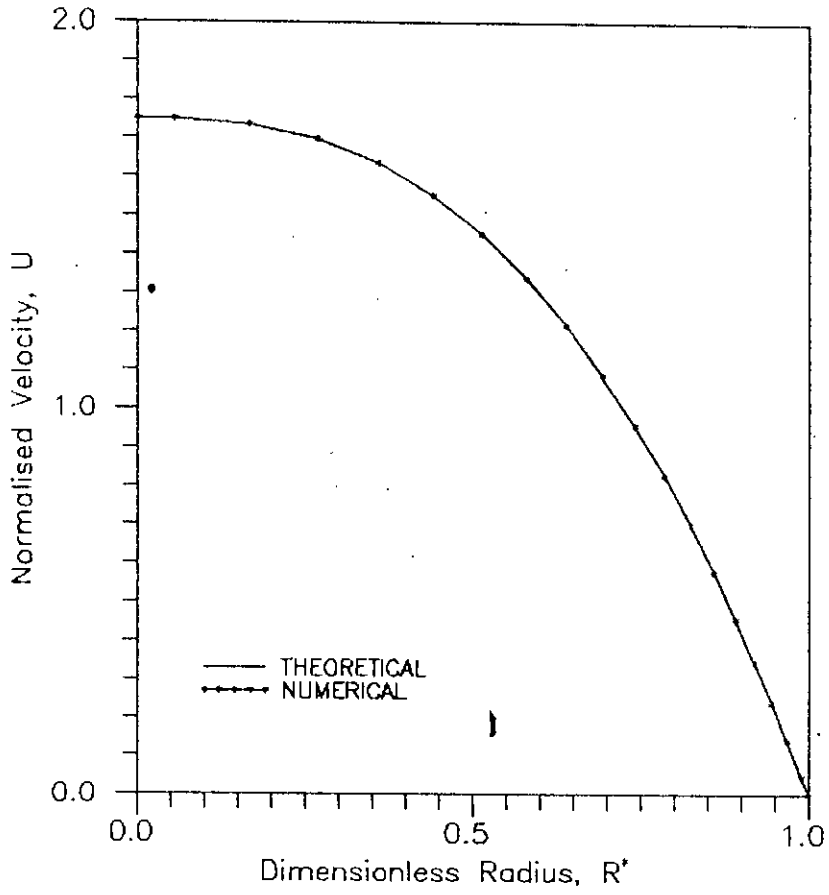


Fig. 5.3 Isothermal Flow Development of Carbopol. $n=0.6$, $EPSY=0.9$.

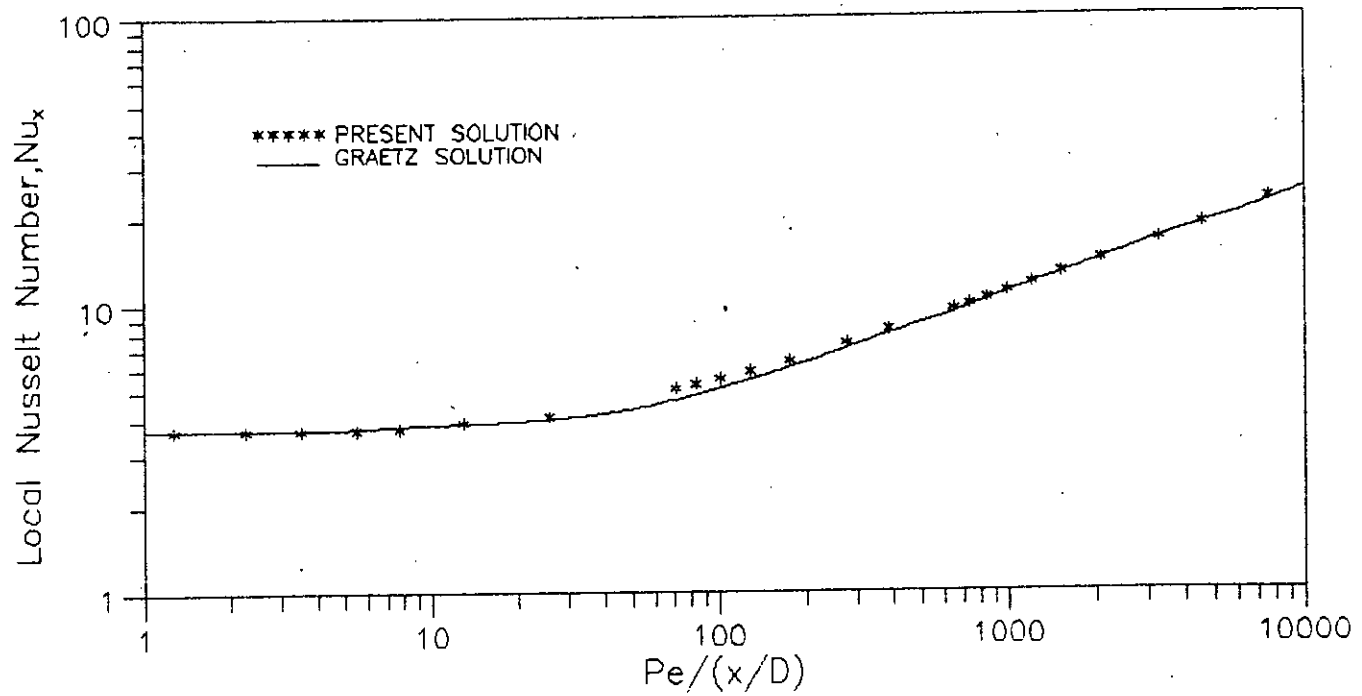


FIG.5.4 Local Nusselt Number for Laminar Flow in Tubes. Velocity Profile Fully Developed.

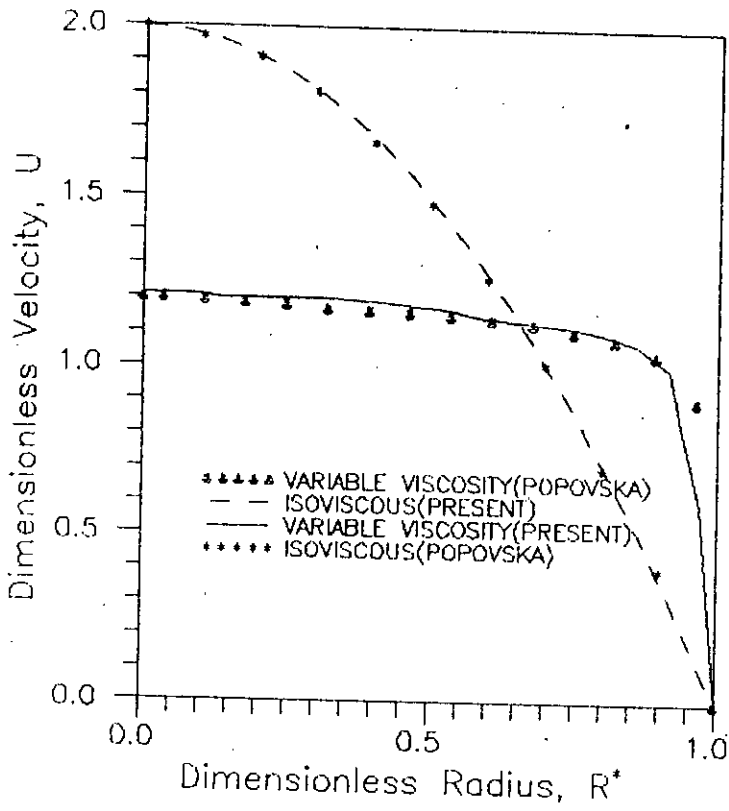


FIG.5.5 Velocity Profiles for Newtonian Oil-heating. $Gz=323$, $T_w/T_i=1.29$ and $D=14.8$ mm.

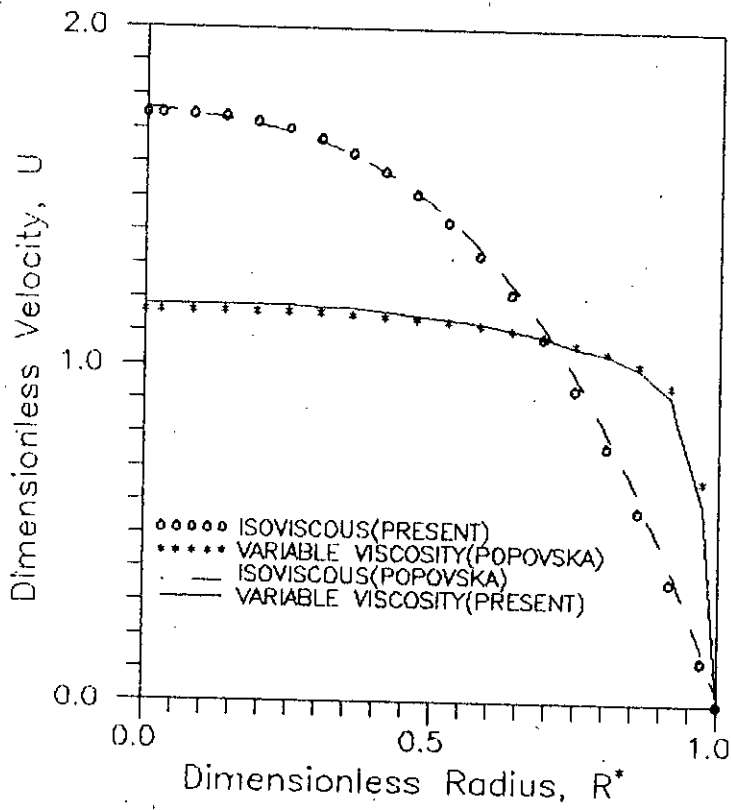


FIG.5.6 Velocity Profiles for Carbopol Heating.
 $n=0.6$, $Gz=359$, $T_w/T_i=1.233$ and $D=17.4$ mm.

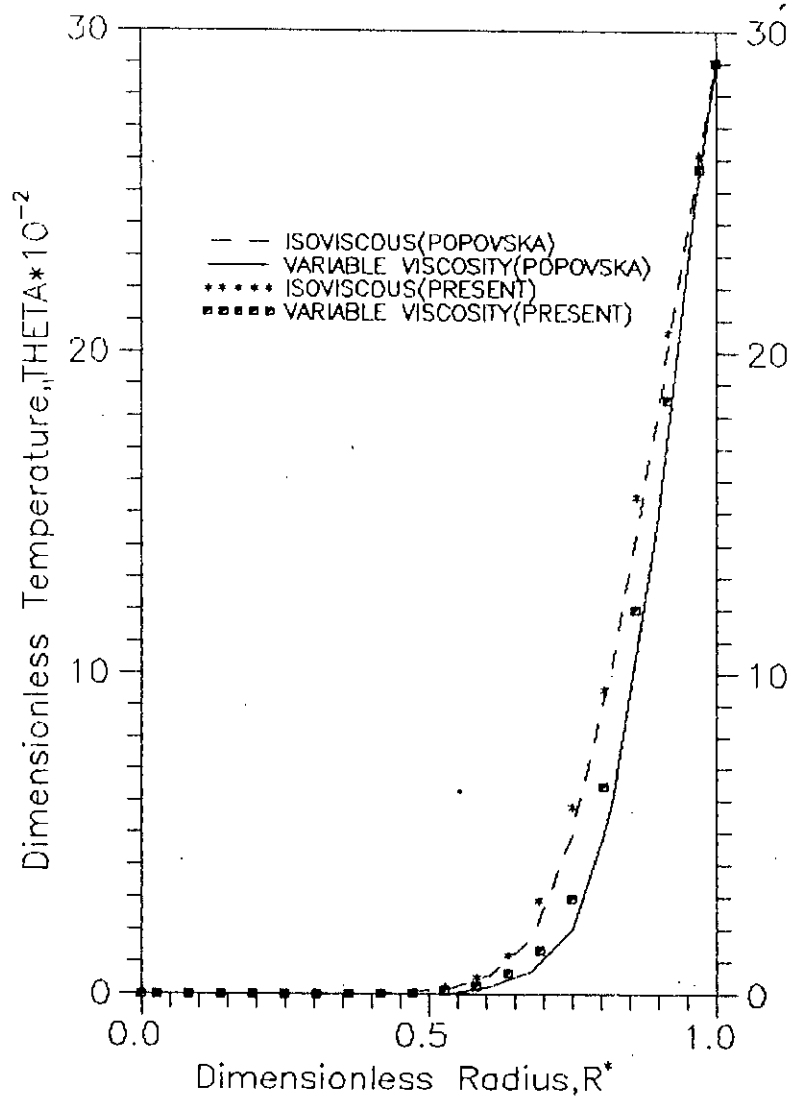


FIG.5.7 Temperature Profiles for Newtonian Oil-heating. $Gz=323$, $T_w/T_i=1.29$, and $D=14.8$ mm.

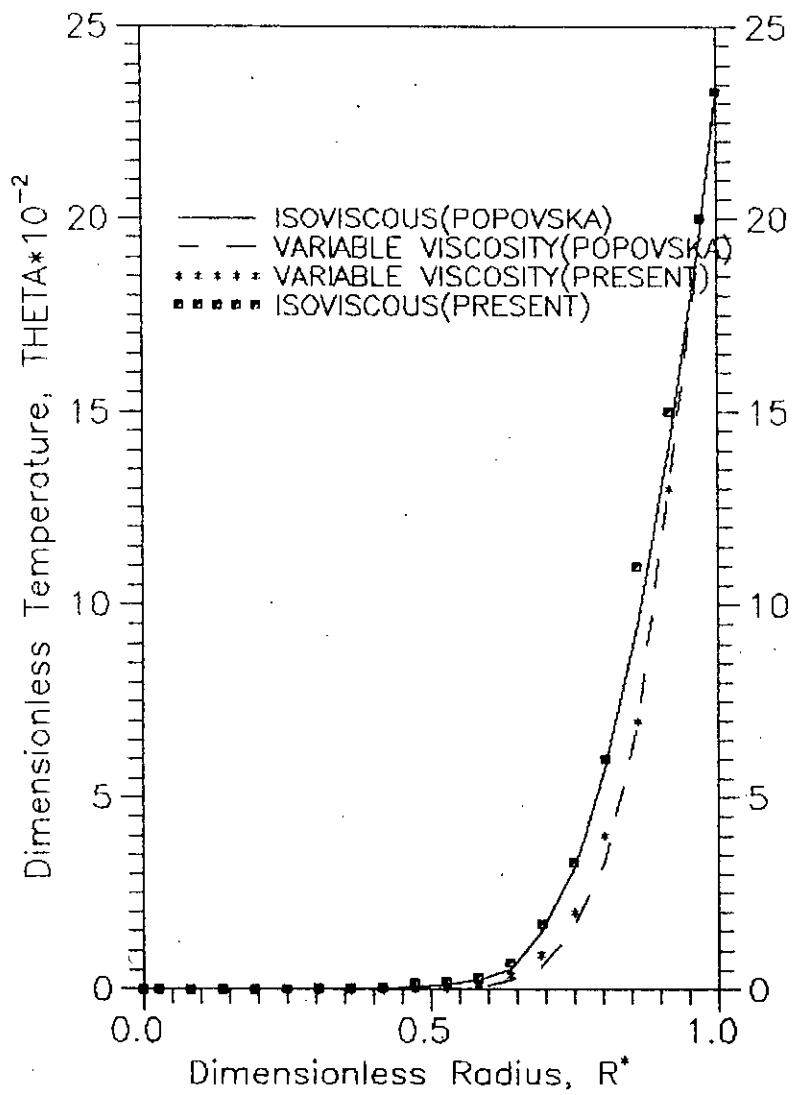


FIG.5.8 Temperature profiles for Carbopol Heating. $n=0.6$, $Gz=359$, $T_w/T_i=1.233$, $D=17.4$ mm.

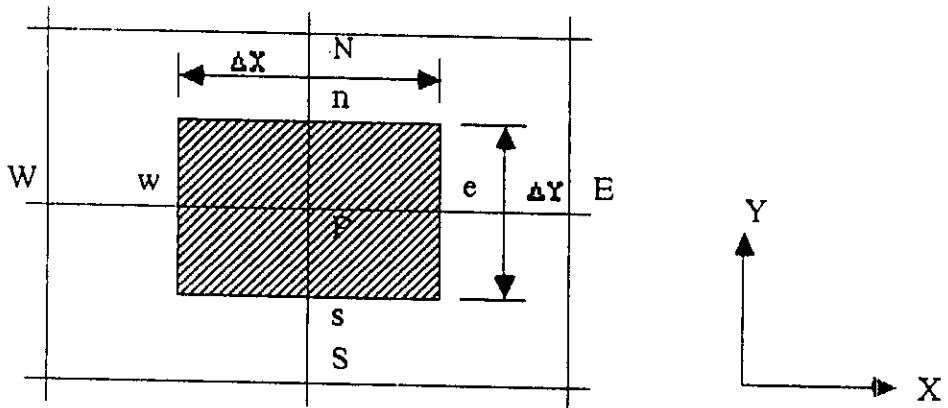


Fig. 6.1 Two dimensional computational cell.

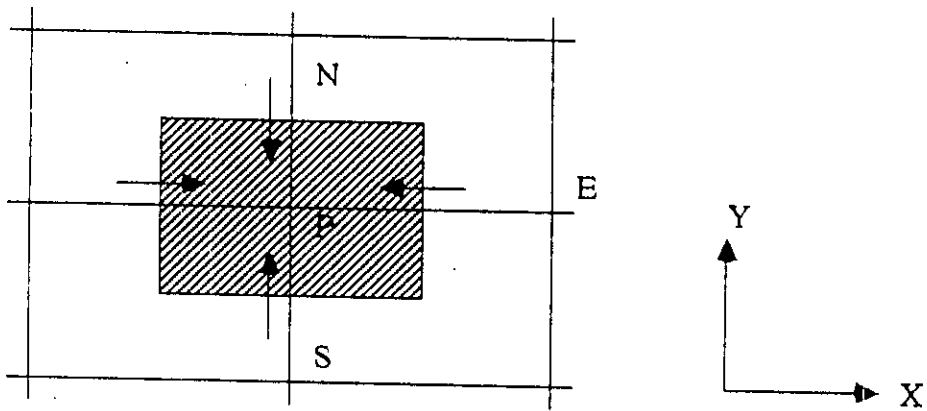


Fig. 6.2 Control volume for continuity equation.

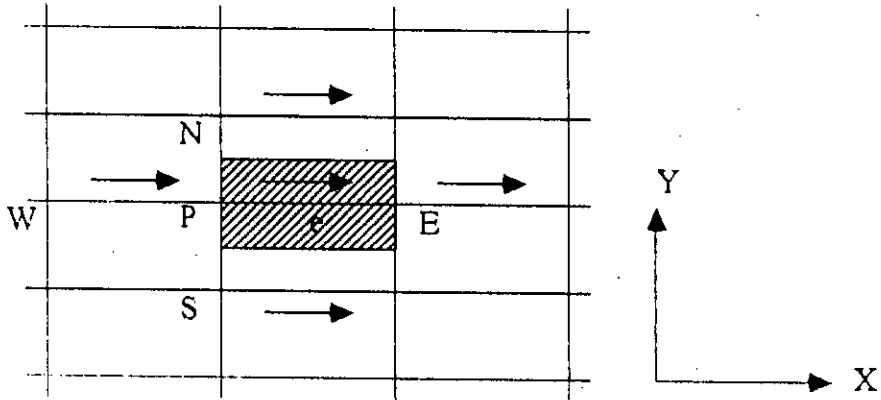


Fig. 6.3 Control volume for U

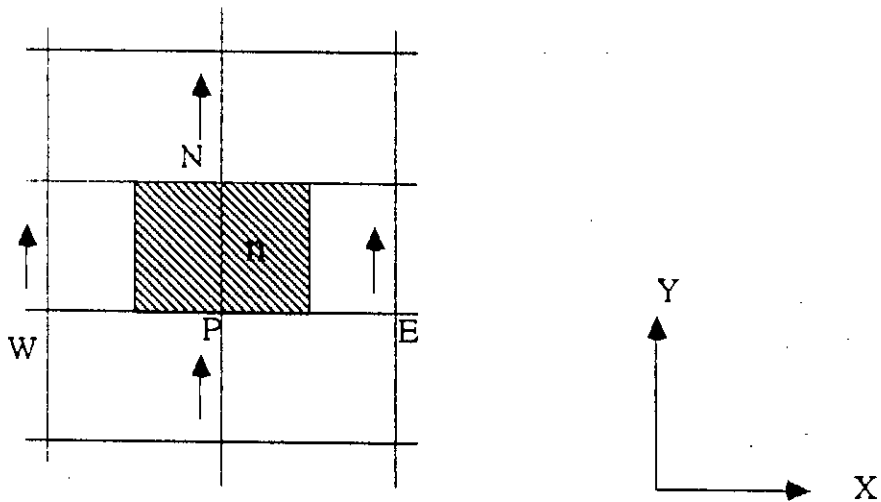


Fig. 6.4 Control volume for V

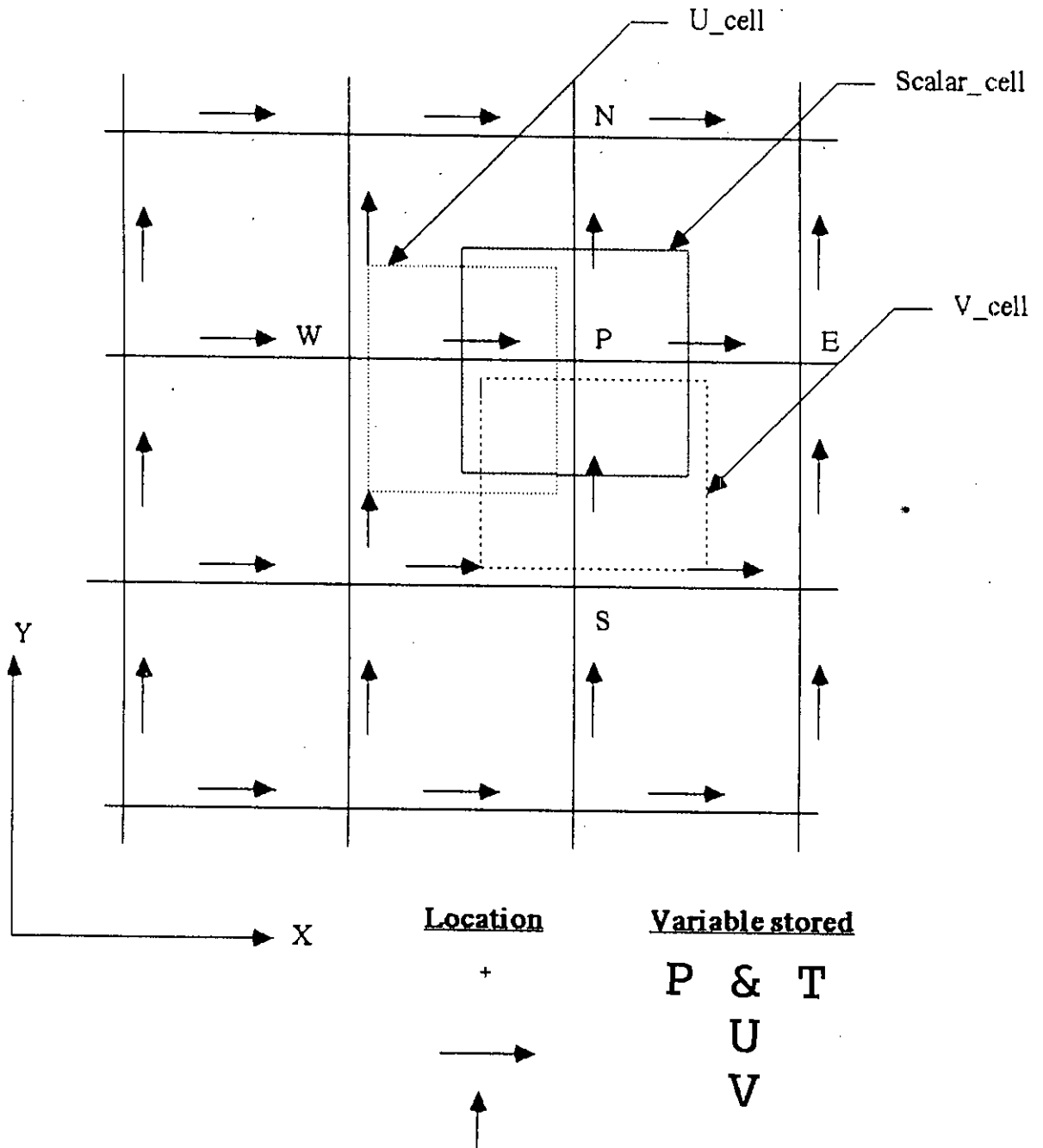


Fig. 6.5 Computational grid, location and control volumes (cells) of scalar variables and axial and radial velocities.

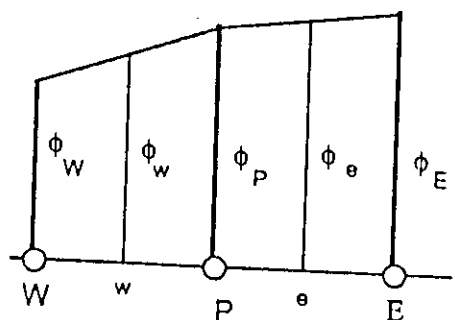


Fig. 6.6 Schematic presentation of CDS

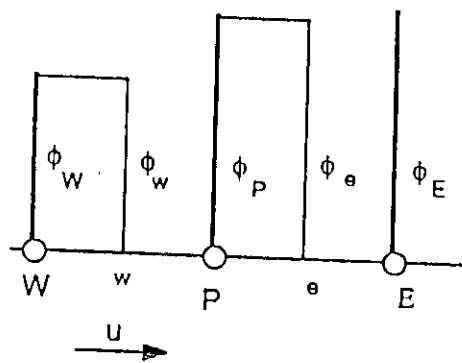


Fig. 6.7 Schematic presentation of UDS

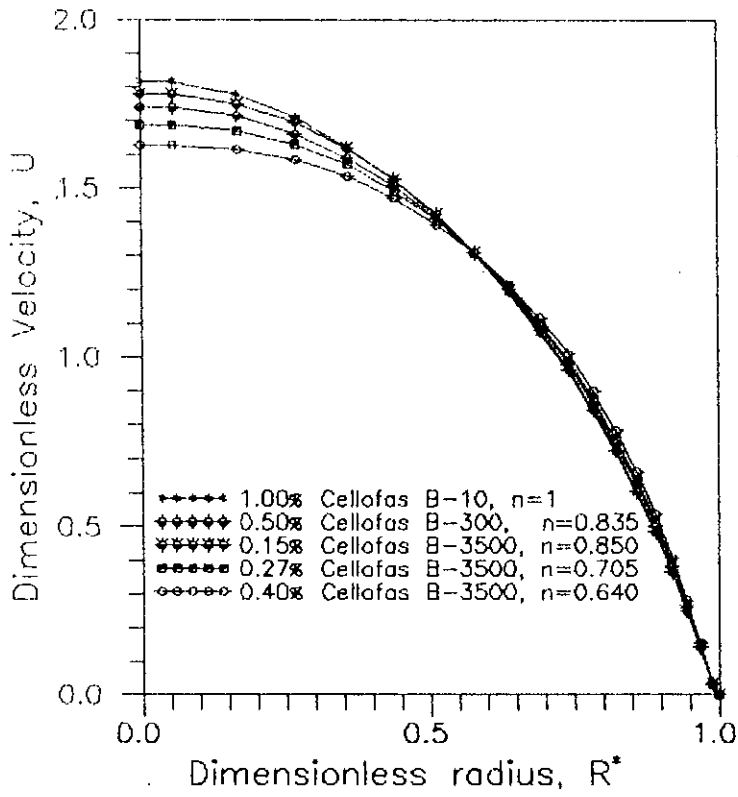


Fig.7.1a Velocity Profiles for Different Types of Cellofas.
 $Gz = 232$, $\Gamma_w/T_i = 1.068$, $D = 17.4$ mm.

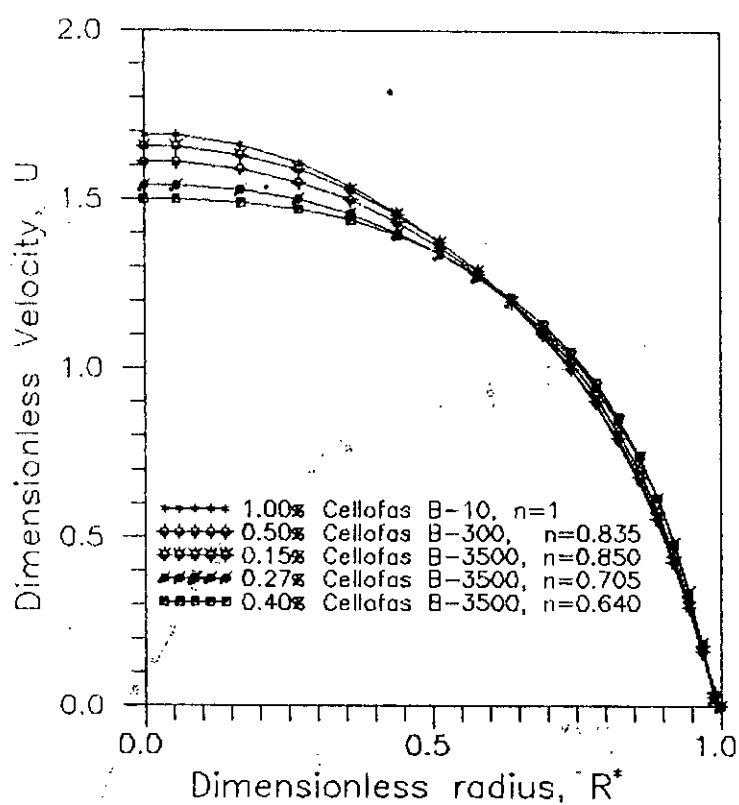


Fig.7.1b Velocity Profiles for Different Types of Cellofas.
 $Gz = 232$, $T_w/T_i = 1.130$, $D = 17.4$ mm.

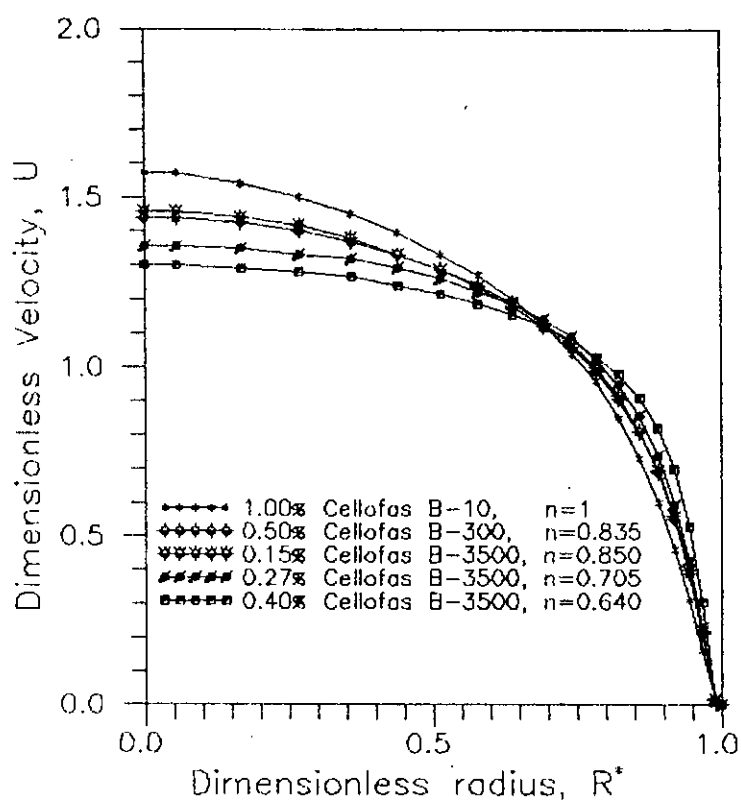


Fig.7.1c Velocity Profiles for Different Types of Cellofas.
 $Gz = 232$, $T_w/T_i = 1.233$, $D = 17.4$ mm.

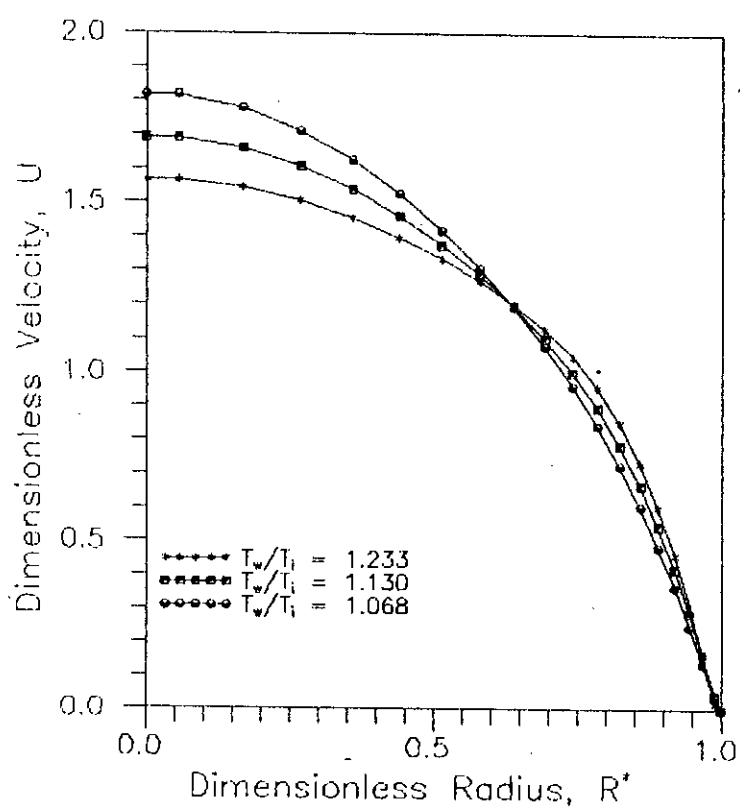


Fig.7.2 Velocity Profiles for 1% Cellofas B-10 at Different T_w/T_i . $Gz = 232$, $D = 17.4$ mm.

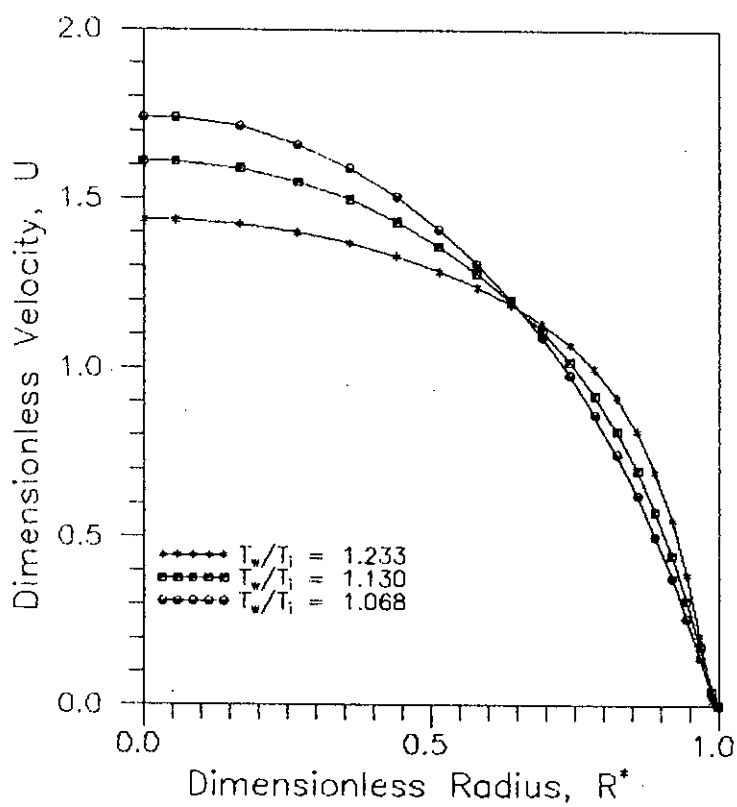


Fig.7.3 Velocity Profiles for 0.5% Cellofas B-300 at Different T_w/T_i . $Gz = 232$, $D = 17.4$ mm.

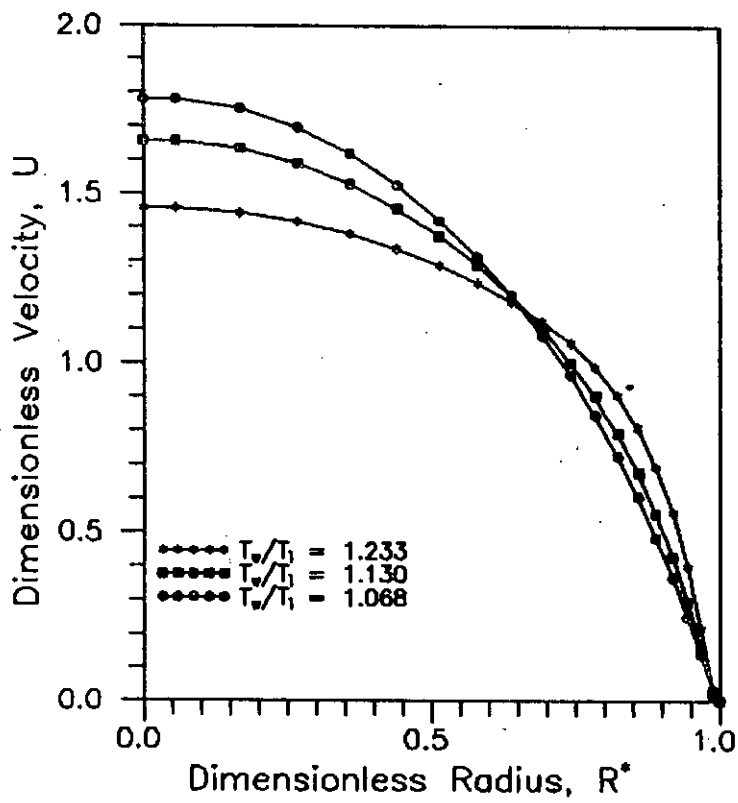


Fig.7.4 Velocity Profiles for 0.15% Cellofas B-3500 at Different T_w/T_1 . $Gz = 232$, $D = 17.4$ mm.

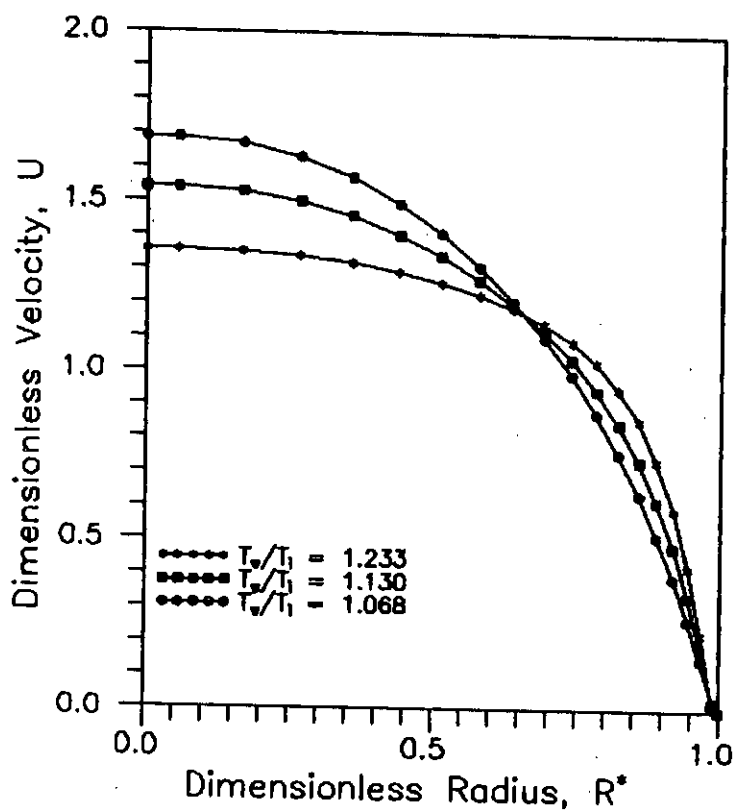


Fig.7.5 Velocity Profiles for 0.27 μ Cellofas B-3500 at Different T_w/T_i . $Gz = 232$, $D = 17.4$ mm.

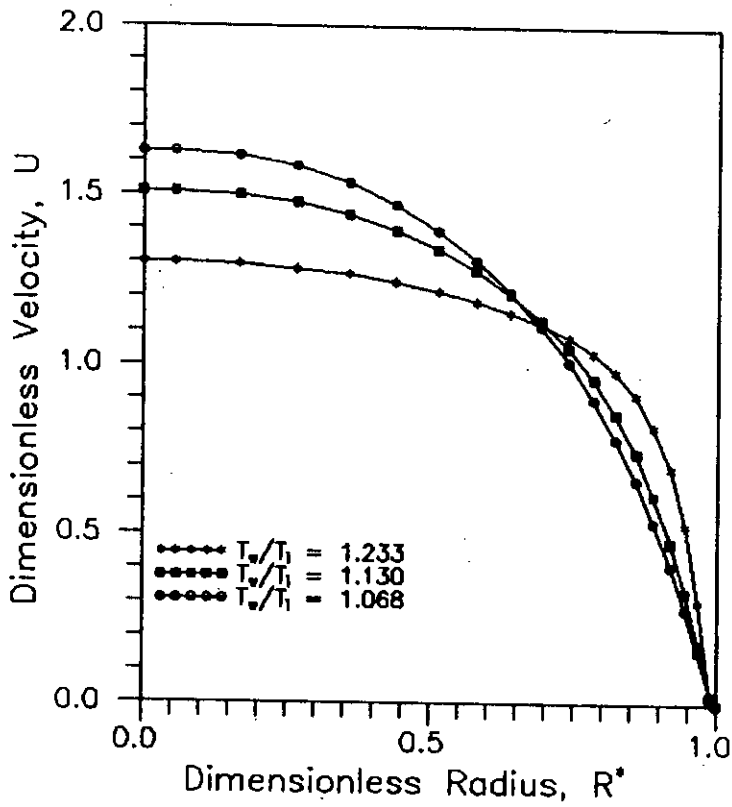


Fig.7.6 Velocity Profiles for 0.40% Cellofas B-3500 at Different T_w/T_i . $Gz = 232$, $D = 17.4$ mm.

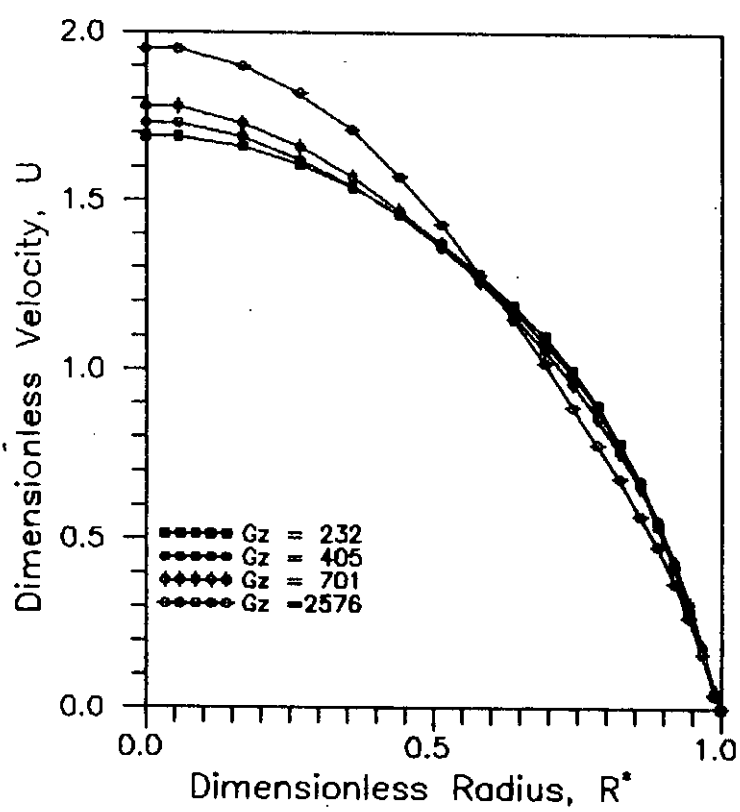


Fig.7.7 Velocity Profiles for 1 \times Cellofas B-10 at Different Gz . $T_w/T_i = 1.130$, $D = 17.4$ mm.

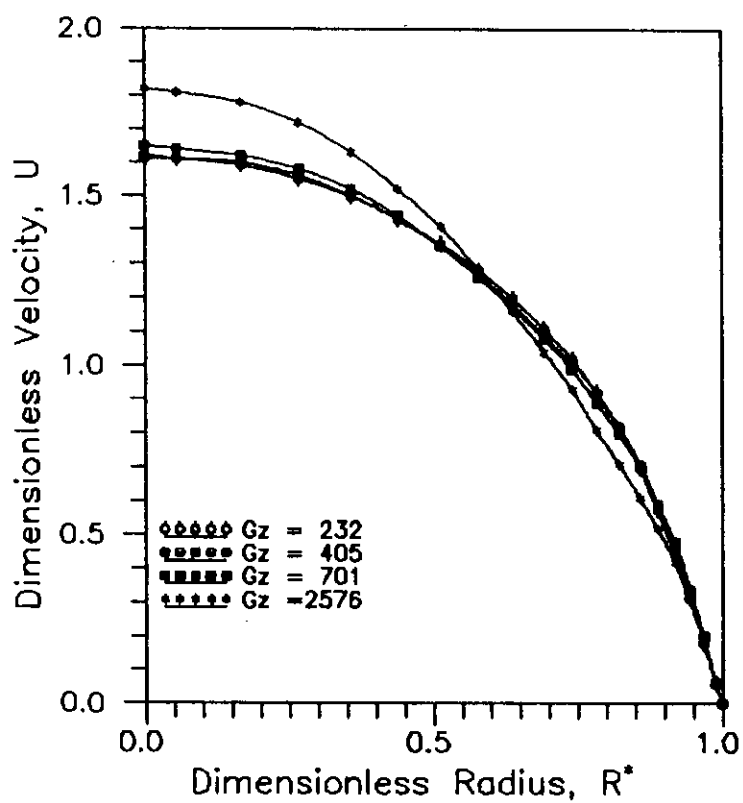


Fig.7.8 Velocity Profiles for 0.5% Cellofas B-300 at Different Gz . $T_w/T_i = 1.130$, $D = 17.4$ mm.

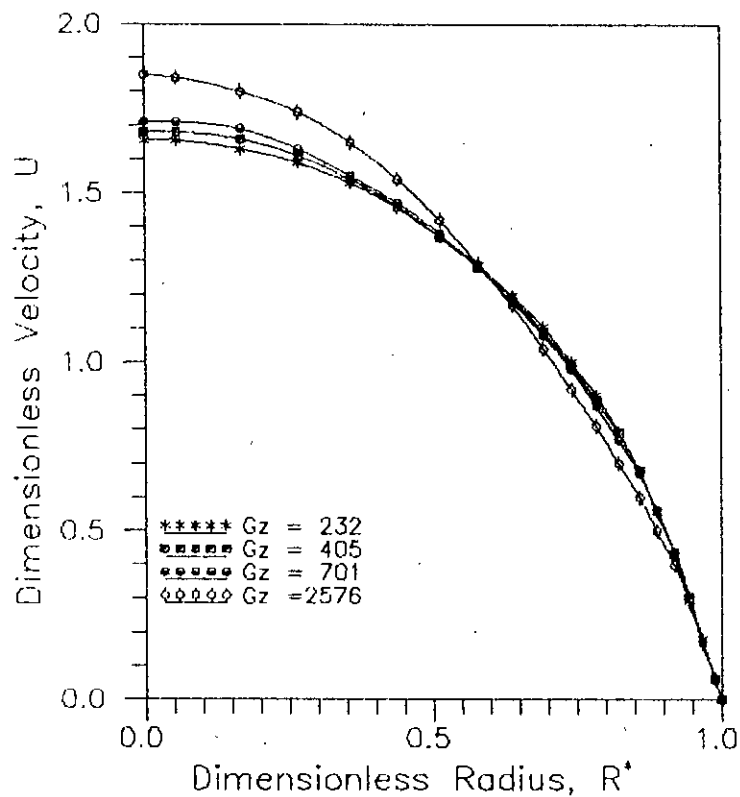


Fig.7.9 Velocity Profiles for 0.15% Cellofas B-3500 at Different Gz. $T_w/T_i = 1.130$, $D = 17.4$ mm.

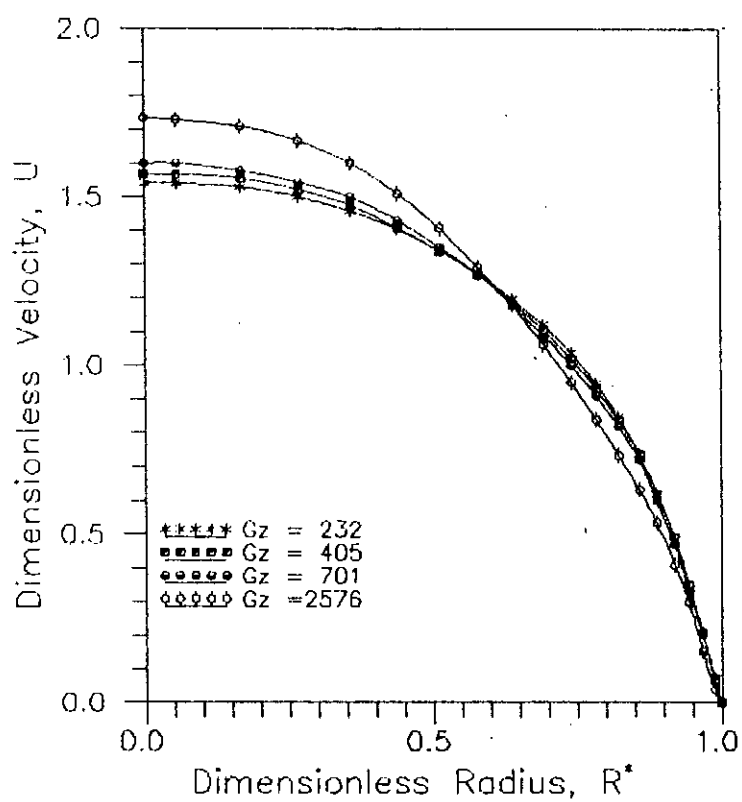


Fig.7.10 Velocity Profiles for 0.27% Cellofos B-3500 at Different Gz. $T_w/T_i = 1.130$, $D = 17.4$ mm.

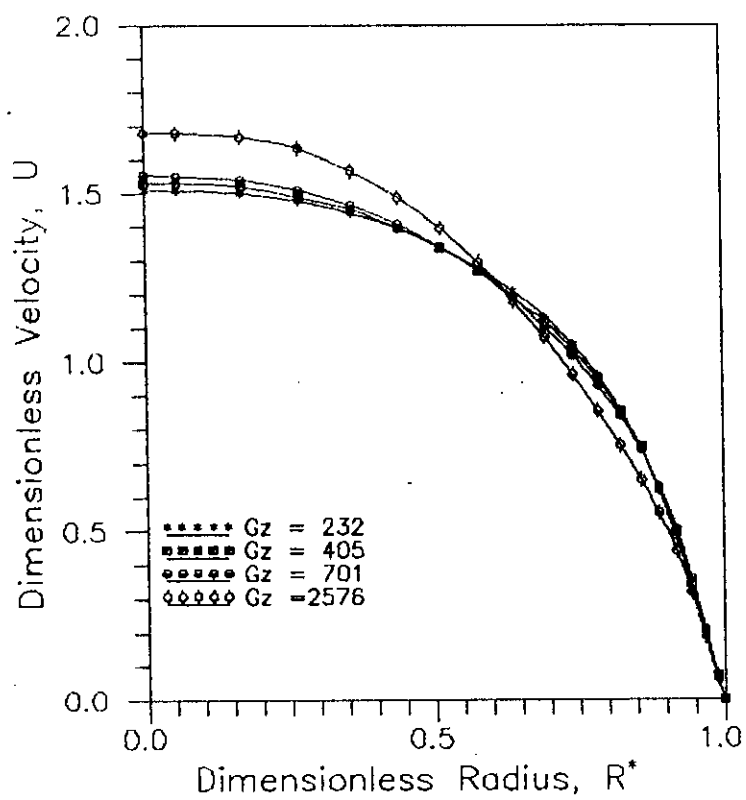


Fig.7.11 Velocity Profiles for 0.40% Cellofas B-3500 at Different Gz . $T_w/T_i = 1.130$, $D = 17.4$ mm.

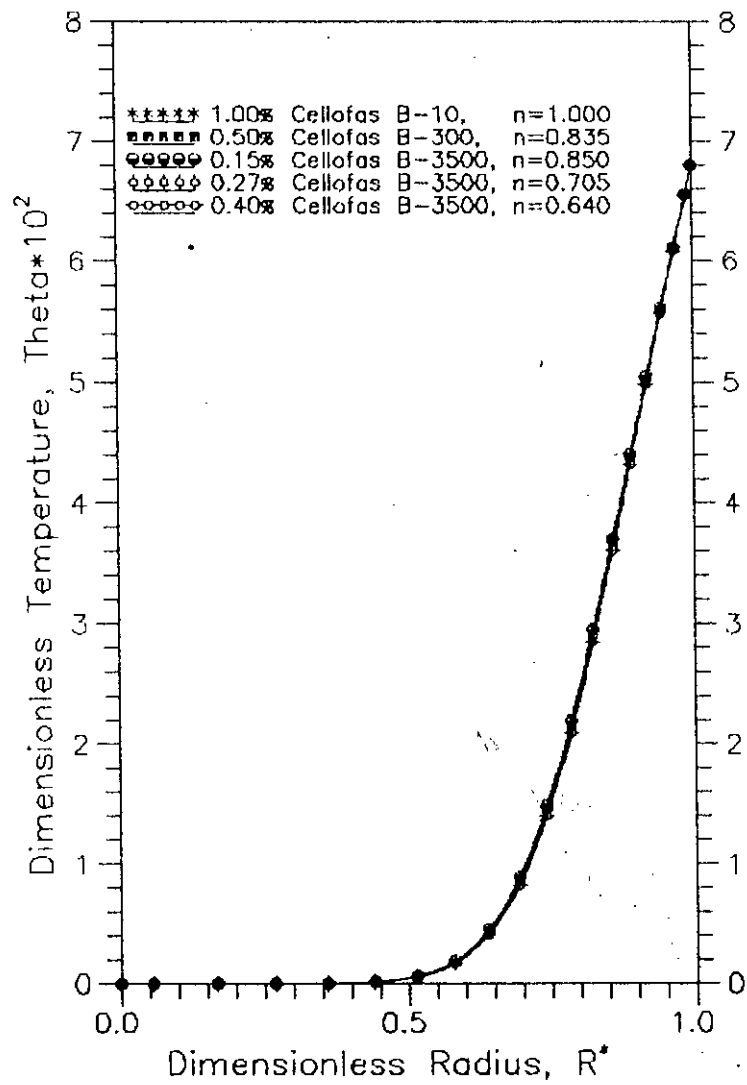


Fig.7.12a Temperature Profiles for Different Types of Cellofas. $Gz=232$, $T_w/T_i=1.068$, $D=17.4$ mm.

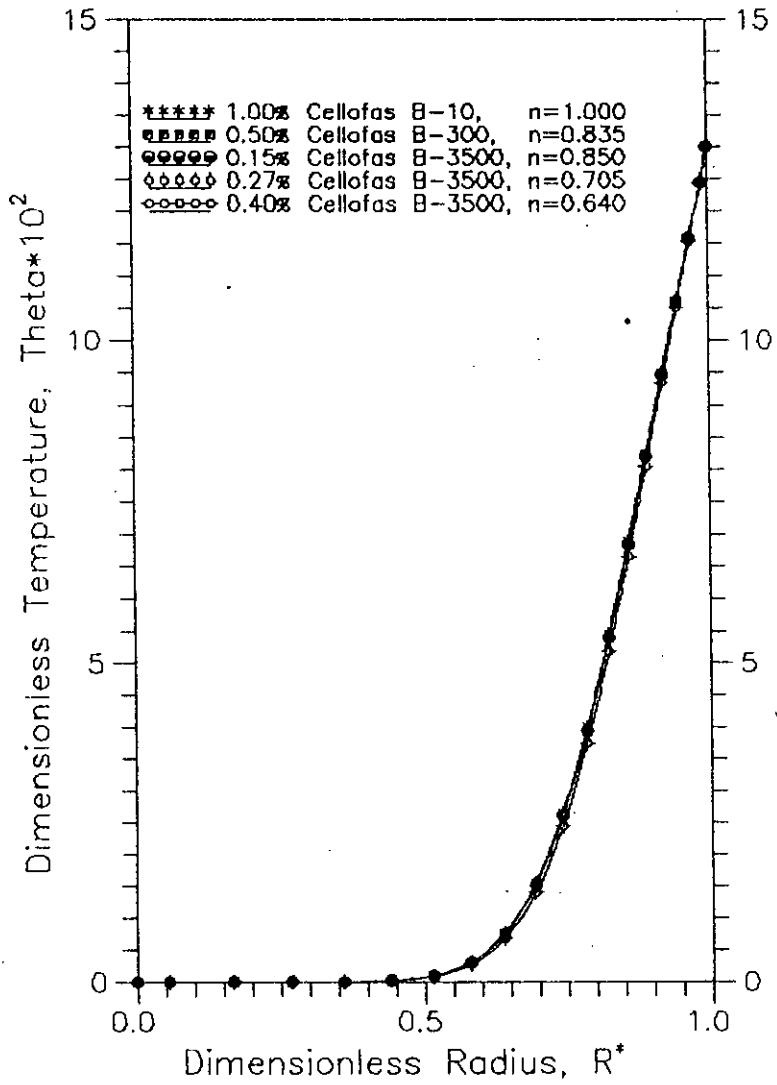


Fig.7.12b Temperature Profiles for Different Types of Cellofas. $Gz=232$, $T_w/T_i=1.130$, $D=17.4$ mm.

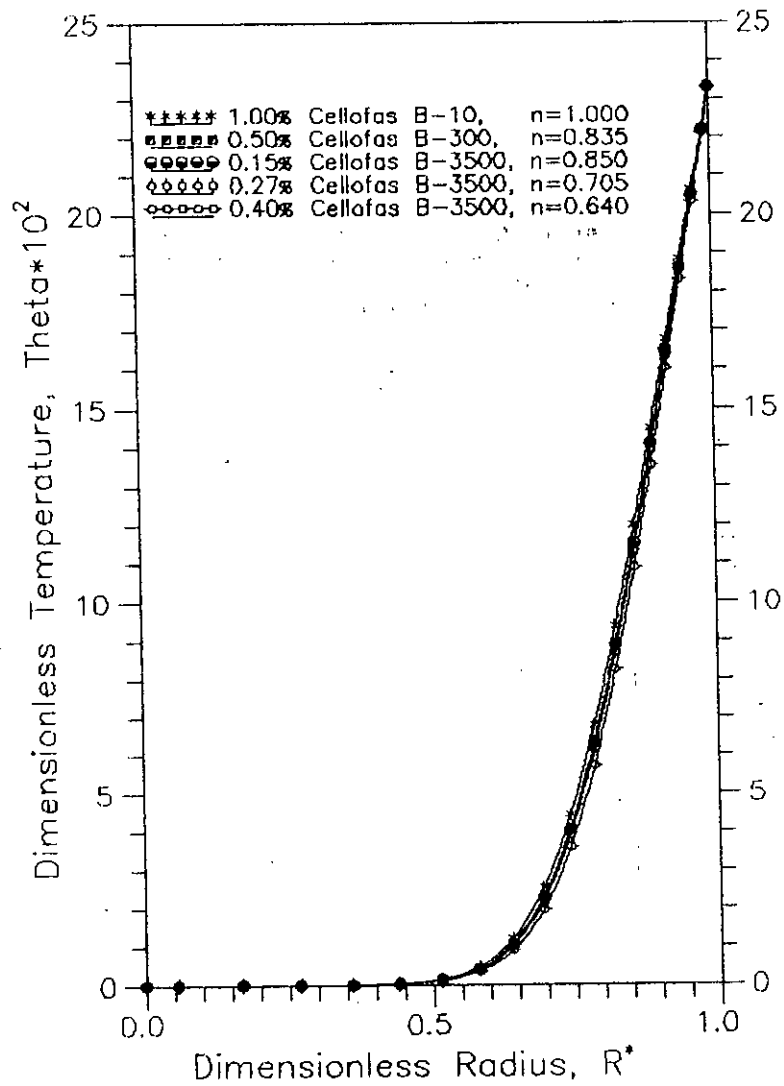


Fig.7.12c Temperature Profiles for Different Types of Cellofas. $Gz=232$, $T_w/T_i=1.233$, $D=17.4$ mm.

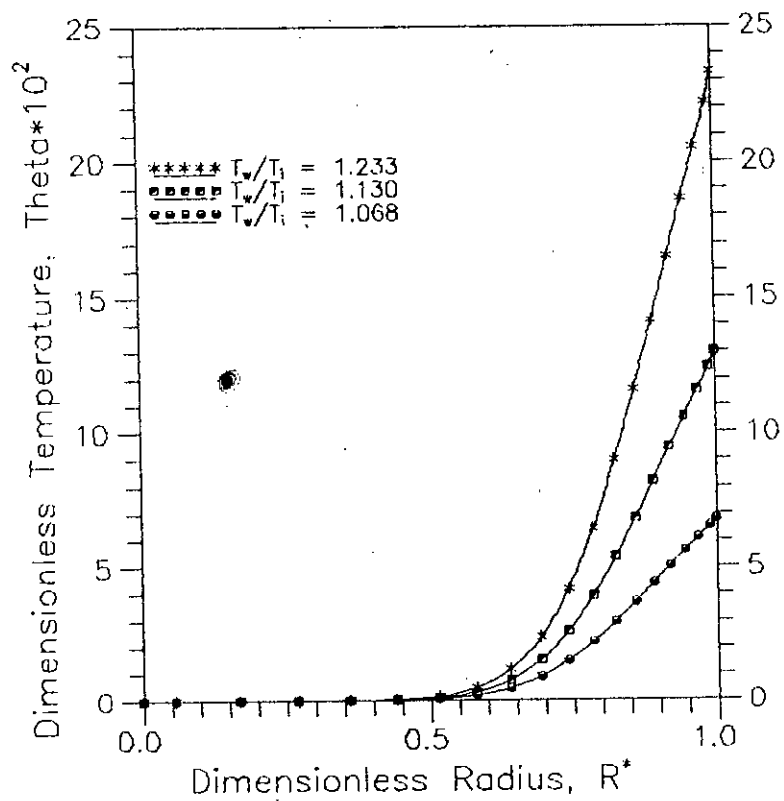


Fig.7.13 Temperature Profiles for 1% Cellofas at Different T_w/T_i . $Gz=232$, $D=17.4$ mm.

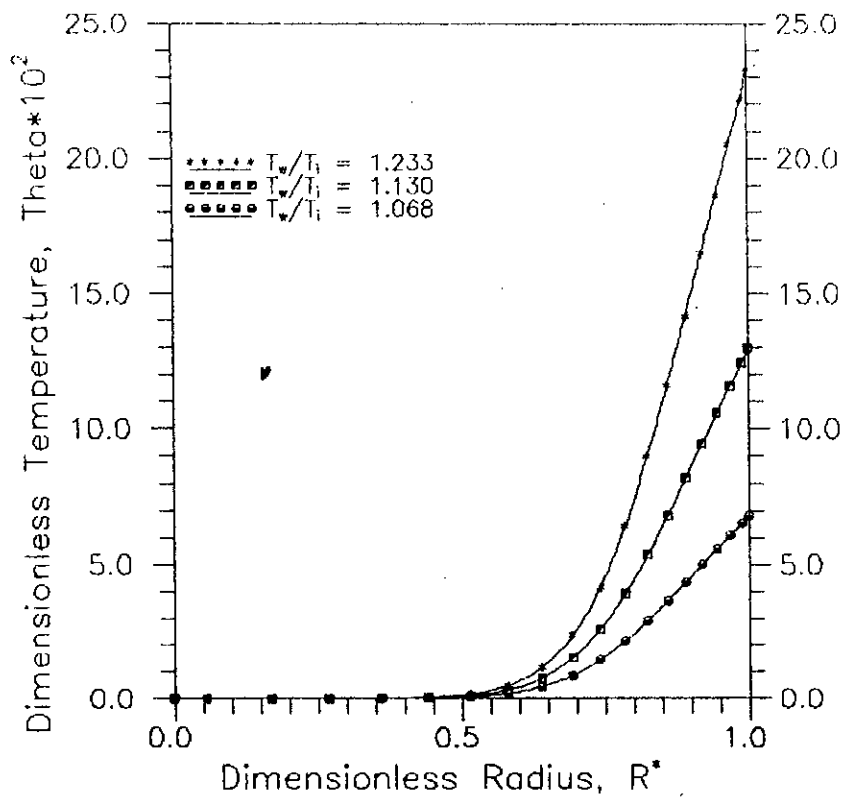


Fig.7.14 Temperature Profiles for 0.5% Cellofas at Different T_w/T_i . $Gz=232$, $D=17.4$ mm.

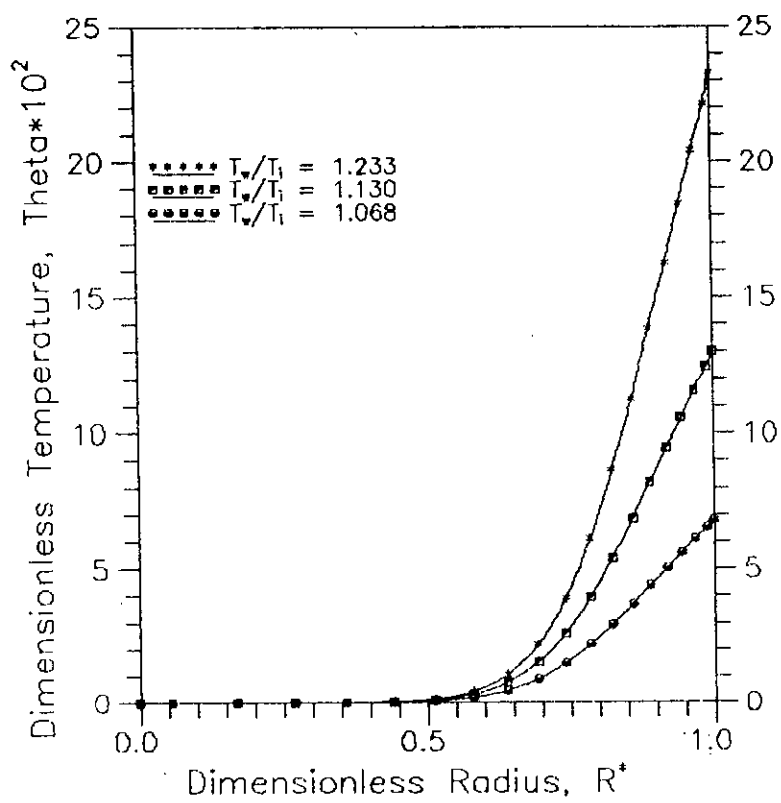


Fig.7.15 Temperature Profiles for 0.15% Cellofas B-3500 at Different T_w/T_i , $Gz=232$, $D=17.4$ mm. ●

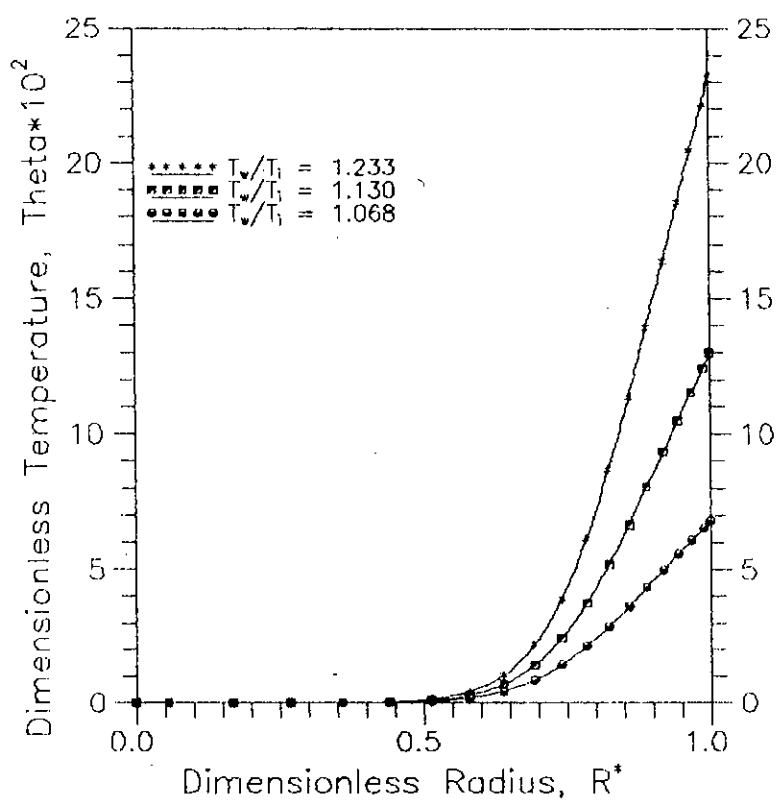


Fig.7.16 Temperature Profiles for 0.27% Cellofas B-3500 at Different T_w/T_i , $Gz=232$, $D=17.4$ mm.

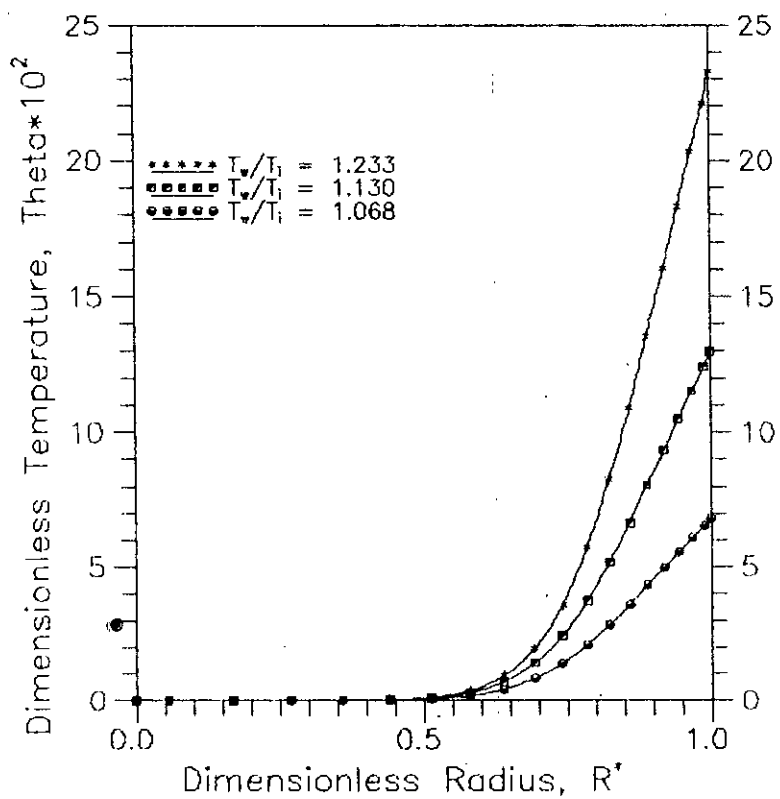


Fig.7.17 Temperature Profiles for 0.40% Cellofas B-3500 at Different T_w/T_i . $Gz=232$, $D=17.4$ mm.

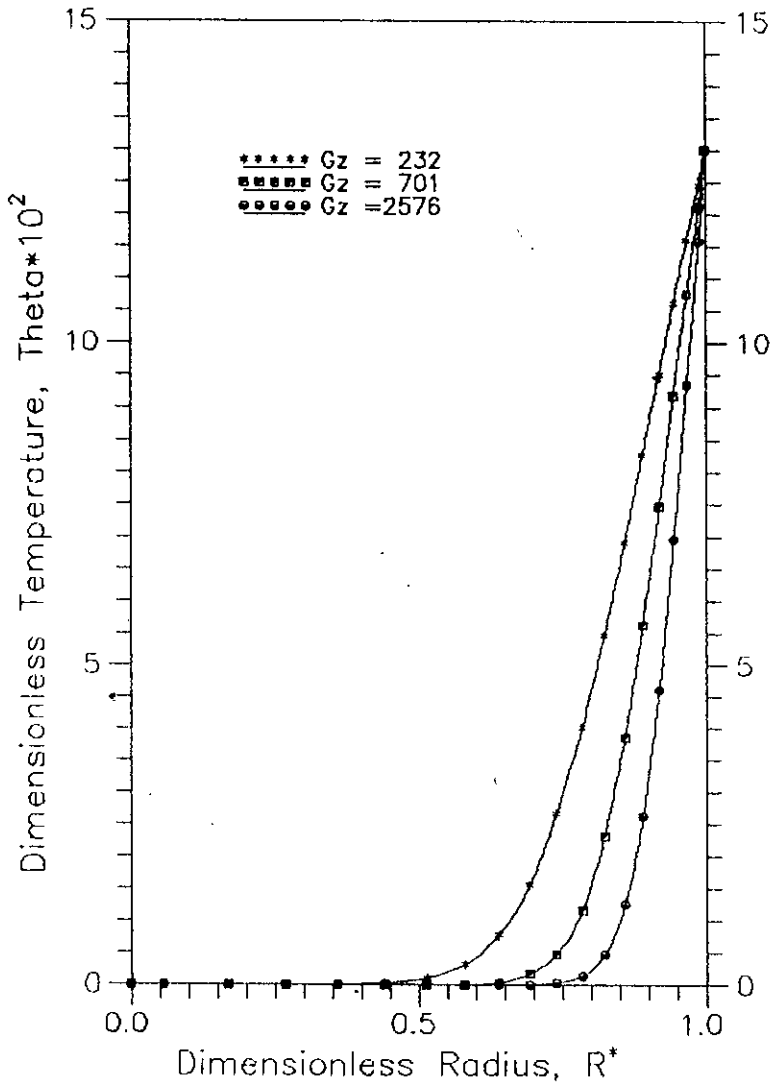


Fig.7.18 Temperature Profiles for 1% Cellofas B-10 at Different Gz . $T_w/T_i = 1.130$, $D = 17.4$ mm.

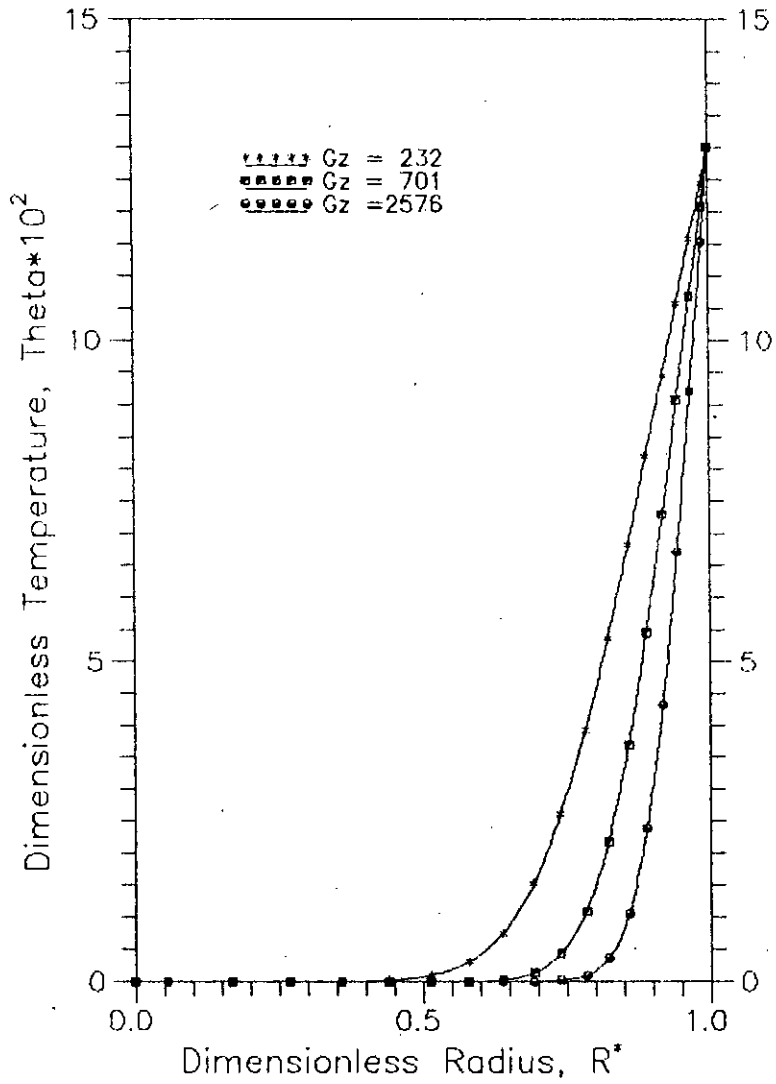


Fig.7.19 Temperature Profiles for 0.5% Cellofas B-300 at Different Gz . $T_w/T_i = 1.130$, $D = 17.4$ mm.

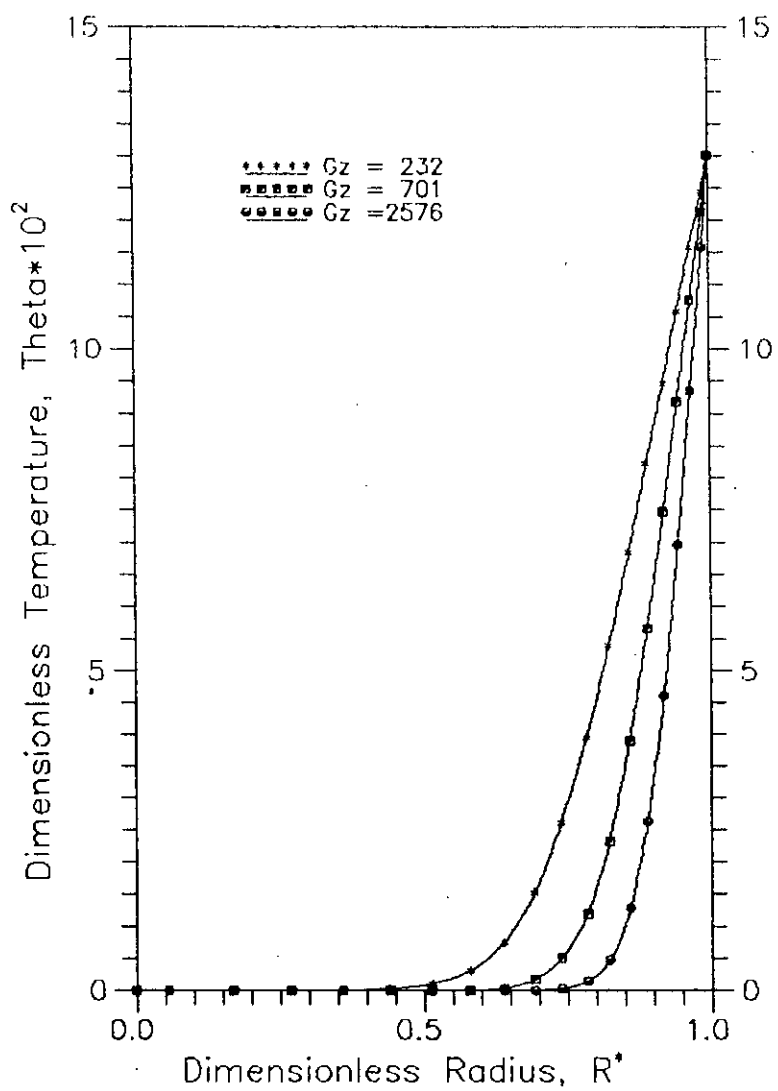


Fig.7.20 Temperature Profiles for 0.15% Cellofas B-3500 at Different Gz . $T_w/T_i=1.130$, $D=17.4$ mm.

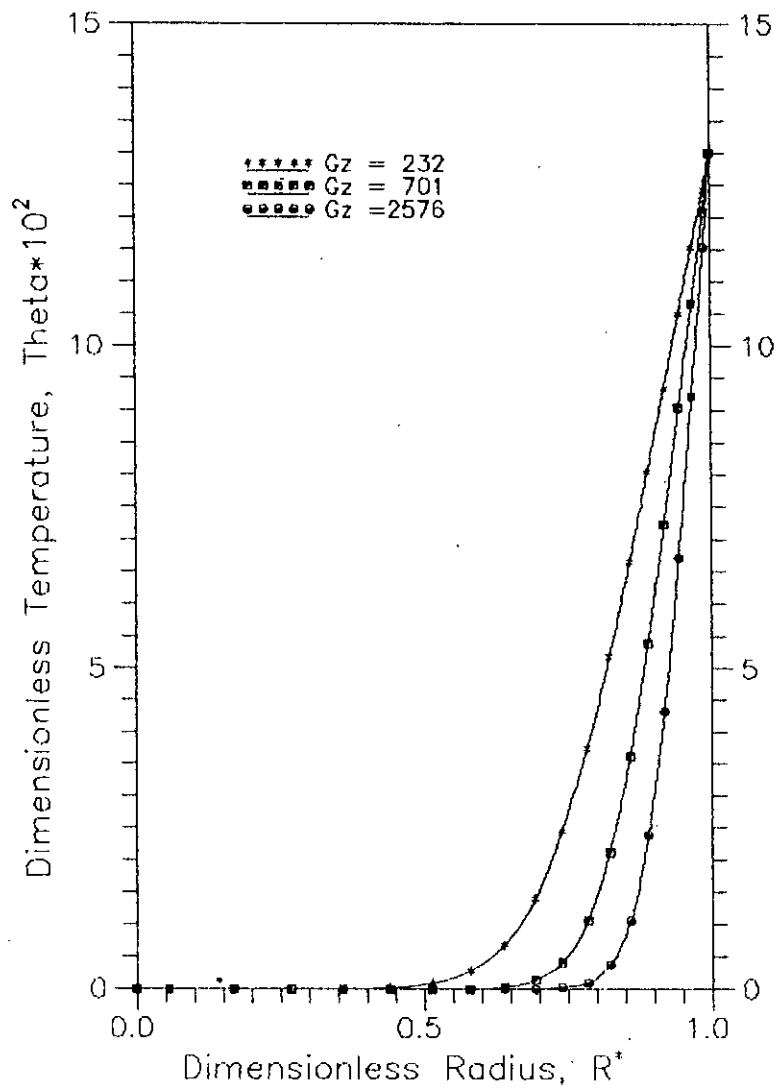


Fig.7.21 Temperature Profiles for 0.27% Cellofas B-3500 at Different Gz . $T_w/T_i = 1.130$, $D = 17.4$ mm.

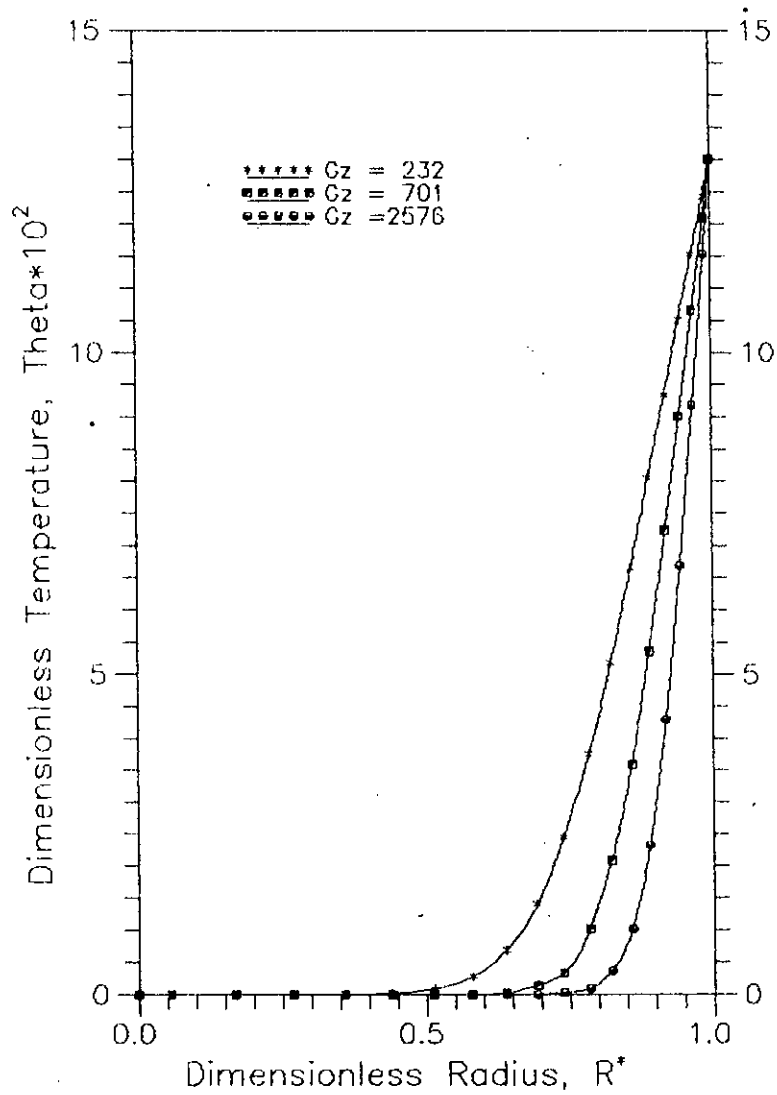


Fig.7.22 Temperature Profiles for 0.40% Cellofas B-3500 at Different Gz . $T_w/T_i = 1.130$, $D = 17.4$ mm.

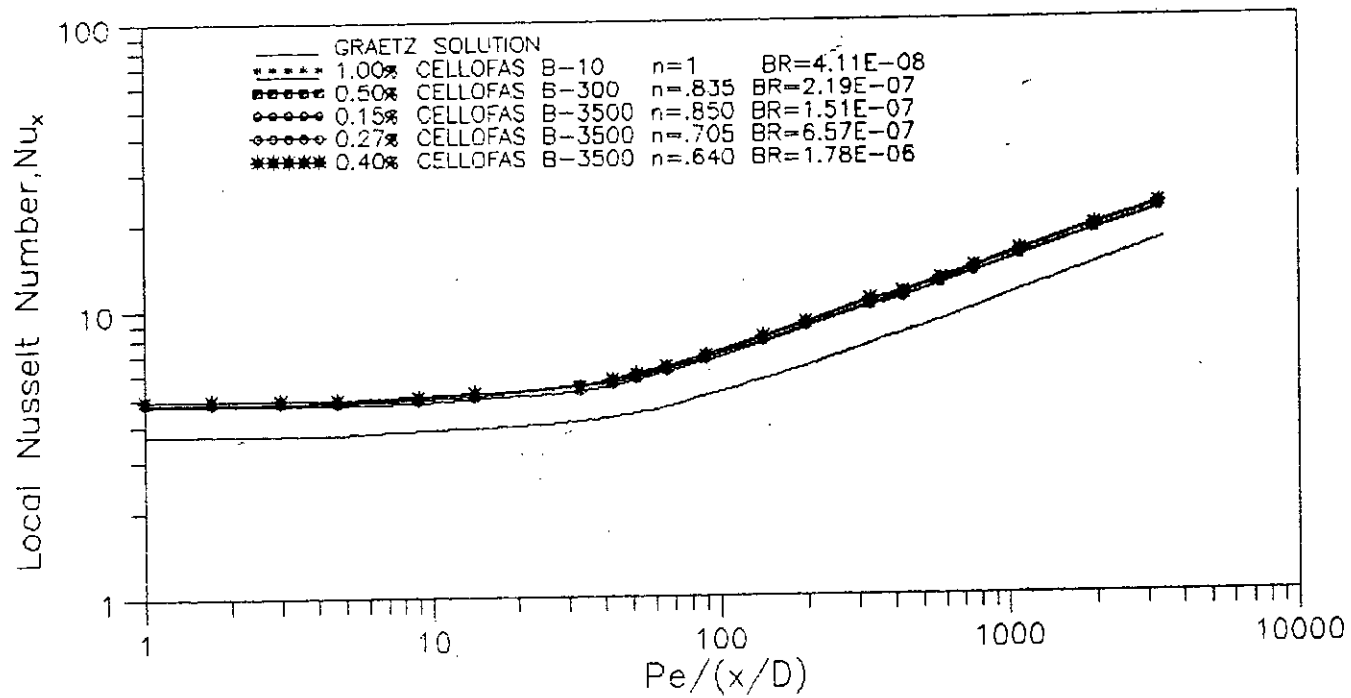


FIG.7.23 Local Nusselt Number for Laminar Flow in Tubes.
Velocity Profile Fully Developed, $T_w/T_i = 1.130$ and $D = 1.7.4$ mm.

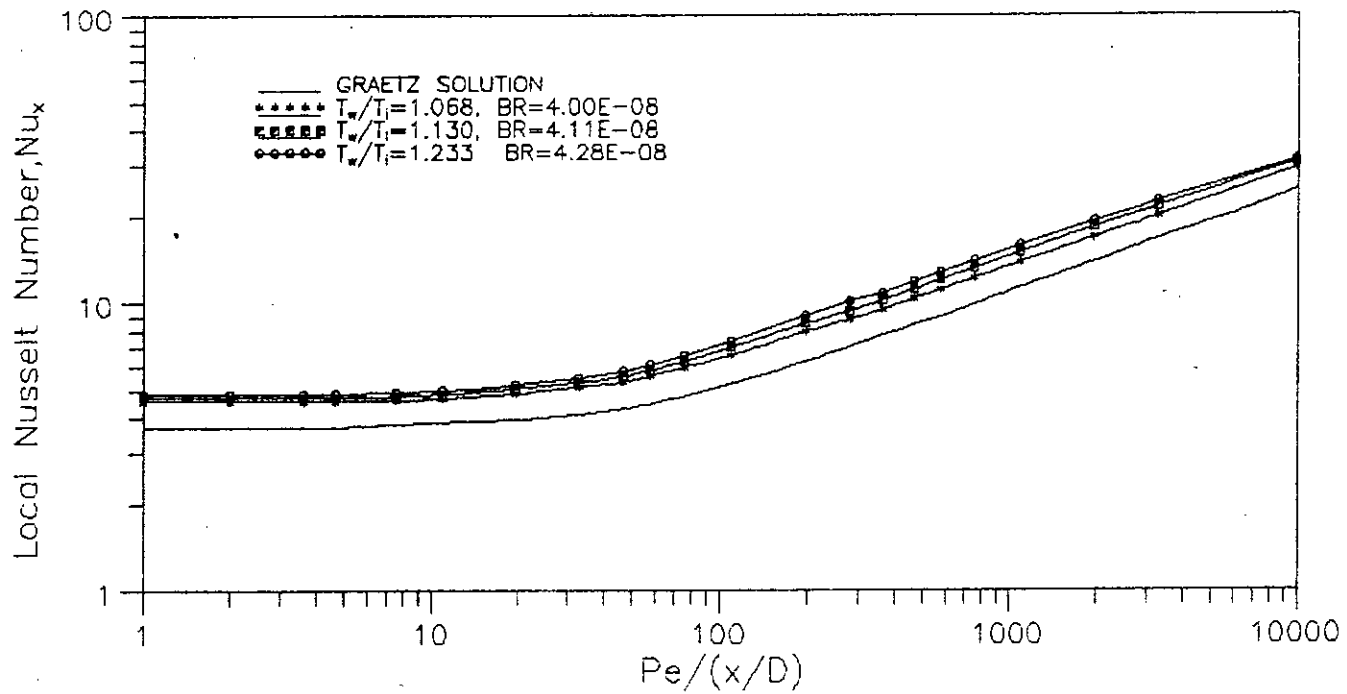


FIG.7.24 Local Nusselt Number for 1.0% Cellofas B-10 at Different T_w/T_i . Velocity Profile Fully Developed, $D = 17.4$ mm.

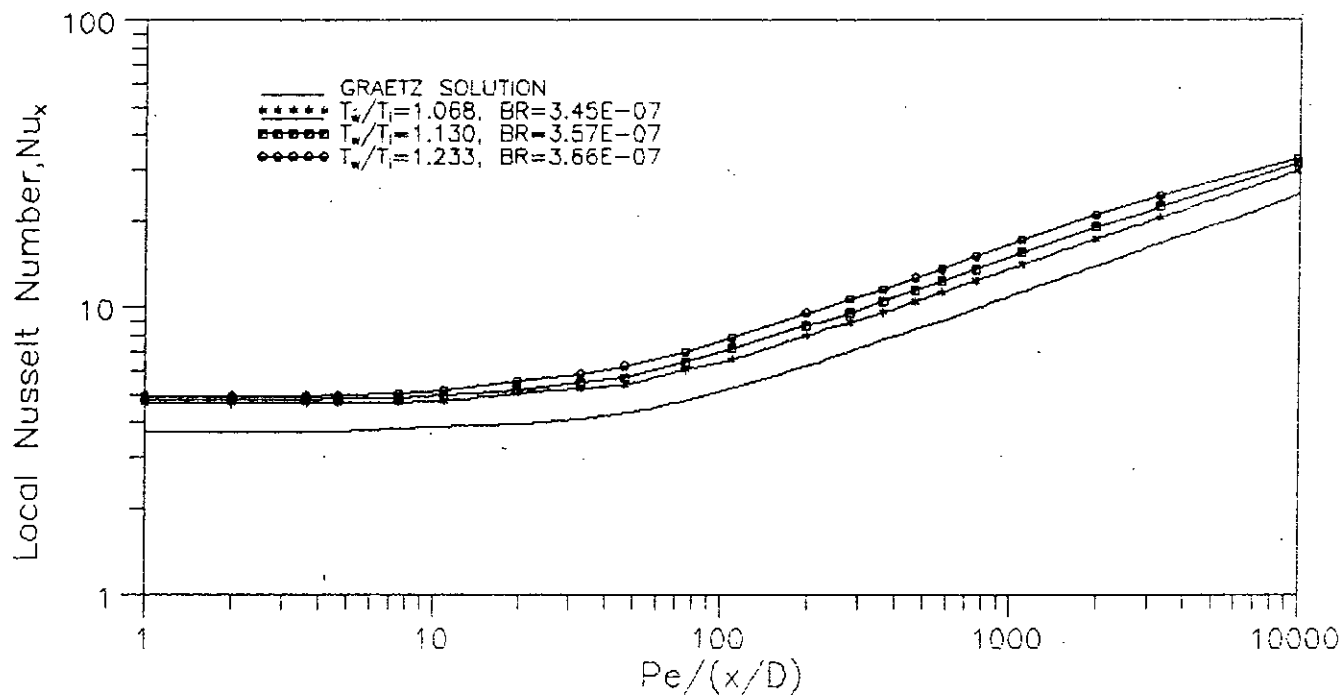


FIG.7.25 Local Nusselt Number for 0.5% Cellofas B-300 at Different T_w/T_i . Velocity Profile Fully Developed, $D = 17.4$ mm.

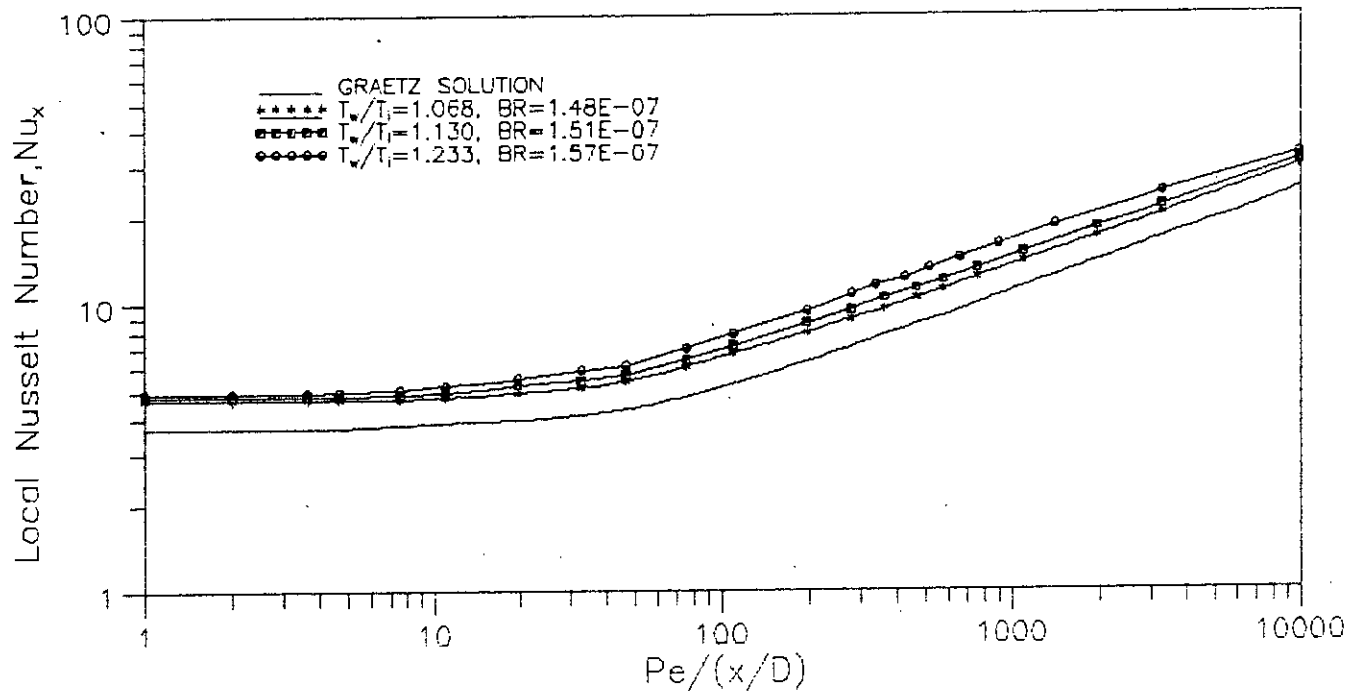


FIG.7.26 Local Nusselt Number for 0.15% Cellofas B-3500 at Different T_w/T_i . Velocity Profile Fully Developed, $D = 17.4$ mm.

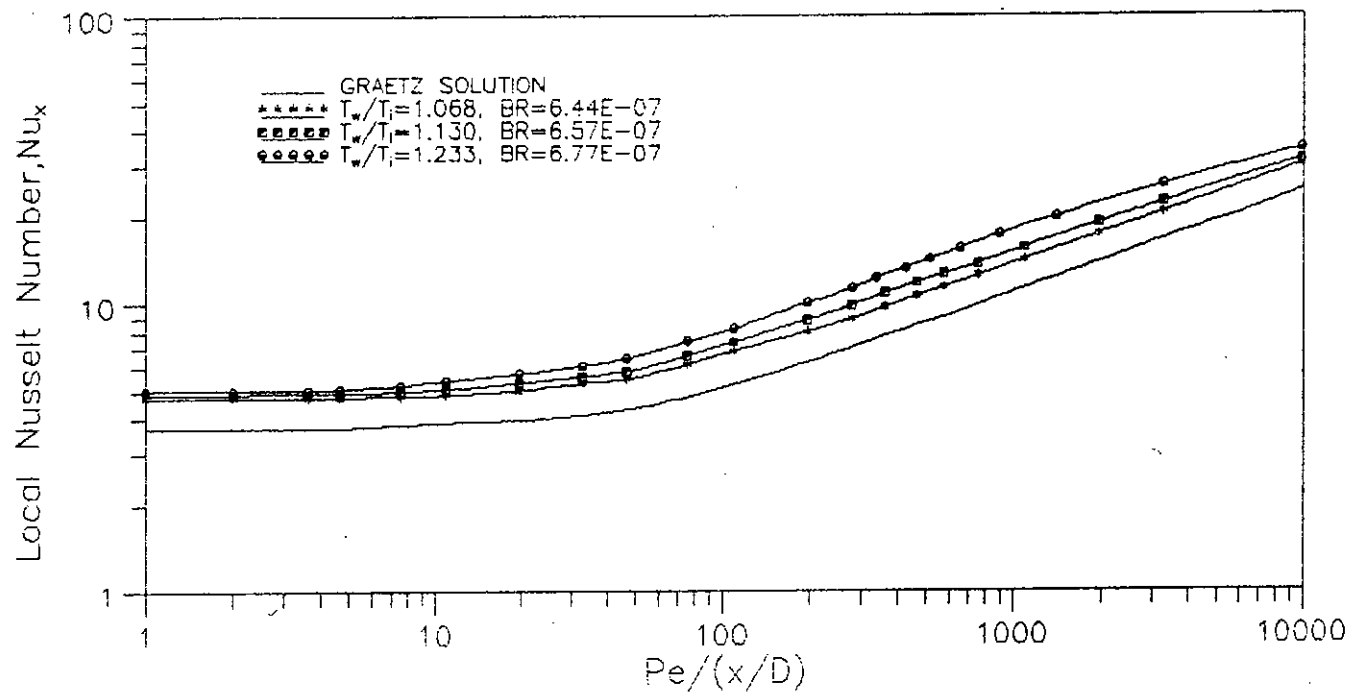


FIG.7.27 Local Nusselt Number for 0.27% Cellofas B-3500 at Different T_w/T_i . Velocity Profile Fully Developed, $D = 17.4$ mm.

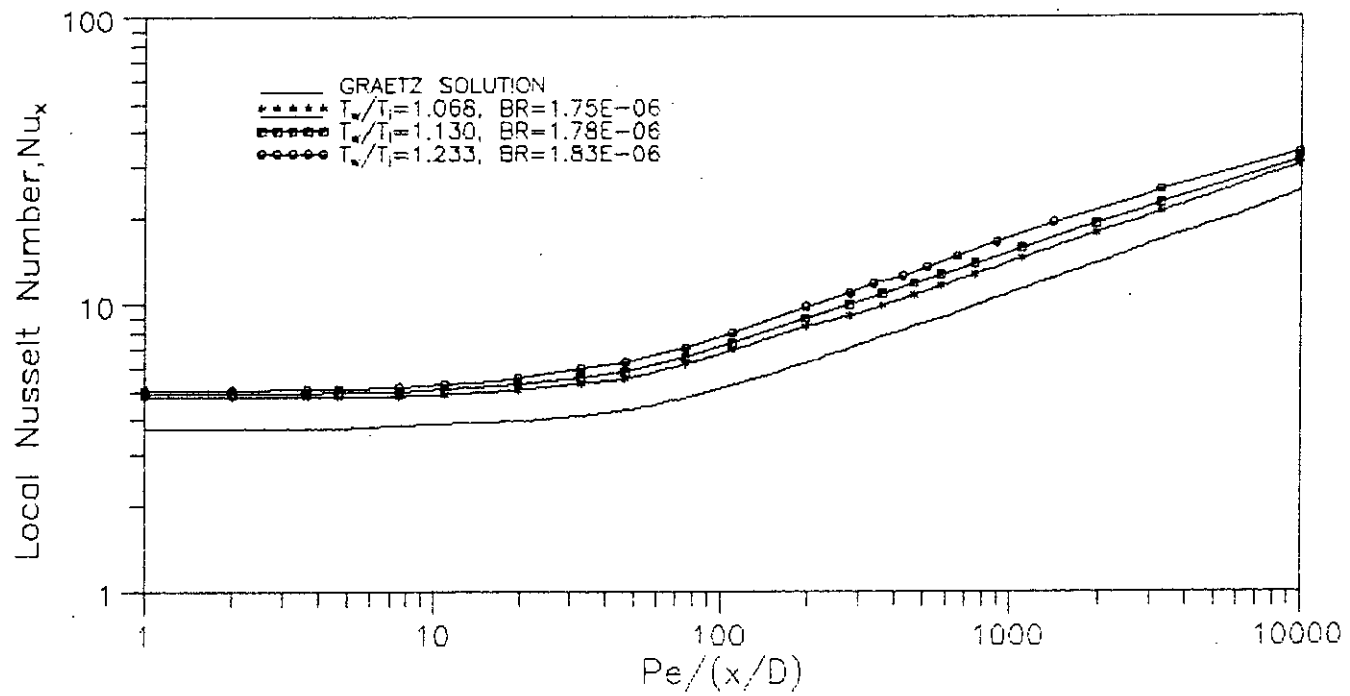


FIG.7.28 Local Nusselt Number for 0.40% Cellofas B-3500 at Different T_w/T_i . Velocity Profile Fully Developed, $D = 17.4$ mm.

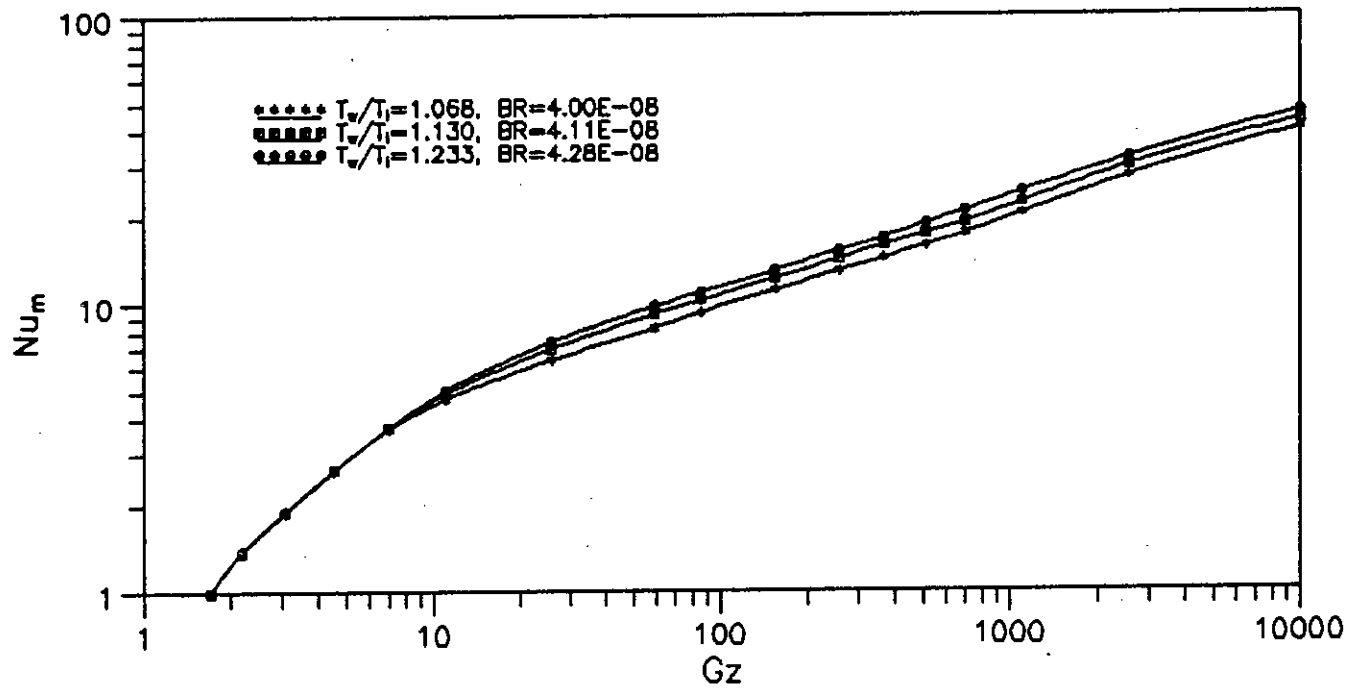


Fig. 7.29 Nu_m vs Gz for the Heating of 1.0% Cellofas B-10 with Constant Temperature at the Tube Wall.

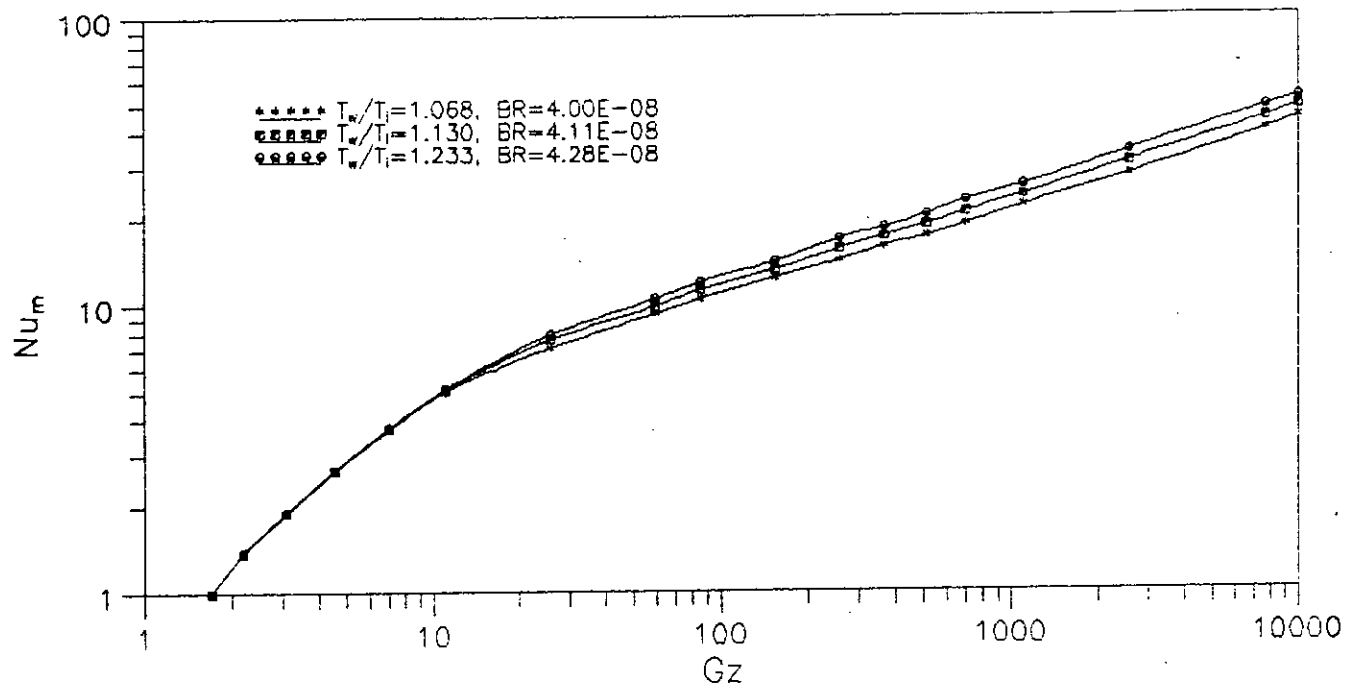


Fig. 7.30 Nu_m vs Gz for the Heating of 0.5% Cellofas B-300 with Constant Temperature at the Tube Wall.

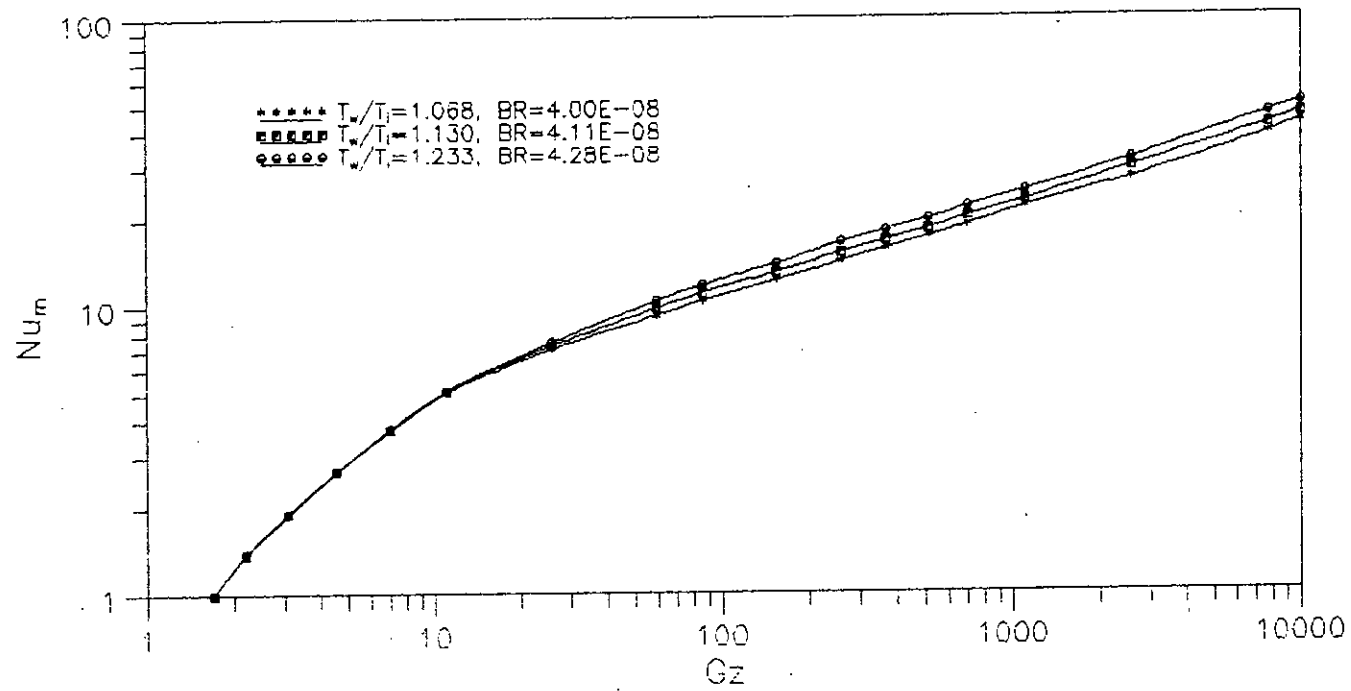


Fig. 7.31 Nu_m vs Gz for the Heating of 0.15 mm Cellofas B-3500 with Constant Temperature at the Tube Wall.

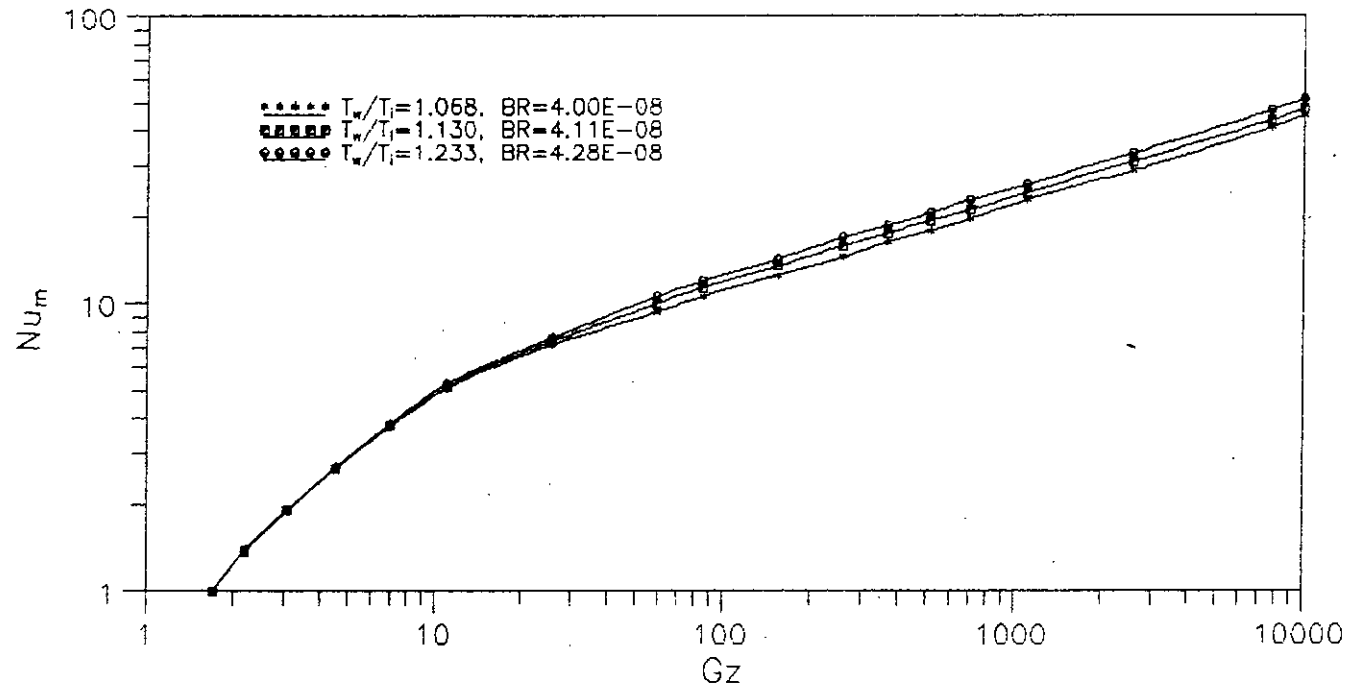


Fig. 7.32 Nu_m vs Gz for the Heating of 0.27x Cellofas B-3500 with Constant Temperature at the Tube Wall.

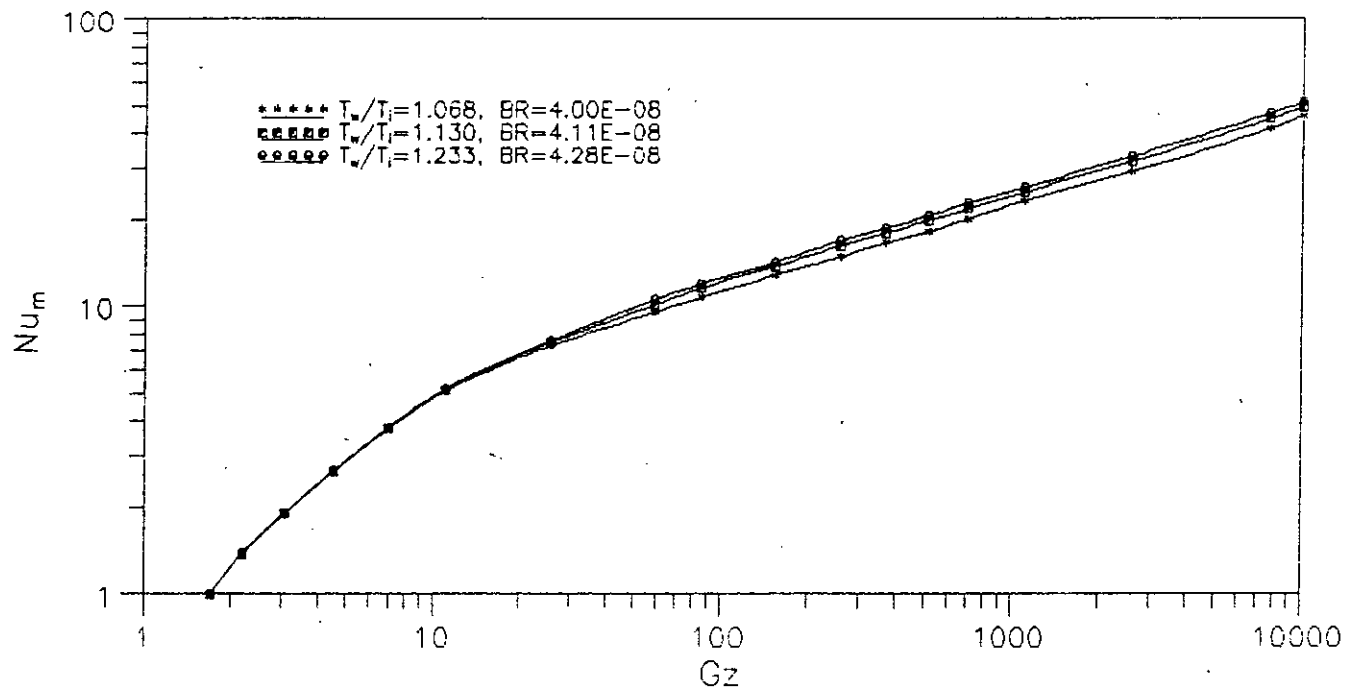


Fig. 7.33 Nu_m vs Gz for the Heating of 0.40% Cellofas B-3500 with Constant Temperature at the Tube Wall.

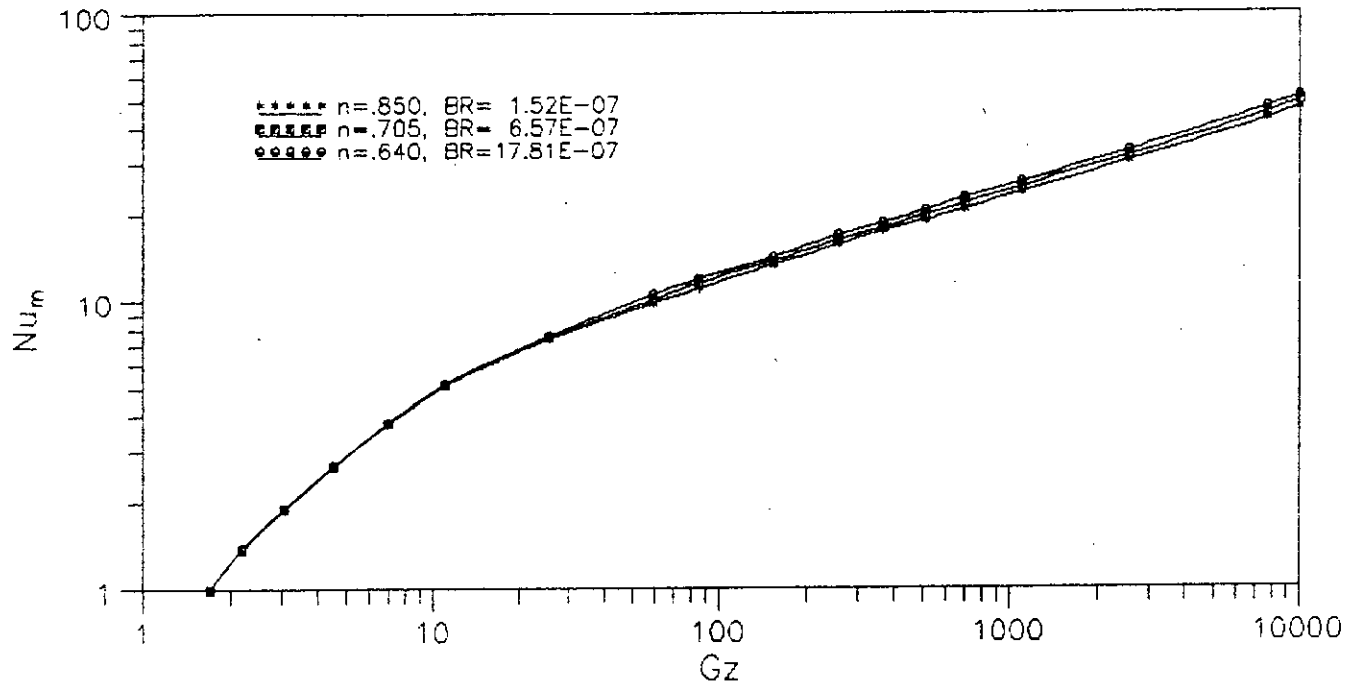
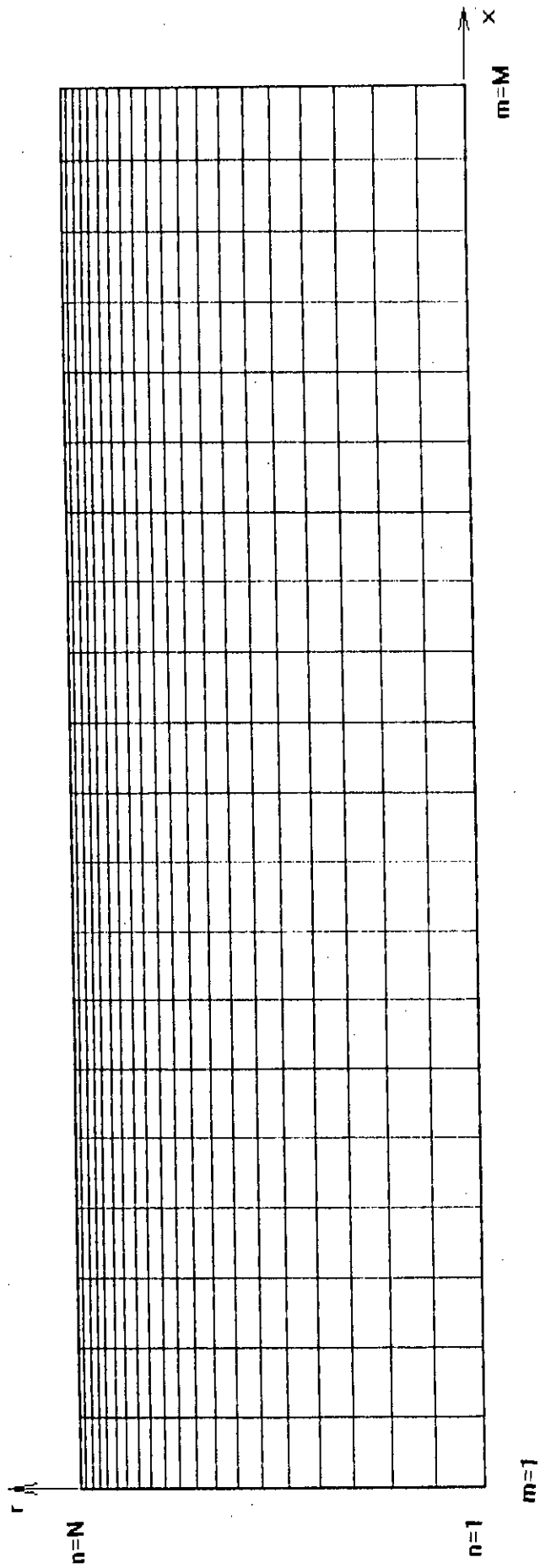


Fig. 7.34 Nu_m vs Gz for the Heating of Cellofas B-3500 with Different Composition at $T_w/T_i=1.13$.

FIG. A.1 COMPUTATIONAL GRID



APPENDIX-A

Finite Difference Form of Equation

The finite difference form of energy equation used in this study is presented here. Due to similar nature and method of discretization, other equations are not shown. The energy equation, eq.(4.5), can be written in the following form

$$\rho C_p u \frac{\partial T}{\partial x} - k \frac{\partial^2 T}{\partial r^2} + \frac{k}{r} \frac{\partial T}{\partial r} + k \frac{\partial^2 T}{\partial x^2} - \tau_{rz} \frac{\partial u}{\partial x}$$

This equation is solved by a finite difference method. A system of grid lines running in x and r directions, i.e. m and n lines, are imposed on the solution domain as shown in Figure A.1. The line at n=1 is located on the centre line and at n=N on the tube wall. The axial grid line at m=1 line is lying on the inlet boundary, x=0. The grid spacing are defined as:

$$\Delta r_1 = r_{n+1} - r_n$$

$$\Delta r_2 = r_n - r_{n-1}$$

$$\Delta x = x_m - x_{m-1}$$

The last term of the energy equation is source term, and is evaluated by integrating the volumetric source over the volume of the computational cell, eq.(6.5). The finite difference forms of the other terms are written as follows:

$$\left(\rho C_p u \frac{\partial T}{\partial x} \right) \Big|_{m,n} - (\rho C_p)_{m,n} u_{m-1,n} \left(\frac{T_{m,n} - T_{m-1,n}}{\Delta x} \right)$$

$$\left(\frac{k}{r} \frac{\partial T}{\partial r} \right) \Big|_{m,n} - \left(\frac{k}{r} \right)_{m,n} \left[\frac{\Delta r_2}{\Delta r_1 (\Delta r_1 + \Delta r_2)} (T_{m,n+1} - T_{m,n}) + \frac{\Delta r_1}{\Delta r_2 (\Delta r_1 + \Delta r_2)} (T_{m,n} - T_{m,n-1}) \right]$$

$$\left(k \frac{\partial^2 T}{\partial r^2} \right) \Big|_{m,n} - k_{m,n} \frac{2}{(\Delta r_1 + \Delta r_2)} \left[\frac{T_{m,n+1} - T_{m,n}}{\Delta r_1} - \frac{T_{m,n} - T_{m,n-1}}{\Delta r_2} \right]$$

$$\left(k \frac{\partial^2 T}{\partial x^2} \right) \Big|_{m,n} - k_{m,n} \left[\frac{T_{m+1,n} - 2T_{m,n} + T_{m-1,n}}{\Delta x^2} \right]$$

So, the final equation obtained is

$$(\rho C_p)_{m,n} u_{m-1,n} \left(\frac{T_{m,n} - T_{m-1,n}}{\Delta x} \right) =$$

$$\left(\frac{k}{r} \right)_{m,n} \left[\frac{\Delta r_2}{\Delta r_1 (\Delta r_1 + \Delta r_2)} (T_{m,n+1} - T_{m,n}) + \frac{\Delta r_1}{\Delta r_2 (\Delta r_1 + \Delta r_2)} (T_{m,n} - T_{m,n-1}) \right]$$

$$+ k_{m,n} \frac{2}{(\Delta r_1 + \Delta r_2)} \left[\frac{T_{m,n+1} - T_{m,n}}{\Delta r_1} - \frac{T_{m,n} - T_{m,n-1}}{\Delta r_2} \right]$$

$$+ k_{m,n} \left[\frac{T_{m+1,n} - 2T_{m,n} + T_{m-1,n}}{\Delta x^2} \right] - \int_v S_s dv$$

where, S_s is the source term.

